# 12 Radiation

## 12.1 INTRODUCTION

Radiation of electromagnetic energy from a circuit, cavity resonator, or wave-guiding system may be important either as an undesired leakage phenomenon or as a desired process for exciting waves in space. In the former case one wishes to minimize the power lost by radiation, and this may be done by changing circuit configuration or by adding shielding. When radiation is desired, the goal is to excite waves from the given source in the required direction or directions, as efficiently as possible. The system that acts as the transition or matching unit between the source and waves in space is known as the *radiator* or *antenna*. The primary stress in this chapter will be on antenna principles, with radiation as the desired result.

In the design of antenna systems, some or all of the following information may be required:

1. The relative field strength for various directions (called the antenna pattern)
2. The total power radiated when the radiator is excited by a known voltage or current
3. The input impedance of the radiator for matching purposes
4. The bandwidth of the antenna with respect to any of the above properties
5. The radiation efficiency, or ratio of power radiated to the total of radiated and dissipated power
6. For high-power antennas, the maximum field strengths at key positions in air or dielectrics that may cause corona or dielectric breakdown

The straightforward approach to any of the above questions might seem to be that of solving Maxwell's equations subject to the boundary conditions of the radiator and at infinity. This is possible in a few cases (to be discussed in a later section), but most antenna configurations are too complicated for this direct approach, and approximations must be made. To make such approximations, it is important to have good physical pictures of radiation phenomena.

One physical picture of radiation is that found in Chapter 4 when we considered circuits that are comparable in size with wavelength. It was found that retardation effects from one part of the circuit to another cause a phase shift, so that induced effects that are only reactive in a small circuit now have a real part also. This real part represents

power radiated from the circuit. From this point of view, an antenna is a circuit comparable with wavelength in size, purposely designed to maximize this retardation effect.

A picture closely related to the preceding but perhaps more direct follows from an examination of fields at a distance from the radiating system. If the system is small in size in comparison with wavelength, fields from positive and negative charges of the system (or oppositely directed current contributions) nearly cancel at large distances. For example, we found fields from a quasistatic electric dipole or small current loop falling off at least as fast as the inverse square of distance from the dipole or loop. But for larger circuits (in comparison with wavelength), there are phase differences from the distant point to various parts of the circuit so that cancellation is not so complete and we find terms inversely proportional to radius from the radiator.

For quantitative use of either of these two pictures, one needs the current distribution on the antenna. Exact determination of this would require solution of the difficult boundary value problem, but for many antennas, reasonable assumptions of current distributions may be made, or they may be found by measurement.

We will examine a variety of radiators in the next section and find that several of these (horns, parabolic reflectors, etc.) utilize large apertures with stress on the field pattern excited in the aperture. For these, it is appropriate to use the concept of the Huygens principle, in which each elemental portion of the wave in the aperture can be considered a source of waves in space. This qualitative picture will be shown to lead to useful quantitative procedures in later sections. There, fields in the aperture are required, and they may often be approximated when not known exactly.

Finally, we may think of the antenna as a matching section between the waves on whatever guiding system we use to excite the antenna and the waves in space. The goal from this point of view is to design the unit for optimum matching over the desired frequency range, just as in matching units between different transmission lines or waveguiding systems. An antenna which illustrates this and also shows the relation between the several points of view is the biconical antenna pictured in Fig. 12.1. This is the biconical transmission line of Sec. 9.6, open to space over the region shown dashed

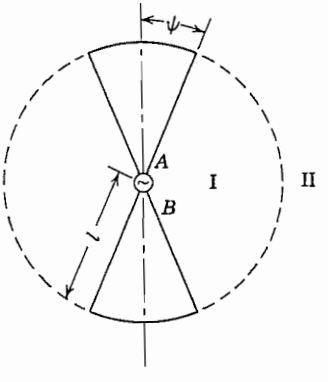


**FIG. 12.1** Axial section through a biconical antenna.

between regions I and II. A source is introduced at the origin, between apexes $A$ and $B$, and this excites primarily the TEM or principal mode studied in Sec. 9.6. To a first approximation the surface at $r = l$ might be considered an open circuit and the principal wave reflection would then produce a sinusoidal standing wave on the cones. High-order waves are then excited in both regions I and II to provide the required field continuity over the dashed portion of the sphere; then the waves in space become the desired radiation fields. This example is interesting in that if cone angle $\psi$ is small, the cones may be thought of as wires, with the current to first order being the sinusoidal principal wave current. Alternatively, we can look at the principal wave fields on the dashed part of the spherical surface between I and II as the source of radiation, with the system considered a biconical horn. So we see that the several pictures are related and the best for quantitative use may depend upon the specific configuration.

Most of the discussion in this chapter will relate directly to radiating or transmitting antennas but the results developed also can be applied to the same antenna when used for receiving applications. The radiating case is easier both for analysis and intuitive understanding and the relation to the receiving situation can be made rigorously using the principle of reciprocity that was introduced in Sec. 11.3.

## 12.2 Some Types of Practical Radiating Systems

To give point to comments and analyses that follow, let us look at some of the typical systems that have been used as radiators. No attempt will be made to provide complete discussions of operation here, since the remainder of the chapter will be devoted to more thorough analyses of some of these systems. Nor does the list cover all types of radiators. The ones given are chosen as examples to make clearer the discussions of principles in sections to follow.

**"Dipole" Antennas** Among the most common radiators is the dipole, which consists of a straight conductor (often a thin wire or circular cylinder of larger diameter) broken at some point where it is excited by a voltage derived from a transmission line, waveguide, or directly from a generator (Fig. 12.2*a*). In most cases, the exciting source is at the center, yielding a symmetric dipole, although asymmetric dipoles are also used. Resonant dipoles, and especially the half-wave dipole with $2l$ approximately equal to a half-wavelength, are common.

**Loop Antennas** Radiation from a loop of wire excited by a generator has been discussed in Chapter 4. Such loop antennas are useful radiators, although often they have many turns, as in Fig. 12.2*b*. The field from a small loop is much like that from the small dipole, with electric and magnetic fields interchanged, and thus is known as a *magnetic dipole.*

**Traveling-Wave Antennas** If the radiator is made to have a traveling wave in one direction with a phase velocity about equal to the velocity of light, waves in space may

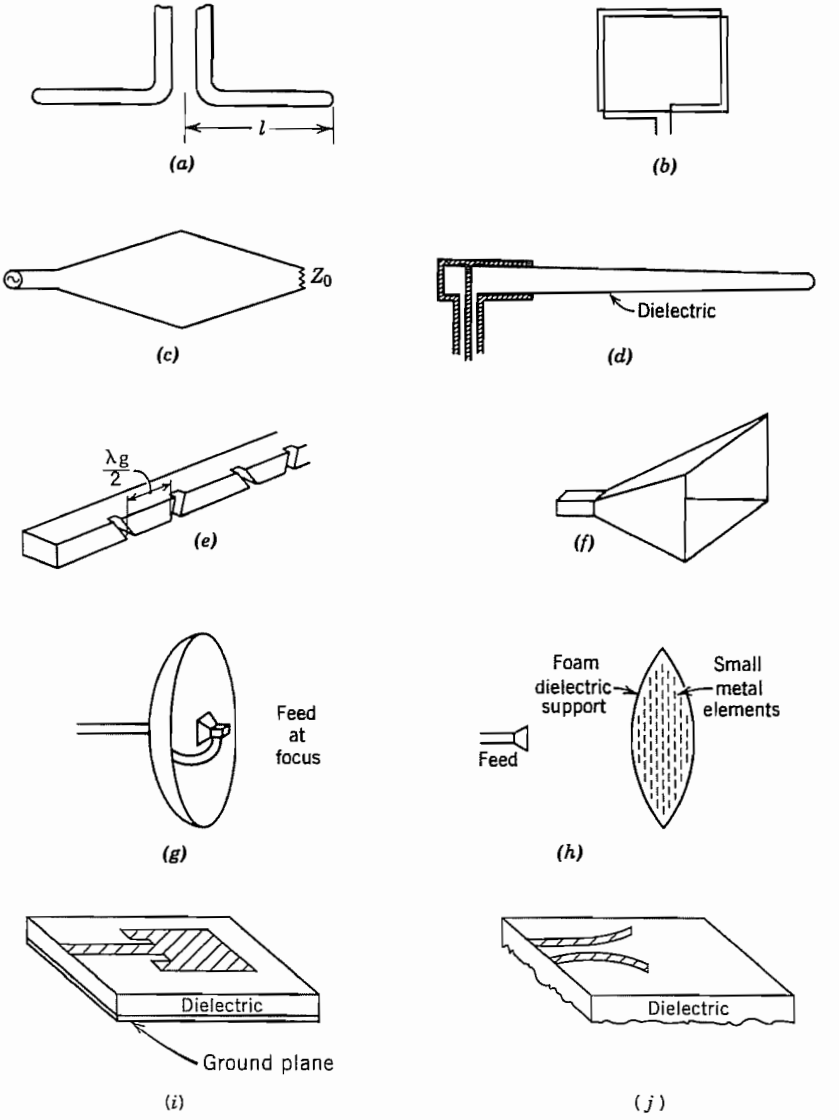


**FIG. 12.2** Typical antennas: (*a*) Dipole. (*b*) Loop. (*c*) Rhombic. (*d*) Dielectric rod. (*e*) Slot array. (*f*) Pyramidal horn. (*g*) Parabolic reflector. (*h*) Artificial dielectric lens. (*i*) Microstrip "patch" antenna. (*j*) Coplanar strip "horn."

be excited strongly in this direction as compared with other directions, thus yielding desired directivity. Figure 12.2*c* shows the important rhombic antenna, which utilizes waves along wires and is analyzed in more detail later. If only one-half of the rhombic

is present, the result is the V antenna. These have been made in thin-film form for use at millimeter-wave frequencies. Figure 12.2*d* shows a version in which the traveling wave is guided by a dielectric as in Sec. 9.2. Near cutoff, phase velocity is approximately the velocity of light and the fields that extend outside a dielectric guide may excite appreciable radiation in space.

**Slot and Aperture Antennas** As noted in Sec. 12.1, fields across an aperture may excite radiation in space. If the apertures are small, they must generally be resonant to excite appreciable amounts of power (although nonresonant holes in cavities may produce enough leakage to damage the $Q$ of low-loss cavities). A narrow resonant half-wave slot has many similarities to the half-wave wire dipole, although electric and magnetic fields are interchanged, as will be seen. Figure 12.2*e* illustrates a series of slots in a rectangular guide to form a "leaky waveguide" array. When apertures are large, they need not be resonant to produce significant radiation. Electromagnetic horns are examples of radiators designed to match waves from a guiding system to a large radiating aperture by properly shaping the transition, much as in the acoustic horns used for sound waves. Figure 12.2*f* gives one example. Since the horns are not resonant, they, like the traveling-wave antennas, are especially useful for broadband signals.

**Reflectors and Lenses** A parabolic reflector, as illustrated in Fig. 12.2*g*, is a most important device for microwave radiation. This may be considered as a mirror, serving to reflect the rays from the primary radiator at the focus. Geometrical optics would then predict an exactly parallel beam emerging from such a reflector if the primary radiator is infinitesimal. Alternatively, it may be considered that the primary source serves to illuminate the aperture, and radiation from this aperture produces the far field. From this point of view (which is also called "physical optics" or "diffraction theory"), there is always spreading of the beam. The spreading decreases as aperture size increases, an aperture 70 wavelengths in diameter producing a beam width of about 1 degree. Lenses serve a similar purpose in directing the rays from a primary radiator. These may be of solid dielectric, artificial dielectrics as illustrated in Fig. 12.2*h*, or metal waveguide paths to supply proper phase shifts to direct the beam. Lenses can also be considered as aperture radiators.

**Integrated-Circuit-Type Antennas** Antennas for use with microwave integrated circuits may be placed on dielectric substrates and are sometimes called *patch* antennas. Figure 12.2*i* illustrates one in microstrip form and Fig. 12.2*j* a horn type for use with coplanar strip.

**Arrays** Any of these radiators may be combined with like or different elements to form arrays that have particular directions in which phases add and radiation is concentrated. A most important use of arrays is in "electrical scanning" of the direction of concentration by control of phase shift from element to element. An example of the two-dimensional array of slot radiators is shown in Fig. 12.2*e*.

# Field and Power Calculations with Currents Assumed on the Antenna

## 12.3 Electric and Magnetic Dipole Radiators

In computing radiated power and the field distributions around an antenna when current distribution is assumed over the surface of the antenna's conductors, the simplest example is that of an ideal short linear element with current considered uniform over its length. Certain more complex antennas can be considered to be made up of a large number of such differential antennas with the proper magnitudes and phases of their currents. We shall consider only the case in which the current varies sinusoidally with time so we express it by its phasor $I_0$ that multiplies the factor $e^{j\omega t}$.

The current element is in the $z$ direction with its location the origin of a set of spherical coordinates (Fig. 12.3*a*). Its length is $h$, with $h$ very small compared with wavelength. By continuity, equal and opposite time-varying charges must exist on the two ends $\pm h/2$, so the element is frequently called a *Hertzian dipole.*

One way of finding fields once current is given requires only the retarded potential **A** as seen in Sec. 3.21. For any point $Q$ at radius $r$, **A** of Eq. 3.21(8) is in the $z$ direction and becomes simply

$$A_z = \mu \frac{hI_0}{4\pi r} e^{-j(\omega r/v)} \tag{1}$$

Or, in the system of spherical coordinates,

$$\begin{aligned} A_r &= A_z \cos\theta = \mu \frac{hI_0}{4\pi r} e^{-jkr} \cos\theta \\ A_\theta &= -A_z \sin\theta = -\mu \frac{hI_0}{4\pi r} e^{-jkr} \sin\theta \end{aligned} \tag{2}$$

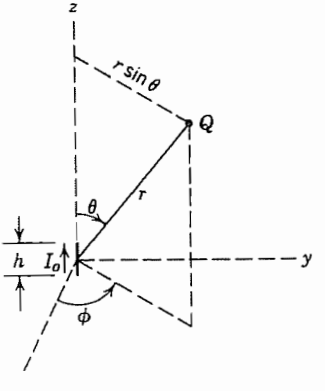


**Fig. 12.3*a*** Hertzian dipole.

where $k = \omega/v = \omega\sqrt{\mu\varepsilon} = 2\pi/\lambda$. There is no $\phi$ component of **A**, and there are no variations with $\phi$ in any expressions because of the symmetry of the structure about the axis. The electric and magnetic field components may be found directly from the components of **A** by use of Eqs. 3.21(6) and (7). Thus,

$$H_\phi = \frac{I_0 h}{4\pi} e^{-jkr}\left(\frac{jk}{r} + \frac{1}{r^2}\right) \sin\theta$$

$$E_r = \frac{I_0 h}{4\pi} e^{-jkr}\left(\frac{2\eta}{r^2} + \frac{2}{j\omega\varepsilon r^3}\right) \cos\theta \tag{3}$$

$$E_\theta = \frac{I_0 h}{4\pi} e^{-jkr}\left(\frac{j\omega\mu}{r} + \frac{1}{j\omega\varepsilon r^3} + \frac{\eta}{r^2}\right) \sin\theta$$

An interesting illustration of the fields produced by the dipole can be obtained by using $E_r$ and $E_\theta$ components in (3) to show the patterns of field lines as functions of time, as was done in Sec. 8.3 for waveguide field patterns.[1] The expressions in (3) are converted into real functions of time in the usual way and plots are made of the electric field lines at various instants in time. At $t = 0$ the dipole current is maximum [Eq. 3.20(9)] so the charges on the ends of the dipole (Prob. 3.20b) are zero and the electric fields near the origin are zero. Previously generated patterns of fields have radiated away as shown in Fig. 12.3*b*. A quarter of a period later, the charge has built up on the ends of the dipole and electric field lines are produced in the neighborhood of the dipole as seen in Fig. 12.3*c*. The loops of the field lines close and "snap off" from the source as the charges return to zero.

For the region very near the element ($r$ small) the most important term in $H_\phi$ is that varying as $1/r^2$. The important terms in $E_r$ and $E_\theta$ are those varying as $1/r^3$. Thus, near the element, magnetic field is very nearly in phase with current, and $H_\phi$ may be identified as the usual induction field obtained from Ampère's law. Electric field in this region may be identified with that calculated for an electrostatic dipole. (By continuity, $I_0/j\omega$ represents the charge on one end of the dipole.) As the important components of electric and magnetic field in this region are 90 degrees out of phase, these components represent no time-average energy flow, according to the Poynting theorem.

At very great distances from the source, the only terms important in the expressions for $E$ and $H$ are those varying as $1/r$:

$$H_\phi = \frac{jkI_0 h}{4\pi r} \sin\theta\, e^{-jkr}$$

$$E_\theta = \frac{j\omega\mu I_0 h}{4\pi r} \sin\theta\, e^{-jkr} = \eta H_\phi \tag{4}$$

$$\eta = \sqrt{\mu/\varepsilon} \approx 120\pi \text{ ohms for space}$$

[1] *S. A. Schelkunoff and H. T. Friis,* Antennas: Theory and Practice, *Wiley, New York, 1952.*

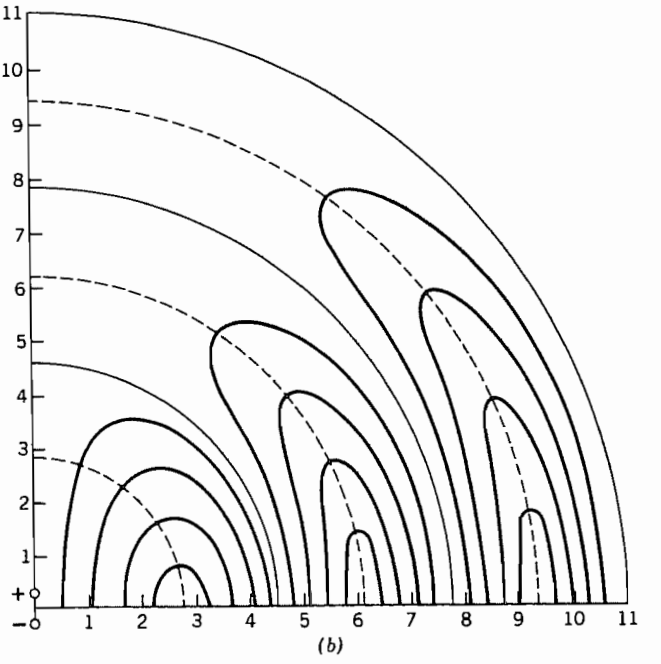


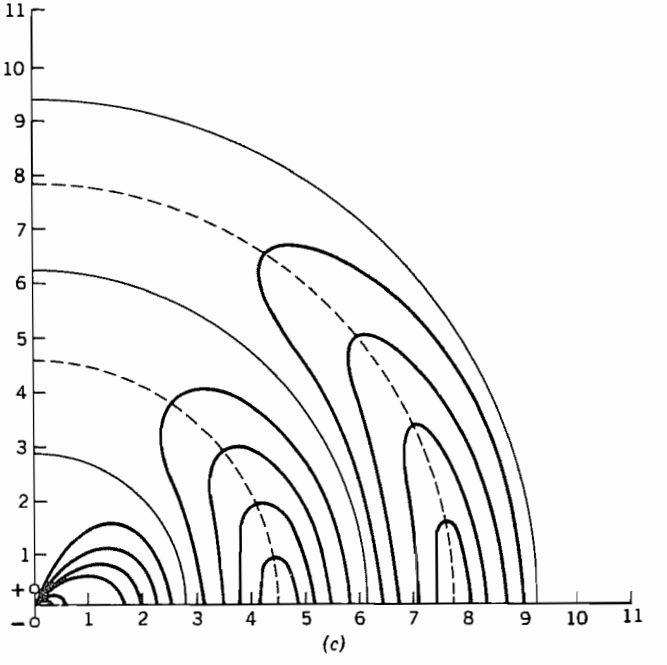


**FIG. 12.3** (*b*) Fields near an oscillating electric dipole when the charges at its ends are zero. (*c*) Fields near an oscillating dipole when the charges at its ends have their maximum values. From S. A. Schelkunoff and H. T. Friis, *Antennas: Theory and Practice.* © 1952, John Wiley and Sons, New York.

Equations (4) show the characteristics typical of uniform plane waves, as might be expected. $E_\theta$ and $H_\phi$ are in time phase, related by $\eta$, and at right angles to each other and the direction of propagation. The Poynting vector is then completely in the radial direction. The time-average $P_r$ is

$$P_r = \frac{1}{2}\,\mathrm{Re}(E_\theta H_\phi^*) = \frac{\eta k^2 I_0^2 h^2}{32\pi^2 r^2}\sin^2\theta \qquad \mathrm{W/m^2} \tag{5}$$

The total power must be the integral of the Poynting vector over any surrounding surface. For simplicity this surface may be taken as a sphere of radius $r$:

$$W = \oint_S \mathbf{P}\cdot\mathbf{dS} = \int_0^\pi P_r 2\pi r^2 \sin\theta\, d\theta$$

$$= \frac{\eta k^2 I_0^2 h^2}{16\pi}\int_0^\pi \sin^3\theta\, d\theta$$

$$W = \frac{\eta\pi I_0^2}{3}\left(\frac{h}{\lambda}\right)^2 \cong 40\pi^2 I_0^2\left(\frac{h}{\lambda}\right)^2 \quad \mathrm{W} \tag{6}$$

It is interesting and important to note that the field of the Hertzian dipole has the same form as the first-order TM spherical wave studied in Sec. 10.7. From Eqs. 10.7(19) with $n = 1$ and the Bessel function taken as the second Hankel form which is appropriate to a region extending to infinity,

$$H_\phi = A_1 r^{-1/2} P_1^1(\cos\theta) H^{(2)}_{3/2}(kr)$$

$$E_\theta = \frac{A_1}{j\omega\varepsilon r^{3/2}}\left[H^{(2)}_{3/2}(kr) - krH^{(2)}_{1/2}(kr)\right]P_1^1(\cos\theta) \tag{7}$$

$$E_r = -\frac{A_1 H^{(2)}_{3/2}(kr)}{j\omega\varepsilon r^{3/2}\sin\theta}\left[\cos\theta\, P_1^1(\cos\theta) - P_2^1(\cos\theta)\right]$$

But, from the relations of Sec. 10.7 it may be shown that

$$H^{(2)}_{3/2}(kr) = \sqrt{\frac{2}{\pi kr}}\, e^{-jkr}\left(\frac{j}{kr} - 1\right)$$

$$P_1^1(\cos\theta) = \sin\theta$$

With these substitutions and appropriate definition of constant $A_1$, (7) and (3) are identical. The electric field lines for this mode are the same as Fig. 12.3*b* or *c*.

**Magnetic Dipole** The concept of duality was introduced in Sec. 9.5, where it was pointed out that exchanges **H** for **E**, $-\mathbf{E}$ for **H**, $\mu$ for $\varepsilon$, and $\varepsilon$ for $\mu$ leave Maxwell's curl equations for source-free regions unchanged. Thus solutions for a problem with an electric source can be adapted to one with a magnetic source. For example, Sec. 2.10 showed that a small current loop of radius $a$ and current $I$ can be represented as a

magnetic dipole $m = I\pi a^2$, and this gave the same form of magnetic field as the electric field given by the electric dipole $p = qh$. The charges $q$ on the ends of the ac dipole are found from the ac current by the continuity equation which gives $j\omega q = I_0$ so that $p = I_0 h/j\omega$. Then replacing $I_0 h/j\omega$ in (3) by $\mu$ times the magnetic dipole and making the other above-stated duality interchanges, we find the fields of a magnetic ac dipole. The field components are

$$
\begin{aligned}
E_\phi &= -\frac{j\omega\mu I a^2}{4} e^{-jkr}\left(\frac{jk}{r} + \frac{1}{r^2}\right) \sin\theta \\
H_r &= \frac{j\omega\mu I a^2}{4} e^{-jkr}\left(\frac{2}{\eta r^2} + \frac{2}{j\omega\mu r^3}\right) \cos\theta \\
H_\theta &= \frac{j\omega\mu I a^2}{4} e^{-jkr}\left(\frac{j\omega\varepsilon}{r} + \frac{1}{j\omega\mu r^3} + \frac{1}{\eta r^2}\right) \sin\theta
\end{aligned}
\tag{8}
$$

In comparing the fields of the electric and magnetic dipole radiators, note that neither has azimuthal ($\phi$) variations, there is a null along the $z$ axis in the far zone, and they have orthogonal polarizations.

## 12.4 Systemization of Calculation of Radiating Fields and Power from Currents on an Antenna

For antennas with known current distributions, or with current distributions that can reasonably be assumed or measured, fields may be calculated from the retarded potentials as in Sec. 12.3, with integration over the current distributions. Or, equivalently, one can assume each infinitesimal element as a dipole and superpose the results of Sec. 12.3 by integration. We shall be able to simplify the procedures, however, whenever we are concerned only with the radiation or far-zone fields. The particular forms used here are useful ones introduced by Schelkunoff.[2]

The following assumptions are justified when field is calculated at a great distance from the radiator:

1. Differences in radius vector to different points of the radiator are unimportant in their effect on *magnitudes*.
2. All field components decreasing with distance faster than $1/r$ are negligible compared with those decreasing as $1/r$.
3. Differences in radius vector to different points on the radiator must be taken into account for phase considerations but may be approximated.

[2] *S. A. Schelkunoff,* Proc. IRE **27**, *660 (1939);* Electromagnetic Waves, *Chap. IX, Van Nostrand, New York, 1943.*

The vector potential at a point $Q$ a distance $r$ from the origin of the coordinate system can be calculated using Eq. 3.21(4), where the integral is taken over the source region $V'$ (Fig. 12.4):

$$\mathbf{A} = \mu \int_{V'} \frac{\mathbf{J} e^{-jkr''}}{4\pi r''} \, dV' \tag{1}$$

If the origin of coordinates is chosen close to the sources so that $r' \ll r$, the law of cosines may be used to find

$$r'' = \sqrt{r^2 + r'^2 - 2rr' \cos \psi} \cong r - r' \cos \psi \tag{2}$$

as suggested by Fig. 12.4. Using the first term of (2) for magnitudes (point 1 above) and both terms for phase (point 3), the vector potential (1) can be written

$$\mathbf{A} = \mu \frac{e^{-jkr}}{4\pi r} \int_{V'} \mathbf{J} \, e^{jkr' \cos \psi} \, dV' \tag{3}$$

The function of $r$ is now outside the integral; *the integral itself is only a function of the assumed current distribution and the direction $\psi$ between $r$ and $r'$*. Define the integral as the *radiation vector* **N**:

$$\mathbf{N} = \int_{V'} \mathbf{J} \, e^{jkr' \cos \psi} \, dV' \tag{4}$$

Then

$$\mathbf{A} = \mu \frac{e^{-jkr}}{4\pi r} \mathbf{N} \tag{5}$$

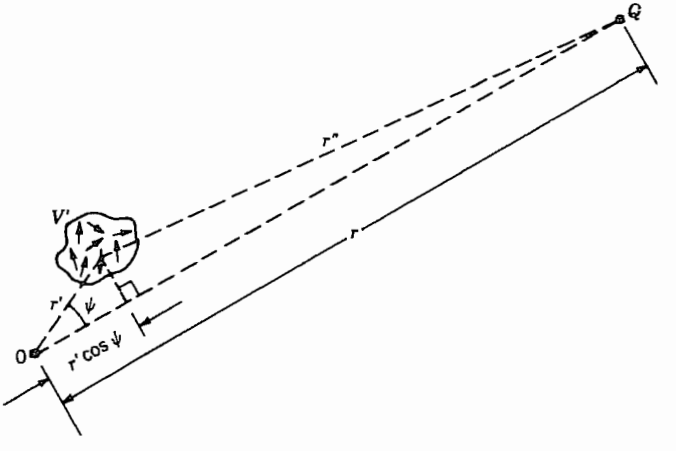


**FIG. 12.4** Coordinates of a general current element in the volume $V'$ and a distant point $Q$, where fields are to be evaluated, with respect to an origin of coordinates near the sources.

In the most general case, **A**, and hence **N**, may have components in any direction. In spherical coordinates, employing the unit vectors,

$$\mathbf{A} = \mu \frac{e^{-jkr}}{4\pi r} (\hat{\mathbf{r}}N_r + \hat{\boldsymbol{\theta}}N_\theta + \hat{\boldsymbol{\phi}}N_\phi)$$

A study of the equation $\mathbf{B} = \nabla \times \mathbf{A}$ in spherical coordinates (see inside front cover) shows that the only components that do not decrease faster than $1/r$ are

$$\begin{aligned} H_\theta &= -\frac{1}{\mu r}\frac{\partial}{\partial r}(rA_\phi) = \frac{jk}{4\pi r} e^{-jkr}N_\phi \\ H_\phi &= \frac{1}{\mu r}\frac{\partial}{\partial r}(rA_\theta) = -\frac{jk}{4\pi r} e^{-jkr}N_\theta \end{aligned} \tag{6}$$

An examination of Eq. 3.21(7)

$$\mathbf{E} = -\frac{j\omega}{k^2}\nabla(\nabla \cdot \mathbf{A}) - j\omega\mathbf{A}$$

shows that the only components of **E** which do not decrease faster than $1/r$ are

$$E_\theta = -\frac{j\omega\mu}{4\pi r} e^{-jkr}N_\theta, \qquad E_\phi = -\frac{j\omega\mu}{4\pi r} e^{-jkr}N_\phi \tag{7}$$

The Poynting vector has a time-average value:

$$P_r = \frac{1}{2}\,\mathrm{Re}[E_\theta H_\phi^* - E_\phi H_\theta^*] = \frac{\eta}{8\lambda^2 r^2}[|N_\theta|^2 + |N_\phi|^2] \tag{8}$$

Total time average power radiated is

$$\begin{aligned} W &= \int_0^\pi \int_0^{2\pi} P_r r^2 \sin\theta \, d\theta \, d\phi \\ &= \frac{\eta}{8\lambda^2}\int_0^\pi \int_0^{2\pi} [|N_\theta|^2 + |N_\phi|^2] \sin\theta \, d\theta \, d\phi \end{aligned} \tag{9}$$

The expression is independent of $r$, as it should be.

The Poynting vector **P** gives the actual power density at any point. To obtain a quantity that does not depend on distance from the radiator, we define $K$, *radiation intensity*, as the power radiated in a given direction per unit solid angle. This is the time-average Poynting vector on a sphere of unit radius:

$$K = \frac{\eta}{8\lambda^2}[|N_\theta|^2 + |N_\phi|^2] \tag{10}$$

and

$$W = \int_0^\pi \int_0^{2\pi} K \sin\theta \, d\theta \, d\phi \tag{11}$$

**Currents All in One Direction** If current in a radiating system flows all in one direction, this may be taken as the direction of the axis of a set of spherical coordinates. Vector **A** (hence **N**) can have a $z$ component only. Then

$$N_\phi = 0, \qquad N_\theta = -N_z \sin\theta$$
$$K = \frac{\eta}{8\lambda^2} |N_z|^2 \sin^2\theta \tag{12}$$

**Aximuthally Directed Currents** If all current in some radiating system is azimuthally directed about an axis, this axis may be taken as the axis of a set of spherical coordinates. Vector **A** (hence **N**) can have a $\phi$ component only. Then, if symmetric in $\phi$,

$$K = \frac{\eta}{8\lambda^2} |N_\phi|^2$$

and

$$W = 2\pi \int_0^\pi K \sin\theta \, d\theta \tag{13}$$

**Useful Relations for Spherical Coordinates** It sometimes may be desirable to calculate $N_\theta$ and $N_\phi$ from the Cartesian components $N_x$, $N_y$, $N_z$:

$$N_\theta = (N_x \cos\phi + N_y \sin\phi)\cos\theta - N_z \sin\theta$$
$$N_\phi = -N_x \sin\phi + N_y \cos\phi \tag{14}$$

The angle $\psi$ appearing in the equation for radiation vector (4) may be found as follows, if $\theta$, $\phi$ are the angular coordinates of the distant point $Q$, and $\theta'$, $\phi'$ are angular coordinates of the source point (see Fig. 12.4):

$$\cos\psi = \cos\theta\cos\theta' + \sin\theta\sin\theta'\cos(\phi - \phi') \tag{15}$$

## 12.5 Long Straight Wire Antenna: Half-Wave Dipole

We argued in Sec. 12.1 that a very thin biconical antenna could serve as a model for a thin-wire antenna. It can be considered as a biconical transmission line with a very strong discontinuity at the end. The current along it should be essentially the same as that on an open-circuited transmission line and therefore nearly zero at the ends. Also, the propagation constant along the line is the same as for plane waves, $k = \omega\sqrt{\mu\varepsilon}$.

The long dipole of Fig. 12.5*a* with voltage applied at its midpoint is shown with an assumed sinusoidal distribution of current. The standing wave has zero current at the

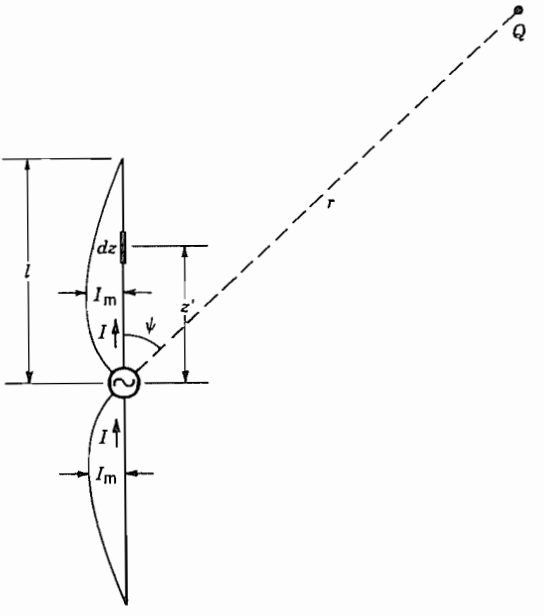


**FIG. 12.5a** Long straight wire antenna with assumed sinusoidal current distribution.

ends, and is selected with distance between zero and a maximum equal to a quarter free-space wavelength.

$$I = \begin{cases} I_m \sin[k(l - z)], & z > 0 \\ I_m \sin[k(l + z)], & z < 0 \end{cases} \tag{1}$$

The fields and power radiated at a great distance from the antenna can be calculated using the general method of the preceding section. Since all current is $z$-directed, **N** and **A** have only $z$ components also. In Eq. 12.4(4), the integral is converted to a line integral along the antenna wire with current density replaced by total current $I$ and $r'$ replaced by $z'$. Then since $\psi = \theta$ for all points along the wire,

$$\begin{aligned} \mathbf{N} &= \hat{\mathbf{z}} \int_{-l}^{l} I e^{jkz' \cos\theta}\, dz' \\ &= \hat{\mathbf{z}} \int_{-l}^{0} I_m \sin[k(l + z')] e^{jkz' \cos\theta}\, dz' \\ &\quad + \hat{\mathbf{z}} \int_{0}^{l} I_m \sin[k(l - z')] e^{jkz' \cos\theta}\, dz' \end{aligned} \tag{2}$$

Using the integral formula

$$\int e^{ax} \sin(bx + c)\, dx = \frac{e^{ax}}{a^2 + b^2} [a \sin(bx + c) - b \cos(bx + c)]$$

equation (2) becomes

$$\mathbf{N} = \hat{\mathbf{z}} \frac{2I_m}{k \sin^2 \theta} [\cos(kl \cos \theta) - \cos kl] \tag{3}$$

Since $N_\theta = -N_z \sin \theta$, Eq. 12.4(7) gives

$$E_\theta = \frac{j\eta I_m}{2\pi r} e^{-jkr} \left[ \frac{\cos(kl \cos \theta) - \cos kl}{\sin \theta} \right] \tag{4}$$

and $H_\phi = E_\theta/\eta$.

The radiation intensity is found from (3) and Eq. 12.4(12) to be

$$K = \frac{\eta I_m^2}{8\pi^2} \left[ \frac{\cos(kl \cos \theta) - \cos kl}{\sin \theta} \right]^2 \tag{5}$$

and the total power radiated is, from Eq. 12.4(11),

$$W = \frac{\eta I_m^2}{4\pi} \int_0^\pi \frac{[\cos(kl \cos \theta) - \cos kl]^2}{\sin \theta} d\theta \tag{6}$$

**Example 12.5**
THE HALF-WAVE DIPOLE

The most important special case of the long center-fed antenna is that of the *half-wave dipole* in which $l = \lambda/4$. Field intensity and radiation intensity, from (4) and (5), with $\eta$ for free space are, respectively,

$$|E_\theta| = \frac{60 I_m}{r} \left| \frac{\cos[(\pi/2) \cos \theta]}{\sin \theta} \right| \quad \text{V/m} \tag{7}$$

$$K = \frac{15 I_m^2}{\pi} \left\{ \frac{\cos[(\pi/2) \cos \theta]}{\sin \theta} \right\}^2 \quad \text{W/steradian} \tag{8}$$

The half-wave antenna is a nearly resonant structure with its maximum of current near the drive point. It is not exactly resonant for any finite wire radius because treatment of the wire antennas as an open-circuited uniform transmission line is only an approximation. The half-length for resonance and the terminal resistance at resonance for different antenna radii $a$ are given in Fig. 12.5*b*.[3]

[3] *R. S. Elliott, Antenna Theory and Design, p. 304, Prentice Hall, Englewood Cliffs, NJ, 1981.*

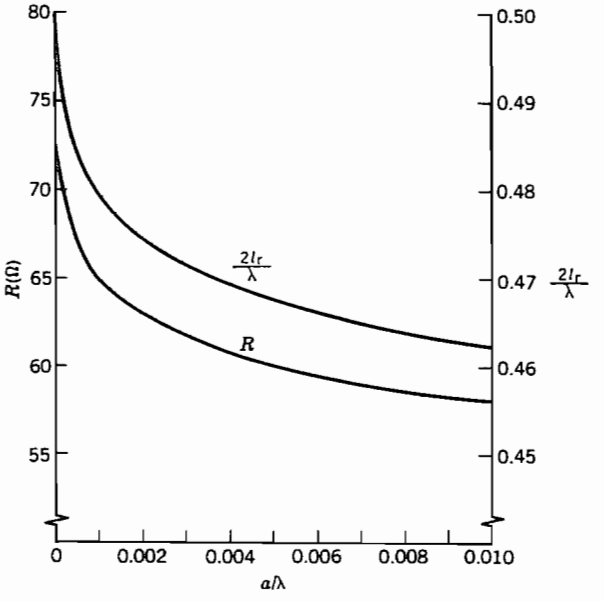


**FIG. 12.5*b*** Resonant length $2l_r$ and resistance at resonance for $\approx \lambda/2$ dipole as a function of radius of wire, normalized to wavelength. From R. S. Elliott, Antenna Theory and Design, © 1981, p. 304. Reprinted by permission of Prentice Hall, Englewoood Cliffs, NJ.

## 12.6 Radiation Patterns and Antenna Gain

We pointed out earlier that the purposes of an antenna are to make an impedance match between a waveguide or transmission line and free space and to send the energy in the desired direction. The methods of characterizing the directivity of antennas will be elaborated in this section.

Figure 12.6*a* shows a surface for which the distance from the origin to a given point on the surface is proportional to the radiation intensity in that direction from the antenna. The surface shown in Fig. 12.6*a* represents the half-wave dipole described by Eq. 12.5(8). The somewhat more complex pattern in Fig. 12.6*b* is for a dipole of length $3\lambda/2$ (Prob. 12.6c). Note that both of these patterns have symmetry about the $z$ axis

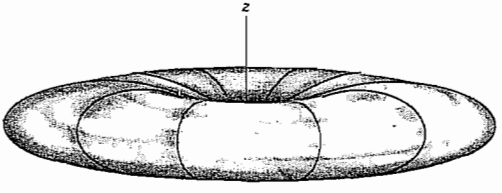


**FIG. 12.6*a*** Pattern of radiation intensity for a half-wave dipole.

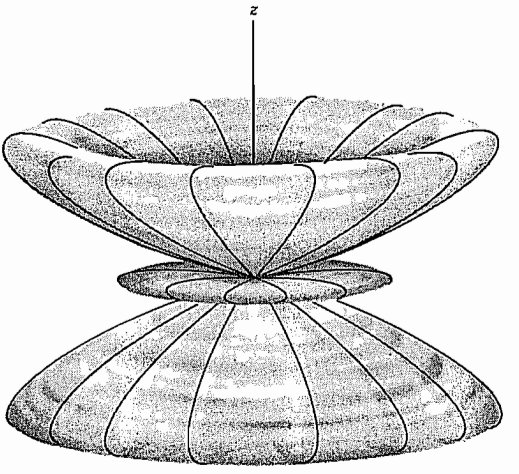


**FIG. 12.6b** Pattern of radiation intensity for a dipole of length $3\lambda/2$.

since current is all $z$ directed. Patterns of this type become quite complicated for asymmetric distributions.

Plots that are more easily made and read quantitatively are the intersections of surfaces like those in Figs. 12.6*a* and *b* with selected principal planes. Clearly, the intersections of planes perpendicular to the $z$ axis with those surfaces are circles, reflecting the symmetry about the $z$ axis. More interesting are the polar plots resulting from the intersection of the surface with a plane containing the $z$ axis. This is shown for the surface of radiation intensity for the half-wave dipole (Fig. 12.6*a*) in Fig. 12.6*c*. Similar plots are shown for the magnitudes of electric field $E_\theta$ for the half-wave dipole and the Hertzian electric dipole, Eq. 12.3(4).

From the patterns in Figs. 12.6*a–c*, it is evident that radiated fields are stronger in some directions than in others. We say then that this antenna has a certain *directivity* as compared with an imagined isotropic radiator which radiates equally in all directions. This is, of course, an advantage if we desire to have the signal radiated in the direction of the maximum, since there is less power required to produce a given field in the desired direction than there would be for the isotropic radiator.

The ratio of the radiation intensity $K(\theta, \phi)$ from an antenna in a given direction, to the uniform radiation intensity for an isotropic radiator with the same total radiation power $W$ is called the *directive gain*

$$g_d(\theta, \phi) = \frac{K(\theta, \phi)}{(W/4\pi)} \tag{1}$$

where the factor $4\pi$ is the number of steradians in a full sphere. The value of directive gain in the direction for which it has its maximum value is called the *directivity* $(g_d)_{max}$.

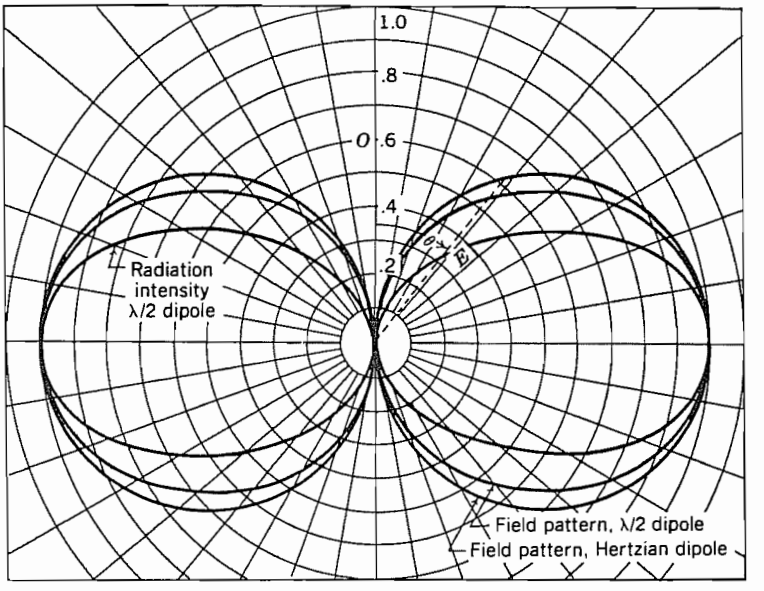


**FIG. 12.6*c*** Polar plots of field and radiation intensity for a half-wave dipole and of field for a Hertzian dipole in plane of dipole.

For example, the directive gain for the half-wave dipole in free space can be found from Eqs. 12.5(5) and 12.5(6):

$$g_d(\theta, \phi) = 1.64\left\{\frac{\cos[(\pi/2)\cos\theta]}{\sin\theta}\right\}^2 \tag{2}$$

which has its maximum at $\theta = \pi/2$, as is clear from Fig. 12.6*a* or *c*, so the directivity is 1.64.

It is interesting to note that a similar calculation for the Hertzian dipole using Eqs. 12.3(5) and 12.3(6) with $\theta = \pi/2$ yields a directivity of 1.5, a value not much different from that of the half-wave dipole. In later parts of this chapter, we will see other antennas, especially antenna arrays, that have much higher directivities.

Another characterizing property of an antenna is the *power gain* $g_p(\theta, \phi)$. For this quantity, the radiation intensity is divided by the uniform radiation intensity that would exist if the total power *supplied to the antenna* by the connected waveguide or transmission line were radiated isotropically:

$$g_p = \frac{K(\theta, \phi)}{W_T/4\pi} \tag{3}$$

Since the total supplied power $W_T$ is the sum of that radiated $W$ and the resistive losses $W_l$, then

$$g_p(\theta, \phi) = \frac{W}{W + W_l} g_d(\theta, \phi) \tag{4}$$

where the factor $W/(W + W_l)$ is called the *radiation efficiency* of the antenna. Although the directivity of a Hertzian dipole is almost equal to that of a half-wave dipole, as mentioned above, their radiation efficiencies are greatly different, even if they are of the same material. This is because the power radiated by the dipole varies as $l^2$ whereas the losses vary as $l$. (The Hertzian dipole, having uniform current, models end-loaded short dipoles.) A similar result obtains for unloaded short antennas with $I = 0$ at the end. For other antennas, radiation efficiency is near unity and there is little difference between directive gain and power gain.

For a given length in comparison with wavelength, antenna diameter also affects radiation pattern and directivity.[4]

## 12.7 Radiation Resistance

The input impedance of an antenna can be represented by a series frequency-dependent impedance $Z = R + jX$ and is of great importance for optimum matching into the antenna. Methods for calculating $R$ and $X$ for certain lossless antennas are discussed in Secs. 12.25 and 12.26. The resistive component, in general, is a measure of the sum of radiated power $W$ and ohmic losses $W_l$, as discussed in connection with power gain in the preceding section. It could be represented by two resistors in series, one for each component,

$$R_r = \frac{2W}{I^2} \tag{1}$$

where $I$ is the magnitude of the terminal current, and

$$R_l = \frac{2W_l}{I^2} \tag{2}$$

The quantity $R_r$ is called *radiation resistance*; for a small dipole current element, it can be found from (1) and Eq. 12.3(6) to be

$$R_r = 80\pi^2\left(\frac{l}{\lambda}\right)^2 \quad \Omega \tag{3}$$

where we use $l$ in place of $h$ for the length. The power loss in the same element is $W_l = \frac{1}{2}\,\mathrm{R_s}|J_s|^2A$ where $J_s = I/2\pi a$, $A$ is the surface area of the wire, $a$ is its radius, and $R_s$ is surface resistance.

$$W_l = \frac{R_s l}{4\pi a} I^2 \tag{4}$$

and

$$R_l = \frac{lR_s}{2\pi a} \tag{5}$$

[4] *J. D. Kraus, Antennas, 2nd ed., Sec. 9–10, McGraw-Hill, New York, 1988.*

Then the efficiency is

$$\frac{W}{W + W_l} = \frac{R_r}{R_r + R_l} = \frac{80(l/\lambda)}{80(l/\lambda) + (\lambda R_s/2\pi^3 a)} \tag{6}$$

Thus, it can be seen that the efficiency decreases as the length $l$ decreases, becoming proportional to $l/\lambda$ in the limit.

For an antenna with $l \ll \lambda$ and no end loading, the current decreases linearly from the source to the end (linear portion of the sinusoidal distribution in Fig. 12.5*a*). In this case the average $I^2$ along the antenna is one-quarter the terminal value $I_m^2$ so the radiated power is also one-quarter the value in the uniform-current case and radiation resistance is

$$R_r = \frac{2W}{I_m^2} = 20\pi^2\left(\frac{l}{\lambda}\right)^2 \tag{7}$$

The average losses are also one-quarter those of the uniform-current case so the conclusion about efficiency is again that it is proportional to the length of the element.

The radiation resistance of a lossless filamentary half-wave dipole can be found using Eq. 12.5(6)

$$R_r = \frac{2W}{I_m^2} = \frac{\eta}{2\pi}\int_0^{\pi} \frac{\cos^2((\pi/2)\cos\theta)}{\sin\theta}\, d\theta \tag{8}$$

which can be shown (Prob. 12.7b) to have the value

$$R_r = 73.09\ \Omega \tag{9}$$

It is seen in Fig. 12.5*b* that this equals the terminal resistance of the half-wave dipole as wire radius goes to zero.

Radiation resistance of the small loop antenna was derived in Eq. 4.12(6) by the induced emf method and may be checked by using a Poynting integration from the fields of Eqs. 12.3(8). It may be written

$$R_r = 20\pi^2\left(\frac{\text{circumference}}{\lambda}\right)^4 \tag{10}$$

## 12.8 Antennas Above Earth or Conducting Plane

Many antennas are placed near plane conductors. If the latter are large enough to be considered effectively infinite, and of high enough conductivity to be considered perfect conductors, it is possible to account for the conductor by imaging the antenna in it. For example, given a single cone with axis vertical above a perfectly conducting plane (Fig. 12.8*a*), the boundary condition of zero electric field tangential to the plane may be satisfied by removing the plane and utilizing a second cone as an image of the first.

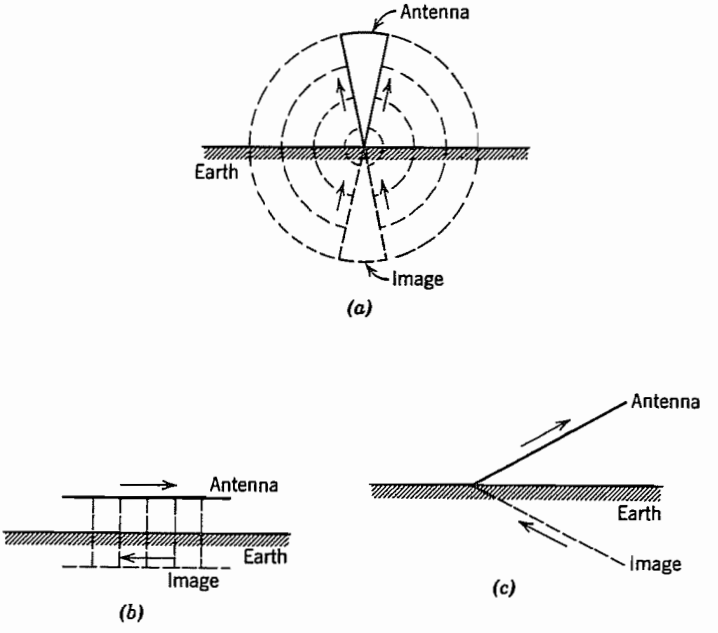


**FIG. 12.8** (*a*) Cone above plane conducting earth and image cone. (*b*) Horizontal wire above plane conducting earth and image wire. (*c*) Inclined wire above plane conducting earth and image wire.

The problem then reduces to that of the biconical antenna discussed in Sec. 12.1. Note that current is in the *same vertical* direction at any instant in the two cones. Given a single wire above a plane conductor and parallel to it, as in Fig. 12.8*b*, our knowledge of symmetry in the transmission-line problem tells us that the condition of electric field lines normal to the earth is met by removing the plane and placing the image with current in the *opposite horizontal direction.* Generalizing from these two cases, we see that current direction in the image will be selected so that vertical components are in the same direction and horizontal components in opposite directions at any instant. An example is shown in Fig. 12.8*c*.

The technique of replacing the conducting plane by the antenna image, of course, gives the proper value of field only above the plane. The proper value below the perfectly conducting plane should be zero. For example, given a long straight vertical antenna above a plane conductor, excited at the base, the image reduces the problem to that solved in Sec. 12.5. Field strength for maximum current $I_m$ in the antenna is given exactly by Eq. 12.5(4) for all points above the earth ($0 < \theta < \pi/2$), but is zero for all points below ($\pi/2 < \theta < \pi$). Thus, for power integration, the integral of Eq. 12.5(5) extends only from 0 to $\pi/2$, and the power radiated is just half that for the

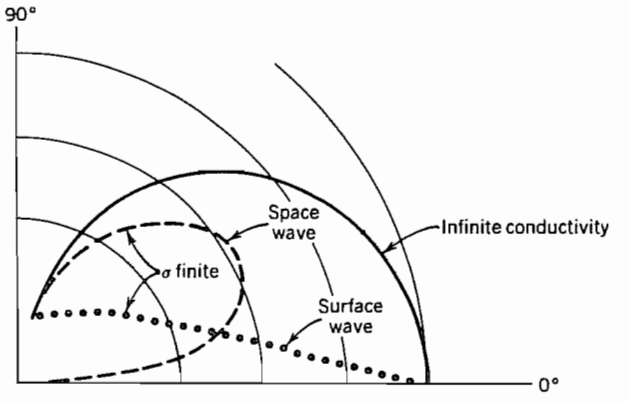


**FIG. 12.8*d*** Radiation pattern for field $E_\theta$ for infinitesimal vertical electric dipole over planes of finite conductivity and infinite conductivity. From E. C. Jordan and K. G. Balmain, *Electromagnetic Waves and Radiating Systems*, 2nd ed., Fig. 16.7. Prentice Hall, Englewood Cliffs, NJ, 1968.

corresponding complete dipole:

$$W = \frac{\eta I_m^2}{4\pi} \int_0^{\pi/2} \frac{[\cos(kl \cos \theta) - \cos kl]^2}{\sin \theta} d\theta \quad \text{W}$$

Calculations of radiation from antennas above an imperfectly conducting earth are much more complicated. The radiation from an electric dipole over a plane, finite-conductivity earth has been calculated. The fields are conveniently divided into a *space wave* and a *surface wave*. The space wave fields decay as $1/r$ and the surface wave fields as $1/r^2$ so the important one at large distances is the space wave. As an example, consider the fields of an Hertzian dipole vertically oriented and at the level of a finite-conductivity earth. The electric field for the case of infinitely conducting earth is shown by the solid line for reference in Fig. 12.8*d*. The space-wave field magnitude ($1/r$ dependence) for a frequency at which the conduction current and displacement current in the earth are equal (typically, 5 MHz) is indicated by the dashed line. The surface wave component of the electric field is shown by the dotted line; it decays as $1/r^2$. Each component is separately normalized; their relative magnitudes depend on the distance from the antenna because of the different dependences on $r$. An important conclusion is that the space wave fields are greatly reduced for angles near the surface of the earth of finite conductivity.[5] Other properties of the real earth, such as curvature and the presence of the troposphere or ionosphere, are important in some frequency ranges and add still more complication.[6]

[5] *E. C. Jordan and K. G. Balmain,* Electromagnetic Waves and Radiating Systems, *2nd ed., Fig. 16.7, Prentice Hall, Englewood Cliffs, NJ, 1968.*

[6] *R. E. Collin,* Antennas and Radiowave Propagation, *McGraw-Hill, New York, 1985.*

## 12.9 TRAVELING WAVE ON A STRAIGHT WIRE

Some important types of antennas involve traveling waves of current rather than the standing waves seen in Sec. 12.5. As preparation, we consider the radiation from a traveling wave of current on an isolated wire. Let us consider a straight wire extending from $z = 0$ to $z = l$, excited by a single traveling wave of current, assumed to be unattenuated and with phase velocity equal to $1/\sqrt{\mu\varepsilon}$ (Fig. 12.9*a*). Since all current is in the $z$ direction, the radiation vector of Eq. 12.4(4) has only a $z$ component. The special forms of Eqs. 12.4(12) then apply:

$$N_z = I_0 \int_0^l e^{-jkz'} e^{jkz' \cos\theta} dz'$$

$$= \frac{I_0[1 - e^{-jkl(1-\cos\theta)}]}{jk(1 - \cos\theta)}$$

$$|N_z| = \frac{2I_0 \sin[(kl/2)(1 - \cos\theta)]}{k(1 - \cos\theta)} \tag{1}$$

$$K = \frac{\eta|N_z|^2}{8\lambda^2} \sin^2\theta = \frac{I_0^2\eta}{2\lambda^2} \frac{\sin^2[(kl/2)(1 - \cos\theta)]}{k^2(1 - \cos\theta)^2} \sin^2\theta \tag{2}$$

In addition, since there is symmetry about the axis,

$$W = 2\pi \int_0^\pi K \sin\theta \, d\theta = 2\pi \int_0^\pi \frac{I_0^2\eta}{2\lambda^2} \frac{\sin^2[(kl/2)(1 - \cos\theta)]}{k^2(1 - \cos\theta)^2} \sin^3\theta \, d\theta$$

$$W = 30I_0^2 \int_0^\pi \frac{\sin^3\theta \sin^2[(kl/2)(1 - \cos\theta)]}{(1 - \cos\theta)^2} d\theta$$

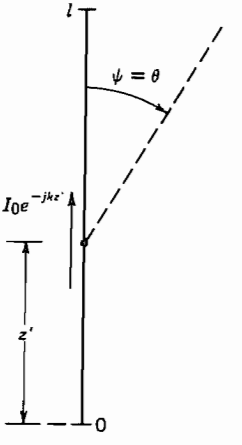


**FIG. 12.9*a*** Thin wire of length $l$ supporting a progressive wave.

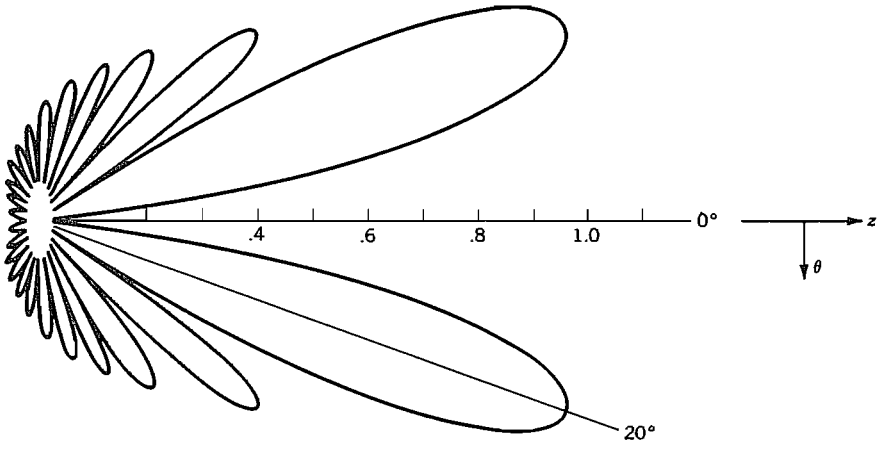


**FIG. 12.9b** Radiation pattern ($E_\theta$) of a traveling wave antenna six wavelengths long. After E. C. Jordan and K. G. Balmain, *Electromagnetic Waves and Radiating Systems*, 2nd ed., p. 357. Prentice-Hall, Englewood Cliffs, NJ, 1968.

If the foregoing integral is evaluated,[7]

$$W = 30I_0^2\left[1.415 + \ln\frac{kl}{\pi} - \text{Ci}(2kl) + \frac{\sin 2kl}{2kl}\right] \tag{3}$$

where

$$\text{Ci}(x) = -\int_x^\infty \frac{\cos x}{x}\,dx$$

This single traveling wave might be expected to produce a maximum of radiation in the direction of propagation. Actually the radiation is zero at $\theta = 0$, as seen from (2), but only because the radiation from each element of current is zero in that direction. A complete radiation pattern of a traveling wave wire radiator six wavelengths long is shown in Fig. 12.9*b*, where it is clear that the lobes near $\theta = 0$ are largest and those near $\theta = \pi$ are smallest.

It should be pointed out that a single traveling wave wire does not make a very desirable antenna because of the large amount of energy in the side lobes. The V-type and rhombic antennas discussed in the following section combine traveling wave wire lines in advantageous ways.

## 12.10 V AND RHOMBIC ANTENNAS

In this section we will study two kinds of antenna, V and rhombic, based on the radiation from a traveling wave given in the preceding section. If the wires of the V are terminated

[7] *J. A. Stratton, Electromagnetic Theory, p. 445, McGraw-Hill, New York, 1941.*

in an appropriate resistance (e.g., by connection of the ends of the V through resistors to ground), there will be a negligible reflected wave. The results of the preceding section can then be used. For example, if two wires carrying traveling wave currents are oriented in a V with an angle between them equal to twice the angular displacement of the main lobe from the wire, the result is a unidirectional pattern, with a maximum in the plane normal to that of the V and containing its bisector. The maximum would also be in the plane of the V if the effect of the ground were not significant; the effect of the image in a perfectly conducting ground is discussed at the end of this section.

We can make a direct calculation of the radiation from the two arms of the V being driven from point 0 in Fig. 12.10*a*, assuming the ends at $C$ and $D$ are matched so there are only waves traveling away from 0. We also neglect, for now, the effect of the earth. The analysis is based on the radiation of a single wire given in the preceding section. The currents in the two arms are in different directions so addition of the effects is by orthogonal components.

The radiation vector for a single wire, with energy traveling at the velocity of light in only one direction, has only the direction of the wire. From 12.9(1),

$$N_s = \frac{I_0[1 - e^{-jkl(1-\cos\psi)}]}{jk(1 - \cos\psi)} = \frac{I_0}{jk} f(\psi) \tag{1}$$

The subscript $s$ denotes the direction of the wire, and $\psi$ is the angle between the wire and the radius vector to the distant point $(r, \theta, \phi)$ at which the radiation field quantities are desired. The angles for the elements, in terms of the coordinates in Fig. 12.10*a*, are

$$\begin{aligned} \cos\psi_{OC} &= \sin\theta\cos(\phi + \alpha) \\ \cos\psi_{OD} &= \sin\theta\cos(\phi - \alpha) \end{aligned} \tag{2}$$

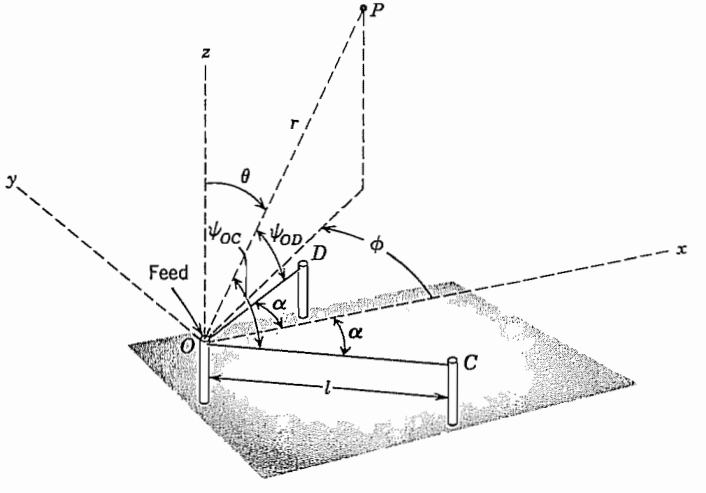


**Fig. 12.10*a*** Coordinates for calculation of radiation from a traveling wave V-type antenna.

The currents at $O$ for $OC$ and $OD$ are 180 degrees out of phase; they may be taken as $I_0$ and $-I_0$, respectively. Components of the radiation vectors of the two wires may be added:

$$N_x = \frac{I_0}{jk} \cos \alpha[f(\psi_{OC}) - f(\psi_{OD})] \tag{3}$$

$$N_y = -\frac{I_0}{jk} \sin \alpha[f(\psi_{OC}) + f(\psi_{OD})] \tag{4}$$

To simplify expressions, we define

$$A \equiv f(\psi_{OC}), \qquad B \equiv f(\psi_{OD}) \tag{5}$$

The components of the radiation vector in spherical coordinates may be written in terms of the Cartesian components $N_x$ and $N_y$ from Eq. 12.4(14):

$$N_\theta = \frac{I_0}{jk} [A \cos(\alpha + \phi) - B \cos(\alpha - \phi)] \cos \theta \tag{6}$$

$$N_\phi = \frac{I_0}{jk} [-A \sin(\phi + \alpha) + B \sin(\phi - \alpha)] \tag{7}$$

Then the radiation intensity [Eq. 12.4(10)] is

$$\begin{aligned} K &= \frac{\eta}{8\lambda^2} [|N_\theta|^2 + |N_\phi|^2] \\ &= \frac{\eta I_0^2}{32\pi^2} \{|A \cos(\alpha + \phi) - B \cos(\alpha - \phi)|^2 \cos^2 \theta \\ &\quad + |-A \sin(\phi + \alpha) + B \sin(\phi - \alpha)|^2\} \end{aligned} \tag{8}$$

Figure 12.10*b* shows the radiation intensity pattern in the plane of the V for a structure with arm lengths of $6\lambda$ and an angle of 32 degrees between arms.[8]

If the V antenna described here is located above earth, as would be required for installing terminating resistors, the effect of the earth must be taken into account. Assuming the earth to be plane and perfectly conducting, the image effect can be accounted for by using the results to be worked out in Prob. 12.10a. The total radiation intensity $K_T$ is

$$K_T = 4K \sin^2(kh \cos \theta) \tag{9}$$

where $K$ is the radiation intensity of a single V given by (8) and $h$ is the height of the antenna above the earth. Although derived for a special case, (9) is a general relation for horizontal antennas above a perfectly conducting earth.

A similar analysis is used for the *rhombic antenna*, which consists of two oppositely directed V antennas with the ends of their arms joined as in Fig. 12.10*c*. It can be

[8] *W. L. Stutzman and G. A. Thiele,* Antenna Theory and Design, *p. 242, Wiley, New York, 1981.*

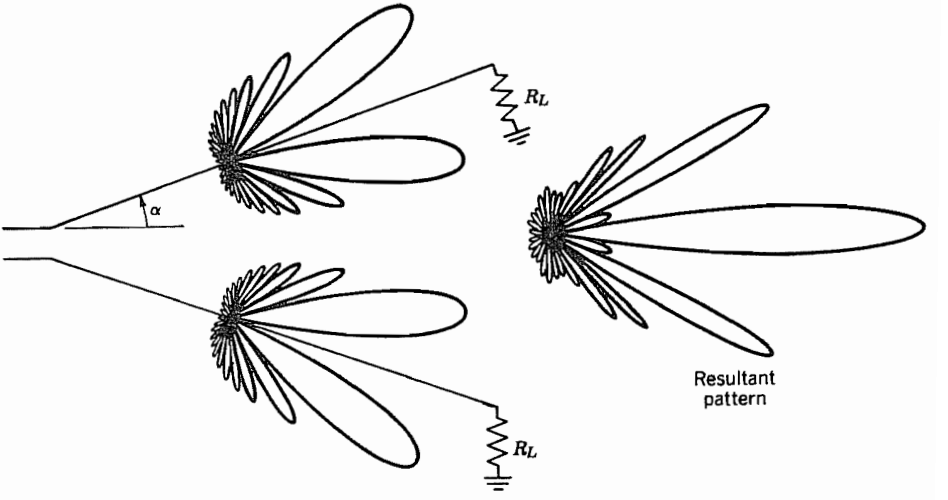


**FIG. 12.10*b*** Radiation intensity pattern for an isolated V antenna with arm lengths of 6λ and 32 degrees between arms. From W. L. Stuzman and G. A Thiele, *Antenna Theory and Design*, p. 242. Reprinted by permission. © John Wiley and Sons, 1981, New York.

demonstrated that the V-type antenna has the same pattern (in the direction of the traveling waves) for either direction of use (Prob. 12.10b) so the radiations from the two V's reinforce each other. Alternatively, the analysis given above can be extended to treat the rhombic antenna. The termination impedance is attached to the apex of the rhombus opposite from the drive point. Operation can be over about a 2:1 frequency range without large changes in the performance. Typical lengths of the arms are 2–7 wavelengths and the rhombus is usually located 1–2 wavelengths above the earth. The acute angles $2\alpha$ are typically 35–60 degrees.

The form of the radiation pattern can be altered significantly by changing the angle $\alpha$ and the lengths of the arms. Moreover, for antennas used with long-distance communication, it is desired to have the beam make a certain angle with the earth for optimum reflection from the ionosphere. This is adjusted by the distance of antenna above earth and calculated for ideal earth as for the V antenna, using (9). Figures 12.10*d* and *e* show, respectively, the calculated pattern in a vertical plane containing the $x$ axis

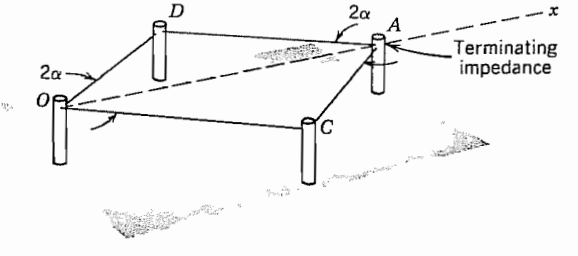


**FIG. 12.10*c*** Rhombic antenna.

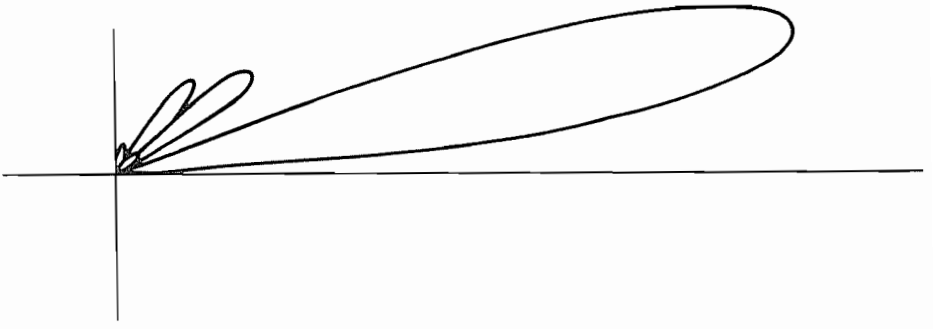

(d)

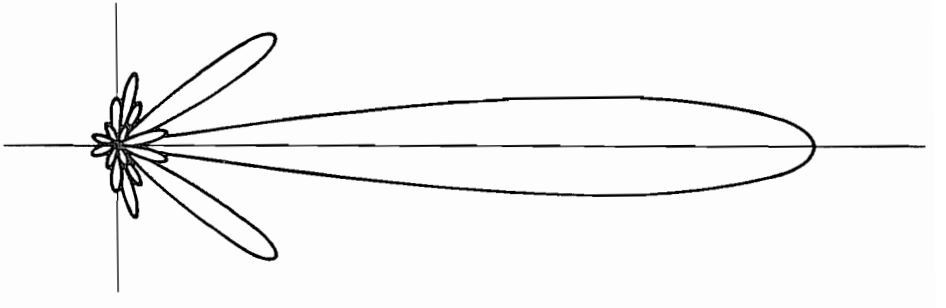

(e)

**FIG. 12.10** (*d*) Radiation intensity pattern in the vertical plane containing the $x$ axis for a typical rhombic antenna (*c*) over a perfectly conducting earth. (*e*) Radiation intensity pattern in the azimuthal plane containing the maximum intensity for the antenna of (*c*). From J. D. Kraus, *Antennas*, 2nd ed., p. 504. © McGraw-Hill, 1988, New York.

and the pattern in an azimuthal plane tilted 10 degrees above the $x$ axis. The arms of the rhombus are $6\lambda$ long, $\alpha = 20$ degrees, and the rhombus is $1.1\lambda$ above the earth,[9] which is assumed perfectly conducting.

## 12.11 METHODS OF FEEDING WIRE ANTENNAS

In this section we consider three aspects of the problem of driving wire antennas. The simplest excitation problem is that of the wire perpendicular to a conducting plane. Another common situation is the feeding of an isolated dipole by a balanced two-wire transmission line, where special techniques must be used to achieve a satisfactory impedance match. Finally, we discuss circuit arrangements to permit the feeding of an antenna, which is balanced with respect to ground, by a transmission line having one side at ground potential (usually the outer conductor of a coaxial line).

[9] *E. A. Laport, in* Antenna Engineering Handbook, *(R. C. Johnson and H. Jasik, Eds.), 2nd ed., McGraw-Hill, New York, 1984.*

**Monopole Perpendicular to a Conducting Plane** Consider first a wire monopole that is effectively an extension of the inner conductor of a coaxial drive line, whose outer conductor is connected to an infinite ground plane, as shown in Fig. 12.11*a*. The load on the coaxial line is resistive when the antenna is resonant. With $l \cong \lambda/4$ the resonant resistance is about 37.5 Ω, with only weak deviations caused by changes of the gap between inner and outer coaxial conductors at the connection to the ground plane.[10] To make the line impedance also 37.5 Ω, the radius ratio should be $b/a = 1.868$ for air dielectric. With available experimental data on the admittance of such structures, it can be deduced that the antenna will have an impedance that is purely resistive and of value ≈ 36.8 Ω at resonance if the radius and length of the antenna are given by $a/\lambda = 0.00159$ and $l/\lambda = 0.236$. Thus, for an antenna operating at 100 MHz, the diameter and length should be 0.95 cm and 0.71 m, respectively. The power reflected at the feed point with this design is less than 0.01%.

**Folded Dipole** Antennas for television and FM broadcast applications are commonly coupled to a two-wire balanced transmission line. Such lines typically have characteristic impedances of 300–600 Ω. If such a line were to drive a half-wave dipole, which has a characteristic impedance on the order of 75 Ω, a serious mismatch would exist. A folded dipole one-half wavelength long with parallel conductors of the same diameter, shorted at the ends as shown in Fig.12.11*b*, has a characteristic impedance four times that of the single half-wave dipole for a mode with currents in the parallel wires in the same direction. The currents are of equal magnitude and in the same direction in the two closely spaced equal-diameter wires. If a terminal current $I_t$ is supplied, the effective radiating current is $2I_t$, so the power is four times that of the single half-wave dipole with current $I_t$. At resonance, the power is related to the input resistance $R$ as $P = \frac{1}{2}I_t^2R$ so the four-fold increase of power for a given $I_t$ implies that $R$ is four times that of the half-wave dipole, or about 300 Ω. If another equal-diameter shorted wire is added in parallel to the folded dipole in Fig. 12.11*b*, the resonant input impedance for the mode with parallel currents in the same direction becomes nine times that of the single half-wave dipole. Another advantage of the folded dipole is that its

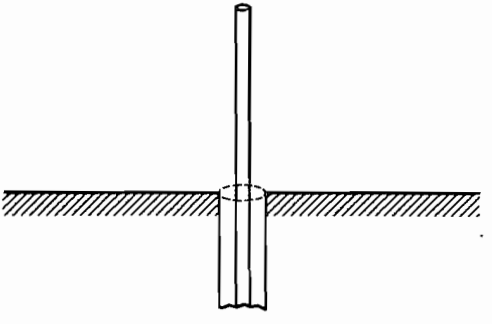

**FIG. 12.11*a*** Coaxial line feeding a monopole through a ground plane.

[10] *R. S. Elliott,* Antenna Theory and Design, *pp. 352–355, Prentice Hall, Englewood Cliffs, NJ, 1981.*

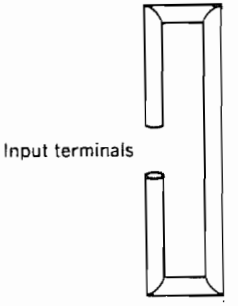


**FIG. 12.11*b*** Folded-dipole antenna.

input impedance is acceptably constant over a larger frequency range than is that of the single dipole. There are many derived forms of the folded dipole giving a wide range of impedances.[11]

**Baluns** An isolated dipole or one oriented parallel to a ground plane is balanced with respect to ground. To avoid unbalancing the antenna, it should be fed by a balanced line, such as a two-wire line. For some situations (for frequencies higher than about 200 MHz or for a dipole mounted parallel to a ground plane), it is preferred to drive the antenna by a coaxial line rather than a two-wire line. Since the outer conductor of the coaxial line is grounded, its direct connection to a balanced dipole would lead to a distortion of the radiation pattern. The connection arrangement that avoids unbalancing a dipole is called a *balun*, a contraction for *balanced/unbalanced*. Baluns take a variety of forms; one is shown in Fig. 12.11*c* for a dipole parallel to a ground plane. At the feed point (marked *F*) the coaxial line drives the dipole and, in parallel electrically, a

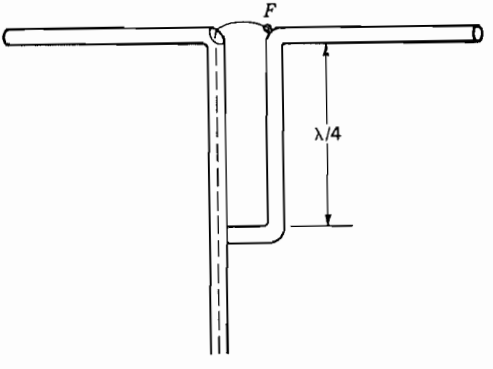


**FIG. 12.11*c*** One type of balun used for feeding a balanced antenna from an unbalanced transmission line (coaxial line in this case). From Edward C. Jordan, Keith G. Balmain, *Electromagnetic Waves and Radiating Systems*, 2nd ed. © 1968, p. 406. Reprinted by permission of Prentice Hall, Englewood Cliffs, NJ.

[11] *J. D. Kraus, Antennas, 2nd ed., Sec. 11–19, McGraw-Hill, New York, 1988.*

two-wire transmission line consisting of its own outer conductor and the parallel support for the dipole. By making the distance to the shorting termination $\lambda/4$, the impedance of the two-wire line, as seen at the drive point, is infinite, so the dipole has equal currents in its two arms and is thus balanced with respect to ground. More complicated matching circuits[12] may be necessary to maintain matching over the bandwidth of broadband systems.

## Radiation from Fields Over an Aperture

### 12.12 Fields as Sources of Radiation

For wire antennas, it is fairly natural to assume a current distribution over the antenna and to consider the current elements as the sources of radiation. For other antennas, such as the electromagnetic horn, slot antennas, parabolic reflectors, lens directors, and all optical systems, it is more natural to think in terms of the fields as sources. The Huygens principle states that any wavefront can be considered the source of secondary waves that add to produce distant wavefronts. Thus the knowledge (or assumption) of field distribution over an aperture should yield the distant field. We wish now to make a quantitative statement of this general principle. There are several possible approaches, but we shall start with one that considers the fields as arising from equivalent current sheets in the aperture. This approach provides good physical pictures and builds directly on the formulations already developed in this chapter.

Consider the aperture in a plane (Fig. 12.12) with sources to the left and the field desired in the region to the right. For present purposes the plane may be considered absorbing, so that it has no fields or currents except in the aperture. The exact boundary value problem can be solved in only a few cases, but it is often possible to make a reasonable estimate of the aperture fields, just as was done for antenna currents in the radiators considered previously. We thus assume that tangential components of fields $E_t(x', y')$ and $H_t(x', y')$ are known in the aperture. Although these fields arise from sources to the left, they may be considered to be produced by equivalent sources located in the aperture plane. In particular, we have seen on many occasions that the relation between tangential magnetic field and a surface current is

$$\mathbf{J}_s = \hat{\mathbf{n}} \times \mathbf{H} \tag{1}$$

[12] *D. F. Bowman, in* Antenna Engineering Handbook *(R. C. Johnson and H. Jasik, Eds.), 2nd ed., McGraw-Hill, New York, 1984.*

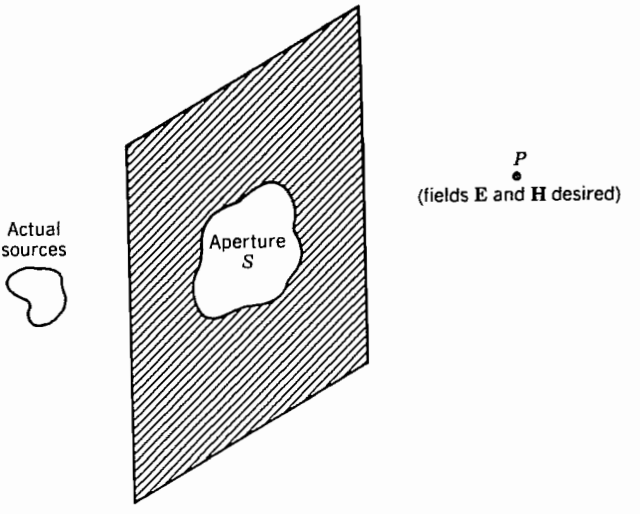


**FIG. 12.12** Radiation through an aperture.

Similarly the tangential electric field can be related to a term which we can interpret as a surface magnetic current $\mathbf{M}_s$:

$$\mathbf{M}_s = -\hat{\mathbf{n}} \times \mathbf{E} \tag{2}$$

Note that (1) and (2) individually assume that the tangential fields $H_t$ and $E_t$ on the left side of the aperture plane are zero. Jointly, $\mathbf{J}_s$ and $\mathbf{M}_s$ produce fields that satisfy that assumption while producing the required fields on the right side. Whether or not true magnetic charges and currents are found in nature, the concept of such equivalent sources is a useful one in a variety of circumstances including this one. Maxwell's equations, augmented by magnetic charge density $\rho_m$ and magnetic current density $\mathbf{M}$, become

$$\begin{aligned} \nabla \cdot \mathbf{D} &= \rho_e \\ \nabla \cdot \mathbf{B} &= \rho_m \\ \nabla \times \mathbf{E} &= -\mathbf{M} - \frac{\partial \mathbf{B}}{\partial t} \\ \nabla \times \mathbf{H} &= \mathbf{J} + \frac{\partial \mathbf{D}}{\partial t} \end{aligned} \tag{3}$$

A second retarded potential $\mathbf{F}$ can be defined in terms of the magnetic sources as $\mathbf{A}$ was related to electric sources. For a homogeneous isotropic medium, the relations in terms of surface currents are

$$\mathbf{A} = \mu \int_{S'} \frac{\mathbf{J}_s e^{-jkr}}{4\pi r} dS', \qquad \mathbf{F} = \varepsilon \int_{S'} \frac{\mathbf{M}_s e^{-jkr}}{4\pi r} dS' \tag{4}$$

and the fields in terms of these potentials are

$$\mathbf{E} = -j\omega\mathbf{A} - \frac{j\omega}{k^2}\nabla(\nabla \cdot \mathbf{A}) - \frac{1}{\varepsilon}\nabla \times \mathbf{F} \tag{5}$$

$$\mathbf{H} = -j\omega\mathbf{F} - \frac{j\omega}{k^2}\nabla(\nabla \cdot \mathbf{F}) + \frac{1}{\mu}\nabla \times \mathbf{A} \tag{6}$$

To calculate fields at any point in the region to the right, the actual sources in the left-hand region are replaced by equivalent sources in the aperture defined by (1) and (2) and the calculation made through the set (4) to (6). If the plane is conducting and not absorbing, any actual currents flowing on the right side of the plane must be added in the calculation of **A** in addition to the equivalent sources in the aperture, although this correction is often negligible.

If we are concerned only with the radiation field, the usual approximations appropriate to great distances can be employed, and the general formulation of Sec. 12.4 extended. A magnetic radiation vector **L** may be related to vector potential **F** as **N** was to **A**. Thus, consistent with the assumptions listed previously

$$\mathbf{A} = \mu\frac{e^{-jkr}}{4\pi r}\mathbf{N}, \qquad \mathbf{F} = \varepsilon\frac{e^{-jkr}}{4\pi r}\mathbf{L} \tag{7}$$

where

$$\mathbf{N} = \int_{S'} \mathbf{J}_s e^{jkr' \cos\psi}\, dS', \qquad \mathbf{L} = \int_{S'} \mathbf{M}_s e^{jkr' \cos\psi}\, dS' \tag{8}$$

Here $r'$ and $\psi$ are as defined in Sec. 12.4.

If electric and magnetic field components are now written in the usual way in terms of these two vector potentials, the only components not decreasing faster than $(1/r)$ are

$$E_\theta = \eta H_\phi = -j\frac{e^{-jkr}}{2\lambda r}(\eta N_\theta + L_\phi) \tag{9}$$

$$E_\phi = -\eta H_\theta = j\frac{e^{-jkr}}{2\lambda r}(-\eta N_\phi + L_\theta) \tag{10}$$

So the radiation intensity, or power per unit solid angle, is

$$K = \frac{\eta}{8\lambda^2}\left[\left|N_\theta + \frac{L_\phi}{\eta}\right|^2 + \left|N_\phi - \frac{L_\theta}{\eta}\right|^2\right] \tag{11}$$

In optics, this far-zone field is called the region of *Fraunhofer diffraction*. For the near zone, or region of *Fresnel diffraction*, better approximations to $r$ are necessary.[13]

One does not need to use the concept of magnetic currents explicitly since the expressions (1) and (2) may be substituted in (4) and then one works with the aperture fields

[13] *M. Born and E. Wolf,* Principles of Optics, *6th ed., p. 660, Pergamon Press, Oxford, 1980.*

directly. In fact Stratton and Chu derived such expressions by direct integration of the field equations.[14] For many purposes, however, the physical pictures inherent in the formulation with magnetic currents is helpful, because of the duality with fields from electric currents.

## 12.13 Plane Wave Sources

The radiation vector and radiation intensity may be calculated for a differential surface element on a uniform plane wave. Such an element might be considered the elemental radiating source in radiation calculations from field distributions, as was the differential current element for radiation calculations from current distributions.

The plane wave source, that is, one that produces **E** and **H** of constant direction, normal to each other, and in the ratio of magnitudes $\eta$ over the area of interest may be replaced by equivalent electric and magnetic current sheets over that area (Fig. 12.13*a*).

If

$$\mathbf{E} = \hat{\mathbf{x}}E_{x0}, \qquad \mathbf{H} = \hat{\mathbf{y}}H_{y0} = \frac{\hat{\mathbf{y}}E_{x0}}{\eta} \tag{1}$$

the equivalent current sheets are

$$J_x = -H_{y0} = -E_{x0}/\eta, \qquad M_y = -E_{x0} \tag{2}$$

If this is a source of infinitesimal area $dS$ (actually it need only be small compared with wavelength for the following results to hold true), the radiation vectors **N** and **L** given by Eq. 12.12(8) are

$$N_x = -\frac{E_{x0}\,dS}{\eta}, \qquad L_y = -E_{x0}\,dS$$

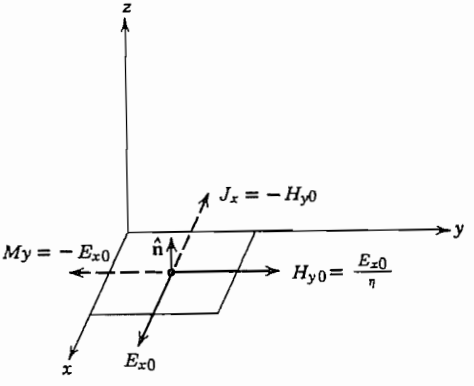


**Fig. 12.13*a*** Small plane-wave source and equivalent current sheets.

[14] *J. A. Stratton,* Electromagnetic Theory, *Sec. 8.14, McGraw-Hill, New York, 1941.*

since the source element is at the origin of coordinates. The components in spherical coordinates are from Eq. 12.4(14),

$$\begin{aligned} N_\theta &= -\frac{E_{x0}\, dS}{\eta} \cos\phi \cos\theta, \qquad N_\phi = \frac{E_{x0}\, dS}{\eta} \sin\phi \\ L_\theta &= -E_{x0}\, dS \sin\phi \cos\theta, \qquad L_\phi = -E_{x0}\, dS \cos\phi \end{aligned} \tag{3}$$

from which far-zone fields, by Eqs. 12.12(9) and (10), are

$$E_\theta = \frac{jE_{x0}\, dS\, e^{-jkr}}{2\lambda r} (1 + \cos\theta) \cos\phi \tag{4}$$

$$E_\phi = -j \frac{E_{x0}\, dS\, e^{-jkr}}{2\lambda r} (1 + \cos\theta) \sin\phi \tag{5}$$

and radiation intensity, by Eq. 12.12(11), is

$$\begin{aligned} K &= \frac{E_{x0}^2 (dS)^2}{8\eta\lambda^2} [(-\cos\phi \cos\theta - \cos\phi)^2 + (\sin\phi + \sin\phi \cos\theta)^2] \\ K &= \frac{E_{x0}^2 (dS)^2}{2\eta\lambda^2} \cos^4 \frac{\theta}{2} \end{aligned} \tag{6}$$

**Paraxial Approximation for Large Apertures** In most cases of radiation from large apertures and horns, we are interested in small values of $\theta$ (*paraxial approximation*) so that $\cos\theta$ may be replaced by unity. Let us also convert to rectangular components in the radiation field:

$$E_x = E_\theta \cos\theta \cos\phi - E_\phi \sin\phi \approx E_\theta \cos\phi - E_\phi \sin\phi \tag{7}$$

$$E_y = E_\theta \cos\theta \sin\phi + E_\phi \cos\phi \approx E_\theta \sin\phi + E_\phi \cos\phi \tag{8}$$

Substituting (4) and (5) with $\cos\theta = 1$,

$$E_x \approx j \frac{E_{x0}\, dS\, e^{-jkr}}{\lambda r}, \qquad E_y \approx 0 \tag{9}$$

Thus in the paraxial approximation, the radiation field is in the direction of the source field and we may drop the subscript on $E$. To integrate over the aperture shown in Fig. 12.13*b*, we must first adapt the above results to an element at an arbitrary location $x'$, $y'$ in the aperture. This can be done using Eqs. 12.12(8) but a direct approach is more convenient here. Within the paraxial approximation, (9) gives the field produced by the element at $x'$, $y'$ if $E_{x0}$ is replaced by $E(x', y')$ and $r$ by $r''$. Now integrating over the given aperture distribution,

$$E(x, y, z) = \frac{j}{\lambda} \int_{S'} \frac{E(x', y') e^{-jkr''}}{r''} dx'\, dy' \tag{10}$$

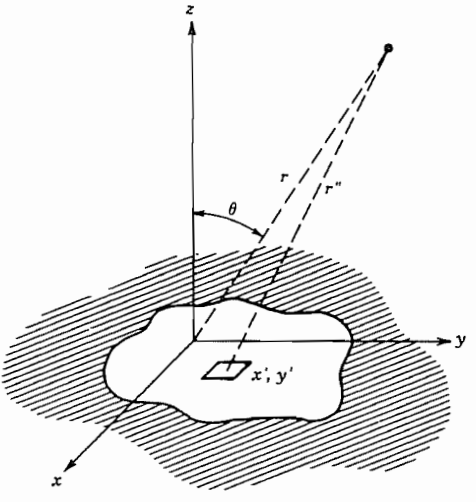


**Fig. 12.13*b*** Plane-wave element as part of a plane aperture located at $z = 0$.

where $r''$ is distance between the element and the field point and may be approximated for the far zone by the binomial expansion

$$r'' = [(x - x')^2 + (y - y')^2 + z^2]^{1/2} \approx r - (xx' + yy')/r \tag{11}$$

Also, as in other radiation problems, the difference between $r$ and $r''$ is important only to phase and not to amplitude. Thus, (10) becomes

$$E(x, y, z) = \frac{je^{-jkr}}{\lambda r} \int_{S'} E(x', y') e^{jk(xx' + yy')/r} dx'\, dy' \tag{12}$$

This is a standard form of diffraction for the Fraunhofer region. Moreover, (12) can be recognized as a two-dimensional version of the Fourier integral (Sec. 7.11), so in the paraxial approximation, the *far-zone field is the Fourier transform of the aperture field.*

## 12.14 Examples of Radiating Apertures Excited by Plane Waves

The expressions developed in the preceding section will now be applied to several important examples. It should be remembered that **E** and **H** at any point in the aperture are assumed to be related as in a plane wave (though strength may vary over the aperture), that we are ignoring contributions from any induced currents outside of the aperture, and that we are restricting ourselves to angles near the polar axis so the paraxial approximation can be used. These assumptions are best satisfied for apertures large compared with wavelength.

**Rectangular Aperture with Uniform Illumination** Consider first a rectangular aperture as in Fig. 12.14*a* with uniform illumination $E_0$ over the aperture. Equation 12.13(12) becomes

$$E(x, y, z) = \frac{je^{-jkr}}{\lambda r} \int_{-a/2}^{a/2} \int_{-b/2}^{b/2} E_0 \, e^{jkxx'/r} e^{jkyy'/r} dx' \, dy' \tag{1}$$

The integrations are readily performed to give

$$E(x, y, z) = \frac{je^{-jkr}}{\lambda r} E_0 ab \left[ \frac{\sin (kax/2r)}{kax/2r} \frac{\sin(kby/2r)}{kby/2r} \right] \tag{2}$$

The pattern in the plane $y = 0$ has nulls of the field at

$$(\theta)_{\text{null}} \approx \left(\frac{x}{r}\right)_{\text{null}} = \frac{m\lambda}{a}, \qquad m = 1, 2, 3, \ldots \tag{3}$$

The pattern in the $x = 0$ plane is of the same form with $y$ replacing $x$ and $b$ replacing $a$. Thus as expected, the primary radiating lobe becomes narrower as the aperture dimensions become larger in comparison with wavelength.

Directivity of this aperture is readily calculated since the maximum field is that at $x = 0$, $y = 0$ so that power radiated by an isotropic radiator of this field strength is

$$(W)_{\text{isotropic}} = 4\pi r^2 \frac{|E_{\max}|^2}{2\eta} = \frac{2\pi E_0^2 a^2 b^2}{\lambda^2 \eta} \tag{4}$$

Actual power radiated may be calculated from the fields in the aperture neglecting currents in the surrounding aperture plane:

$$W = \frac{E_0^2}{2\eta} ab \tag{5}$$

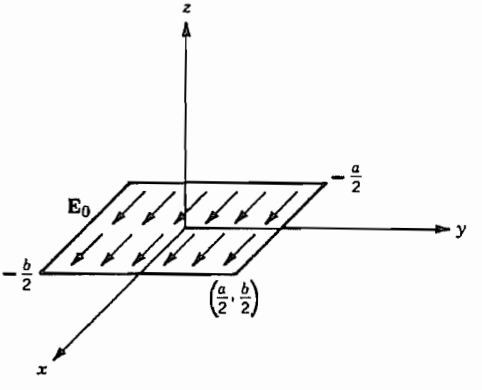


**Fig. 12.14*a*** Uniformly illuminated aperture.

Thus directivity is

$$(g_d)_{max} = \frac{W_{isotropic}}{W} = \frac{4\pi ab}{\lambda^2} = \frac{4\pi(\text{area})}{\lambda^2} \tag{6}$$

which is most accurate for large apertures. The relation between directivity and area is very important and will be found for other aperture radiators.

**Long Slit** A long slit is often used to demonstrate diffraction effects with visible light and, if uniformly illuminated, is just a special case of the above. With $b$ very long in comparison with wavelength, one would expect an extremely thin pattern in the plane $x = 0$, and this is the case if the light used is coherent (in phase) over the length of the slit. In many demonstrations this is not the case, so that there are no appreciable interferences and, therefore, no variations in the long $y$ direction, but only over the shorter $x$ direction. The degree of coherence of a source is described by a *coherence length.* We are then assuming width of the slit less than this coherence length but length large compared with that measure. The resulting radiation intensity can be found as proportional to $|E|^2$ using only the variable $x$ in (2). Since this problem has only two-dimensional symmetry, it is advantageous to express it in cylindrical coordinates with $\phi$ measured about the $y$ axis and $\phi = 0$ along the $x$ axis. Then in the approximation $x/r \approx \cos\phi$, radiation intensity is

$$K = A\left\{\frac{\sin[(ka/2)\cos\phi]}{(ka/2)\cos\phi}\right\}^2 \tag{7}$$

where $A$ is a constant related to the illumination of the aperture. The resulting pattern is shown in Fig. 12.14*b*. We will return to this point, showing patterns using visible light, when we consider multiple slits in Sec. 12.20.

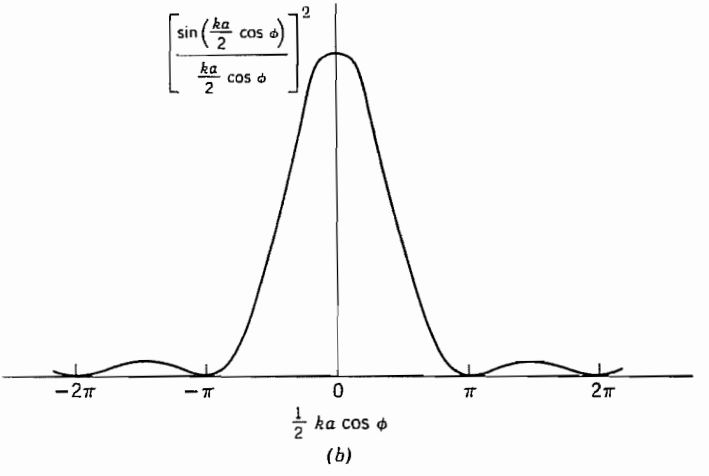


**FIG. 12.14*b*** Radiation intensity variation in one coordinate for a rectangular aperture.

**Circular Aperture with Uniform Illumination** In considering the circular aperture, let us first transform to polar coordinates. Let

$$x = r \sin\theta \cos\phi, \qquad y = r \sin\theta \sin\phi, \qquad x' = r' \cos\phi', \qquad y' = r' \sin\phi'$$

Then Eq. 12.13(12) becomes

$$E(r, \theta, \phi) = \frac{je^{-jkr}}{\lambda r} \int_0^{2\pi} \int_0^a E(r', \phi') e^{jkr' \sin\theta \cos(\phi - \phi')} r' \, dr' \, d\phi' \tag{8}$$

If $E(r', \phi')$ is independent of $\phi'$, $E(r, \theta, \phi)$ is independent of $\phi$, so we may take $\phi = 0$ and for the $\phi'$ integration we may use the integral[15]

$$\int_0^{2\pi} e^{jq \cos\psi} \, d\psi = 2\pi J_0(q) \tag{9}$$

where $J_0(q)$ is a zeroth-order Bessel function. Then

$$E(r, \theta) = \frac{2\pi j e^{-jkr}}{\lambda r} \int_0^a E(r') J_0(kr' \sin\theta) r' \, dr' \tag{10}$$

If $E(r')$ is a constant $E_0$, Eq. 7.15(20) may be utilized to give

$$E(r, \theta) = \frac{2\pi j e^{-jkr}}{\lambda r} E_0 a^2 \frac{J_1(ka \sin\theta)}{ka \sin\theta} \tag{11}$$

The magnitude of the last term in $E(r, \theta)$ is plotted as a function of $ka \sin\theta$ in Fig. 12.14*c*. The first null is reached at an angle

$$\theta_0 = \sin^{-1}\left(\frac{3.83\lambda}{2\pi a}\right) \approx \frac{0.61\lambda}{a} \tag{12}$$

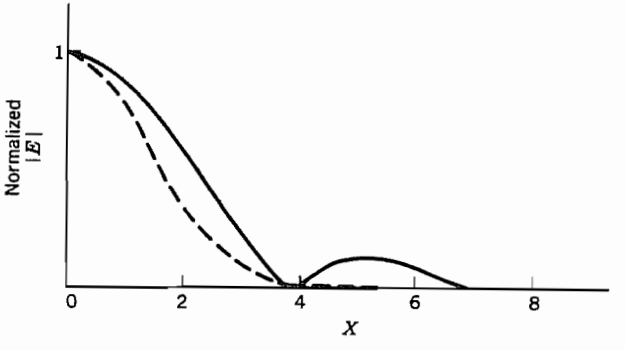


**FIG. 12.14c** Normalized electric field magnitude for circular aperture with uniform illumination (solid) and gaussian illumination (dashed). $X = ka \sin\theta$ for uniform case and $X = kw \sin\theta$ for gaussian illumination, with $a$ and $w$ defined in text.

[15] *I. S. Gradshteyn and I. M. Ryzhik,* Table of Integrals, Series and Products, *corrected and enlarged edition prepared by A. Jeffrey, 8.411(1), Academic Press, San Diego, CA, 1980.*

Directivity of the circular aperture may be calculated in the same fashion as for the rectangular aperture, taking the ratio of power from an isotropic radiator having intensity the same as that at $\theta = 0$ to that of the plane-wave power through the actual aperture:

$$(g_d)_{max} = \frac{(4\pi r^2/2\eta)(2\pi E_0 a^2/2\lambda r)^2}{(\pi a^2 E_0^2/2\eta)} = \left(\frac{4\pi}{\lambda^2}\right)(\pi a^2) \tag{13}$$

Directivity is thus related to aperture area exactly as for the rectangular aperture in (6).

**Circular Aperture with Gaussian Illumination** To compare the effects of tapered illumination with uniform illumination, we next consider a gaussian distribution of field over the circular aperture,

$$E(r', \phi') = E_0 e^{-(r'/w)^2} = E_0 e^{-(x'^2+y'^2)/w^2} \tag{14}$$

but assume that **E** and **H** are related as in a plane wave. The quantity $w$ is beam radius to the $1/e$ point in field. We assume that $w$ is small compared with aperture radius $a$ so that the latter may be assumed effectively infinite. Since field is a function of $r'$ only, we could use (10) directly, but it is simpler to return to the rectangular form, Eq. 12.13(12):

$$E(x, y, z) = \frac{je^{-jkr}}{\lambda r} \int_{-\infty}^{\infty} \int_{-\infty}^{\infty} E_0 e^{-(x'^2/w^2 - jkxx'/r)} e^{-(y'^2/w^2 - jkyy'/r)}\, dx'\, dy' \tag{15}$$

The imaginary parts of the complex exponentials are odd functions and integrate to zero, so

$$E(x, y, z) = \frac{4je^{-jkr}}{\lambda r} \int_0^{\infty} \int_0^{\infty} E_0 \left[ e^{(-x'^2/w^2)} \cos \frac{kxx'}{r} \right] \left[ e^{(-y'^2/w^2)} \cos \frac{kyy'}{r} \right] dx'\, dy' \tag{16}$$

This integral is tabulated[16] and gives

$$E(x, y, z) = \frac{je^{-jkr}}{\lambda r} E_0 \pi w^2 e^{(-k^2(x^2+y^2)w^2/4r^2)} = \frac{je^{-jkr}}{\lambda r} E_0 \pi w^2\, e^{-(k^2 w^2 \sin^2\theta)/4} \tag{17}$$

The angle $\theta_0$ in the direction where the radiation field is $e^{-1}$ of its value at $\theta = 0$ is

$$\theta_0 = \sin^{-1}\left(\frac{2}{kw}\right) \approx \frac{2}{kw} = \frac{\lambda}{\pi w} \tag{18}$$

The pattern as a function of $kw \sin\theta$ is compared with that for the case of uniform illumination in Fig. 12.14*c*. It is seen that the tapered illumination eliminates the side lobes present in the uniformly illuminated example.

[16] *I. S. Gradshteyn and I. M. Ryzhik,* Table of Integrals, Series and Products, *corrected and enlarged edition prepared by A. Jeffrey, 3.896(4), Academic Press, San Diego, CA, 1980.*

**Practical Parabolic Reflectors** The preceding examples give some information about the important parabolic reflector with circular aperture. If illumination were uniform, (11) would apply. In general it is not uniform, both because of the practical difficulties in making it so and also because decreased illumination near the edge has the desirable effect of decreasing side lobes, as illustrated by the gaussian example above. For most primary sources at the focus, such as a small horn or dipole radiator, there is a difference in illumination of the reflector in two orthogonal planes, resulting in a difference of radiation patterns between those planes. Taking into account the above practical problems, a typical design value for beam angle between half-power directions, for a paraboloid of radius $a$, is[17]

$$(2\theta_0)_{\text{half-power}} \approx (70°)(\lambda/2a)$$

## 12.15 Electromagnetic Horns

The electromagnetic horns discussed qualitatively in Sec. 12.2 are of interest both as directive radiators in themselves and also as feed systems for reflectors or directive lens systems. In the horn, there is a gradual flare from the waveguide or transmission line to a larger aperture. This large aperture is desired to obtain directivity, and also to produce more efficient radiation by providing a better match to space. Usually, a fair approximation to aperture field may be made by studying the fields in the feeding system and the possible modes in the horn structure. This then makes possible approximate radiation calculations starting from these fields, by the methods discussed in preceding sections. The idealized examples of Sec. 12.14 give some ideas of the patterns and directivity for certain practical cases. In general, however, there is not only a variation of fields across the aperture, but also a relation between electric and magnetic fields in the aperture somewhat different from that of a plane wave and some effect of currents induced on the exterior surfaces or supporting members.

We consider first the effect of variations across the aperture assuming **E** and **H** related as in a plane wave and neglecting currents on exterior surfaces and supports. For a rectangular horn excited by the $TE_{10}$ mode of rectangular guide (Fig. 12.15), a reasonable approximation to aperture field is

$$E(x', y') = E_0 \sin\left(\frac{\pi x'}{a}\right) \tag{1}$$

Use of Eq. 12.13(12) for the radiation field gives the integral

$$E(x, y, z) = \frac{je^{-jkr}}{\lambda r} \int_{-b/2}^{b/2} \int_{-a/2}^{a/2} E_0 \sin\left(\frac{\pi x'}{a}\right) e^{jk(xx' + yy')/r} dx'\, dy' \tag{2}$$

[17] *R. C. Johnson and H. Jasik (Eds.),* Antenna Engineering Handbook, *2nd ed., pp. 1–15, McGraw-Hill, New York, 1984.*

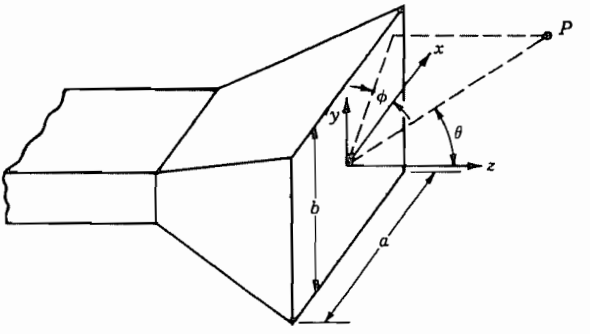


**FIG. 12.15** Waveguide horn.

These integrals are standard and yield

$$E(x, y, z) = \frac{2E_0ab}{\pi}\frac{e^{-jkr}}{\lambda r}\left[\frac{\cos(kax/2r)}{1 - (kax/\pi r)^2}\right]\frac{\sin(kby/2r)}{kby/2r} \tag{3}$$

The dependence on $y$ is of the same form as with the uniform distribution (since $E$ is not a function of $y$), but that for $x$ will be found to be somewhat broader than that of Eq. 12.14(2). Directivity for this case is

$$(g_d)_{max} = \frac{(4\pi r^2/2\eta)(2E_0ab/\pi\lambda r)^2}{(E_0^2ab/4\eta)} = \frac{4\pi}{\lambda^2}\left(\frac{8ab}{\pi^2}\right) \tag{4}$$

The quantity $8ab/\pi^2$ can be considered an equivalent area [by comparing with Eqs. 12.14(6) or (13)] and is slightly less than the actual area.

Extension to $TE_{mn}$ mode excitation, including allowance for reflection at the aperture, is given in the literature.[18]

## 12.16 Resonant Slot Antenna

Another important class of radiators in which the emphasis is on the field in the aperture is that of the slot antenna mentioned qualitatively in Sec. 12.2. Let us consider the resonant slot antenna (approximately a half-wave long) in an infinite plane conductor,[19] as shown in Fig. 12.16*a*. For apertures in perfectly conducting planes, it is only nec-

[18] *S. Silver,* Microwave Antenna Theory and Design, *Chap. 10, IEEE Press, Piscataway, NJ, 1984.*

[19] *R. E. Collin,* Antennas and Radiowave Propagation, *Sec. 4.12, McGraw-Hill, New York, 1985.*

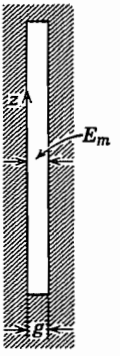


**FIG. 12.16a** Resonant half-wave slot.

essary to consider the electric field in the aperture to specify completely the boundary conditions since tangential **E** is zero along the conductor and dies off at infinity (see uniqueness argument, Sec. 3.14). We will take the electric field in the aperture to be uniform in $x$ and to have a half-sine distribution in $z$ with its maximum at the center. By reference to Eq. 12.12(2), the magnetic current sheet equivalent to this would be found to lie in the $z$ direction and to be equal to $E_x$:

$$M_z = E_x = E_m \cos kz \tag{1}$$

Since $E_z$ is assumed to be zero behind $M_z$, the gap can be considered closed with an electric conductor. It is convenient to account for the infinite conductor by replacing it with the image of $M_z$. As shown in Prob. 12.16a, $M_z$ and its image are in the same direction so the value in (1) must be doubled in using free-space field expressions.

If gap width $g$ is taken as small, the equation for magnetic radiation vector, Eq. 12.12(8), becomes

$$L_z = \int_{-\lambda/4}^{\lambda/4} 2gE_m \cos kz' \, e^{jkz' \cos\theta} \, dz' \tag{2}$$

The integral is evaluated to give

$$L_z = \frac{4gE_m \cos[(\pi/2)\cos\theta]}{k \sin^2\theta} \tag{3}$$

Then, utilizing Eq. 12.12(10), we see that the fields are

$$E_\phi = -\eta H_\theta = \frac{je^{-jkr}gE_m}{\pi r}\left\{\frac{\cos[(\pi/2)\cos\theta]}{\sin\theta}\right\} \tag{4}$$

We should note here that this is of the same form as the expression for fields about a half-wave dipole antenna (Sec. 12.5) except for the interchange in electric and magnetic fields.

The power radiated corresponding to (4), assuming radiation only into one side, is

$$W = \frac{\pi(gE_m)^2}{2\pi^2\eta} \int_0^{\pi} \frac{\cos^2[(\pi/2)\cos\theta]}{\sin\theta}\, d\theta \tag{5}$$

This may be interpreted in terms of a radiation conductance defined in terms of the maximum gap voltage:

$$(G_r)_{slot} = \frac{2W}{(gE_m)^2} = \frac{1}{\pi\eta} \int_0^{\pi} \frac{\cos^2[(\pi/2)\cos\theta]}{\sin\theta}\, d\theta \tag{6}$$

By comparing with the expression for radiation resistance of the half-wave dipole, Eqs. 12.7(8) and (9), we find

$$(G_r)_{slot} = \frac{2(R_r)_{dipole}}{\eta^2} \approx 0.00103 \text{ S} \tag{7}$$

If radiation is to both sides, conductance is double the above value. The reciprocity between results for the slot and dipole can also be shown to follow from *Babinet's principle*,[20] which is an extension of the principle of duality discussed in Sec. 9.5. For a strip dipole of general shape, and its complementary slot, Booker has shown from Babinet's principle that radiation fields are of the same form but of orthogonal polarization. Impedances, if the slot radiates to both sides of the conducting plane, are related by

$$Z_{strip}Z_{slot} = \eta^2/4 \tag{8}$$

A possible means of exciting the slot is shown in Fig. 12.16*b*.

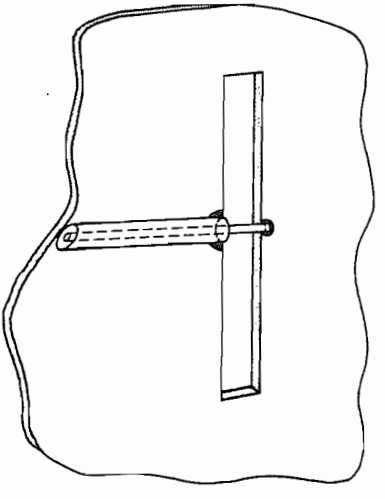

**FIG. 12.16*b*** Coaxial-line feed for resonant-slot antenna.

[20] *R. E. Collin,* Field Theory of Guided Waves, *Sec. 1.8, IEEE Press, Piscataway, NJ, 1990.*

## 12.17 Lenses for Directing Radiation

The lenses used in radiating systems, like the parabolic reflector, act to focus the radiation from primary sources into desired directions. Most lenses are conceived from the point of view of geometrical optics, and in this approximation would produce a plane-parallel beam of radiation from an ideal point radiator at the focus. The actual lens behavior is disturbed from this ideal by the finite character of the primary radiator and by diffraction arising from the finite aperture of the lens. The latter effect causes the beam to spread in a manner predicted by the aperture analysis of Sec. 12.14. Thus, we will leave this aspect of the matter and consider the various first-order designs suggested by geometrical optics.

The most direct conception is that of a primary source placed at the focus of a converging lens so that the beam emerges parallel. The technique is well developed at optical frequencies, including the coating of the surfaces to eliminate reflections (Ex. 6.8c). The solid lenses most often used are small enough for convenient handling. The use of solid dielectric lenses can be extended to submillimeter and millimeter wavelengths. However, for microwaves the lenses are large and heavy if the aperture is made large enough to produce a reasonably narrow beam. Thus one of the two variants to be described is commonly used.

A fairly direct extension of the solid lens concept to microwaves is possible with reasonable weights through the use of "artificial dielectrics." These lenses are made of metal spheres, disks, strips, or rods embedded in a light material such as polyfoam.[21] If the metal particles are small in comparison with wavelength, they act very much as individual molecules in a solid dielectric. That is, the metal particles are "polarized" by the applied field (Fig. 12.17*a*), with the positive and negative charges displaced from each other. Each particle then acts as a small dipole, contributing to total displacement and thus to an effective dielectric constant. In general both electric and magnetic field components contribute to the polarization of the metallic particles. In spherical particles, for example, the electric and magnetic effects tend to cancel. Particles having the form of thin sheets (disks or strips) parallel to the electric and magnetic fields, as in Fig. 12.2*h*, have negligible magnetically induced polarization and therefore give a larger $n$. They are also lighter than the other shapes. Kock[21] gave a simple formula for disks, $\varepsilon_r = 1 + 5.3Na^3$, where $a$ is the disk radius and $N$ is the number per unit volume. Values depend, however, upon orientation of the disks with respect to field polarization and direction of propagation. Very high values of $\varepsilon_r$ have been obtained but practical values are generally only a few times unity.[22] Inhomogeneous properties are also possible by varying spacing or size of particles; this technique may be used instead of shaping to produce focusing action.

One of the most important lenses that utilizes an inhomogeneous effective dielectric

[21] *W. E. Kock*, Bell Syst. Tech. J. **27**, *58 (1948).*

[22] *R. E. Collin*, Field Theory of Guided Waves, *Chap. 12, IEEE Press, Piscataway, NJ, 1990.*

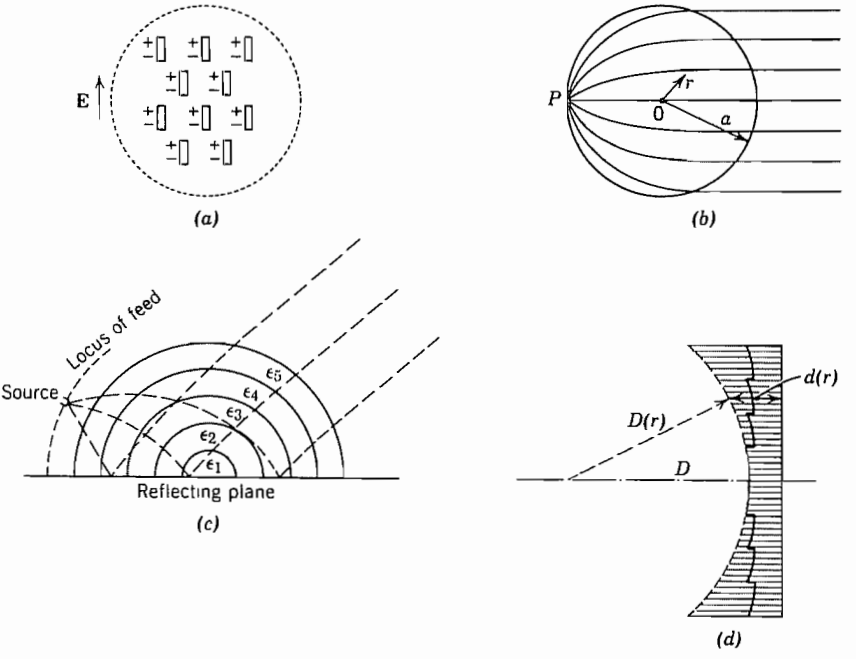


**FIG. 12.17** (*a*) Artificial dielectric lens. (*b*) Luneberg lens. (*c*) Practical form of Luneberg lens. (*d*) Metal lens antenna.

constant is the Luneberg lens.[23] This is made in the form of a sphere with effective dielectric constant varying with radius as

$$\varepsilon_r(r) = 2 - (r/a)^2, \qquad r \leq a \tag{1}$$

Techniques for analyzing rays in inhomogeneous media will be given in Chapter 14. Use of these can show that all rays originating from a point on the surface will emerge from the other side as a parallel beam in the direction of the diameter through the source point (Fig. 12.17*b*). This lens is important because small-distance movements of the source along the surface can provide substantial angular scanning of the beam. It is more practical to have the source point a small distance away from the surface of the lens, to use a reflection plane to eliminate half the sphere, and to use steps in effective dielectric constant, as illustrated in Fig. 12.17*c*. A number of variations have been utilized.[24]

[23] *R. F. Rinehart,* J. Appl. Phys. ***19****, 860 (1948).*

[24] *R. C. Johnson and H. Jasik (Eds.),* Antenna Engineering Handbook, *2nd ed., Secs. 16–10 and 18–2, McGraw-Hill, New York, 1984.*

An interesting and different means of realizing lens-type focusing action is with the *metal lens antenna*[25] which utilizes sections of parallel-plane waveguides, as illustrated in Fig. 12.17*d*. Polarization is such that the mode between the plates is a TE mode, normally with one half-sine variation in field distribution. The ratio of spacing to wavelength is such that phase velocity $v_p$ is appreciably greater than that in free space. The concept used is one in which all paths from focus to the lens plane yield the same phase,

$$\frac{D}{c} + \frac{d(0)}{v_p} = \frac{D(r)}{c} + \frac{d(r)}{v_p} \tag{2}$$

where $v_p$ is given by Eq. 8.3(18) and $r$ is distance from the axis in cylindrical coordinates. Since the waveguide sections advance rather than delay phase, the outer parts of the lens are longer than the center parts for a converging lens, as illustrated in Fig. 12.17*d*. Whole wavelengths contribute nothing from the point of view of phase, so these may be cut out to save weight, resulting in the final stepped configuration shown by the solid lines of the figure.

## Arrays of Elements

### 12.18 Radiation Intensity with Superposition of Effects

If there are several complete radiators operating together, currents or fields might be assumed over the entire group, and a complete calculation made for potentials or fields at any point in the radiation field. If the radiation pattern of the individual elements is known, however, some labor may be saved by superposing these with proper attention to phase, direction, and magnitude of the fields. This is actually only an extension of the procedure we have already used to add up the effects of infinitesimal elements. As a practical matter, the synthesis of desired antenna patterns by the addition of individual radiators is a most important tool, so that efficient methods for the analysis of arrays are essential. A few of these, with examples, are set down in this and several following sections.

The usual problem in array theory is that of identical radiators with similar current or field distributions (although magnitudes and phases of currents or fields in individual radiators may differ). The radiation vectors for one of these alone may be calculated as $\mathbf{N}_0$ and $\mathbf{L}_0$. ($\mathbf{N}_0$ alone is sufficient if we consider contributions only from electric current

[25] *W. E. Kock,* Proc. IRE **34**, *828 (1946). Also see J. D. Kraus,* Antennas, *2nd ed., Sec. 14–4, McGraw-Hill, New York, 1988.*

elements.) In adding contributions from the individual radiators for the far-zone field, the usual approximation is made in that differences in distances to the individual radiators need be taken into account only with respect to phase; also, the approximate form for distance differences may be calculated by assuming the field point far removed. The form of the radiation vectors can be found by evaluating the distance $r''$ from an element of radiating current to the field point in terms of the parameters of the array. We can see from Fig. 12.18*a* that for an element on the $n$th radiator, $r''$ can be expressed in terms of the distance $r$ from the arbitrary reference point in the array to the field point as

$$r'' \approx r - r_n' \cos \psi_n - r_0' \cos \psi_0 \tag{1}$$

where $r_n'$ and $\psi_n$ locate the $n$th radiator relative to the reference point and $r_0'$ and $\psi_0$ determine the location of the differential radiating element relative to the reference point on the radiator. Since all radiators have the same orientation, $r_0'$ and $\psi_0$ apply equally to all $n$ radiators. Substituting (1) in Eq. 12.4(1), we get the far-field vector potential at $P$ for the $n$th radiator:

$$\begin{aligned} \mathbf{A}_n &= \frac{\mu e^{-jkr}}{4\pi r}\left[e^{jkr_n' \cos \psi_n} \int_{V_n'} \mathbf{J}_n e^{jkr_0' \cos \psi_0}\, dV_n'\right] \\ &= \frac{\mu e^{-jkr}}{4\pi r}\left[C_n e^{jkr_n' \cos \psi_n} \mathbf{N}_0\right] \end{aligned} \tag{2}$$

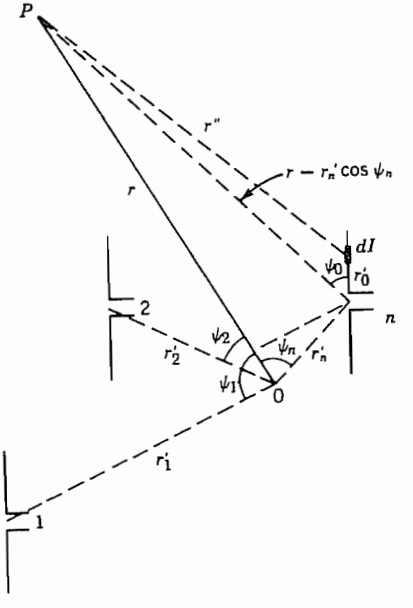


**FIG. 12.18*a*** Array of identical radiators, all with the same orientation.

where $C_n$ is a complex constant and $\mathbf{N}_0$ is the normalized radiation vector for one of the identical radiators. Thus, the radiation vector for a system of radiators with electric current is

$$\mathbf{N} = \mathbf{N}_0(C_1 e^{jkr_1' \cos \psi_1} + C_2 e^{jkr_2' \cos \psi_2} + \cdots) \tag{3}$$

Likewise, for radiators with magnetic currents,

$$\mathbf{L} = \mathbf{L}_0(C_1 e^{jkr_1' \cos \psi_1} + C_2 e^{jkr_2' \cos \psi_2} + \cdots) \tag{4}$$

It follows that the total radiation intensity may be written in terms of the radiation intensity $K_0$ for one radiator alone:

$$K = K_0 |C_1 e^{jkr_1' \cos \psi_1} + C_2 e^{jkr_2' \cos \psi_2} + \cdots|^2 \tag{5}$$

Examples will follow to make the use of these forms more specific. We should note one important point, however, that will not be touched on specifically in the examples. Mutual couplings between the elements, including effects from the near-zone fields, may affect the amount and phase of current that a given array element receives from the driving source, so that the excitation problem may become quite difficult. A discussion of the coupling problems is given for one type of array in Sec. 12.22.

### Example 12.18
ARRAY OF TWO HALF-WAVE DIPOLES

Consider two half-wave dipoles separated by a quarter-wavelength and fed by currents equal in magnitude and 90 degrees out of time phase, as in Fig. 12.18*b*. For a single dipole, we have Eq. 12.5(8):

$$K_0 = \frac{15}{\pi} I_m^2 \frac{\cos^2[(\pi/2) \cos \theta]}{\sin^2 \theta}$$

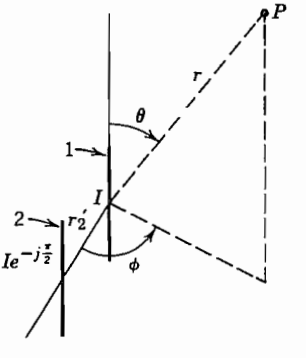


**FIG. 12.18*b*** Combination of two half-wave dipoles.

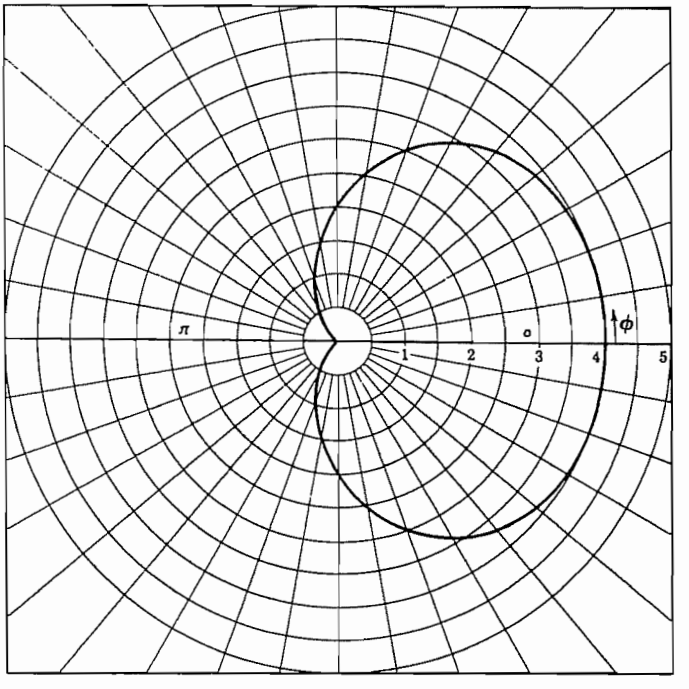


**FIG. 12.18c** Polar plot of relative power intensity radiation for array in Fig. 12.18*b* in the plane $\theta = \pi/2$.

For the two dipoles with the origin as shown in Fig. 12.18*b*,

$$r_1' = 0, \qquad r_2' = \frac{\lambda}{4}, \qquad \theta_2' = \frac{\pi}{2}, \qquad \phi_2' = 0$$

Using the general formula, Eq. 12.4(15),

$$\cos \psi_2 = \sin \theta \cos \phi$$

If

$$I_2 = I_1 e^{-j(\pi/2)}$$

then (5) gives

$$\begin{aligned} K &= K_0 |1 + e^{-j(\pi/2)} e^{j(\pi/2)(\sin \theta \cos \phi)}|^2 \\ &= 4K_0 \cos^2 \left[ \frac{\pi}{4} (\sin \theta \cos \phi - 1) \right] \end{aligned}$$

A horizontal radiation intensity pattern is plotted in Fig. 12.18*c*.

## 12.19 LINEAR ARRAYS

An especially important class of arrays is that in which the elements are arranged along a straight line, usually with equal spacing between them, as indicated in Fig. 12.19*a*. Let the line be the $z$ axis, with the basic spacing $d$ and coefficients $a_0, a_1, \ldots, a_{N-1}$ representing the relative currents in elements at $z = 0, d, \ldots, (N-1)d$. (Note that any of the elements can be missing, in which case the coefficient is zero, so the elements need only be of commensurate spacing instead of equal spacing.) If the elements have a radiation vector $\mathbf{N}_0$, Eq. 12.18(3) becomes for this case

$$\mathbf{N} = \mathbf{N}_0[a_0 + a_1 e^{jkd\cos\theta} + \cdots + a_{N-1}e^{j(N-1)kd\cos\theta}] = \mathbf{N}_0 S(\theta) \tag{1}$$

where $S(\theta)$ may be called the *space factor* of the array:

$$S(\theta) = \sum_{n=0}^{N-1} a_n e^{jnkd\cos\theta} \tag{2}$$

The radiation intensity from Eq. 12.18(5) is then

$$K = K_0|S|^2 \tag{3}$$

**Broadside Array** If all currents in the linear array are equal in magnitude and phase, it is evident from physical reasoning that the contributions to radiation will add in phase in the plane perpendicular to the axis of the array ($\theta = \pi/2$). For this reason, the array is called a *broadside array*. Moreover, it is evident that, if the total length $l = (N-1)d$ is long compared with wavelength, the phase of contributions from various elements will change rapidly as angle is changed slightly from the maximum, so that maximum in this case would be expected to be sharp. To see this from (2), let all $a_n = a_0$:

$$S(\theta) = a_0 \sum_{n=0}^{N-1} e^{jnkd\cos\theta} = a_0 \frac{1 - e^{jNkd\cos\theta}}{1 - e^{jkd\cos\theta}} \tag{4}$$

Summation (4) is effected by the rule for a geometric progression. Then

$$|S| = a_0 \left| \frac{\sin \frac{1}{2}(Nkd\cos\theta)}{\sin \frac{1}{2}(kd\cos\theta)} \right| \tag{5}$$

Relation (5) is plotted as a function of $kd\cos\theta$ in Fig. 12.19*b* for $N = 10$. Note that the peak of the main lobe occurs at $kd\cos\theta = 0$ (or $\theta = \pi/2$) as expected. The width of the main lobe may be described by giving the angles at which radiation goes to zero.

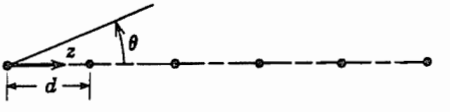


**FIG. 12.19*a*** Coordinate system for a linear array.

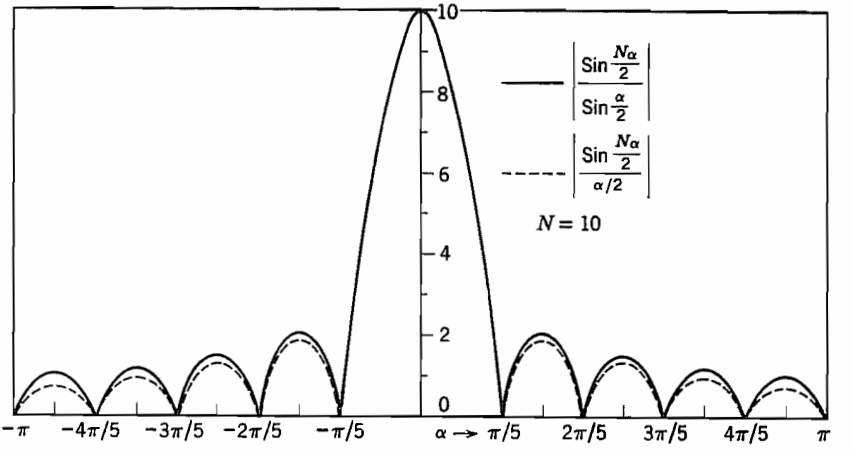


**FIG. 12.19*b*** Plot of magnitude of space factor and approximation with 10 elements. $\alpha$ is $kd \cos\theta$ for a broadside array and $kd(1 - \cos\theta)$ for an end-fire array.

If we set these angles as $\theta = \pi/2 \pm \Delta/2$,

$$Nkd \cos\left(\frac{\pi}{2} \pm \frac{\Delta}{2}\right) = \mp 2\pi$$

$$\Delta = 2 \sin^{-1}\left(\frac{\lambda}{Nd}\right) \approx \frac{2\lambda}{l} \tag{6}$$

The last approximation is for large $N$. So we see that the beam becomes narrow as $l/\lambda$ becomes large, as predicted.

If $N$ is large the denominator of (5) remains small over several of the lobes near the main lobe. Over this region it is then a good approximation to set the sine equal to the angle in the denominator:

$$|S| \approx Na_0 \left|\frac{\sin\frac{1}{2}(Nkd \cos\theta)}{\frac{1}{2}Nkd \cos\theta}\right| \tag{7}$$

This approximation is compared as a dotted curve with the accurate curve for $N = 10$ in Fig. 12.19*b*, and is found to agree well over several maxima. Thus, for large $N$, this universal form applies near $\theta = \pi/2$ and the first secondary maximum is observed to be about 0.045 of the absolute maximum, or 13.5 dB below.

The directivity of an array is usually expressed as though the elements were isotropic radiators. It is of course modified if actual elements having some directivity are employed, but for high-gain arrays, the modification is small. (Note that it is not correct to multiply directivity of the array by directivity of a single element.) For the array,

$$(g_d)_{\max} = \frac{4\pi|S_{\max}|^2}{2\pi \int_0^\pi |S|^2 \sin\theta \, d\theta} \tag{8}$$

The high-gain broadside array gives most of its contribution to the integal in the denominator near $\theta = \pi/2$, where the approximate expression (7) applies,

$$\int_0^{\pi} |S|^2 \sin\theta \, d\theta = \frac{2N^2a_0^2}{Nkd} \int_0^{Nkd} \frac{\sin^2 \alpha/2}{(\alpha/2)^2} \, d\alpha \approx \frac{4N^2a_0^2}{Nkd} \cdot \frac{\pi}{2}$$

where $Nkd$ is effectively infinite. From (8),

$$(g_d)_{\max} \approx \frac{2l}{\lambda} \qquad \left(\text{large } \frac{l}{\lambda}\right) \tag{9}$$

**End-Fire Arrays** If the elements of the array are progressively delayed in phase just enough to make up for the retardation of the waves, it would be expected that the radiation from all elements of the array could be made to add in the direction of the array axis. Such an array is called an *end-fire array.* To accomplish this, let

$$a_n = a_0 e^{-jnkd} \tag{10}$$

Then in (2),

$$S = a_0 \sum_{n=0}^{N-1} e^{-jnkd(1-\cos\theta)} = a_0 \frac{1 - e^{-jNkd(1-\cos\theta)}}{1 - e^{-jkd(1-\cos\theta)}} \tag{11}$$

$$|S| = \frac{\sin \frac{1}{2}[Nkd(1 - \cos\theta)]}{\sin \frac{1}{2}[kd(1 - \cos\theta)]} a_0 \tag{12}$$

By comparison with (5), it is recognized that the plot of Fig. 12.19*b* made for a broadside array may be utilized for the end-fire array also if the abscissa is interpreted as $kd(1 - \cos\theta)$. The pattern as a function of $\theta$ of course looks different, but the ratio of secondary to primary maxima is the same. It may also be shown to follow that the formula for directivity (9) applies also to an end-fire array with large $l/\lambda$. To obtain the angular width of the main lobe, let $\Delta/2$ be the angle at which $S$ goes to zero:

$$Nkd\left(1 - \cos\frac{\Delta}{2}\right) = 2\pi$$

$$\Delta \approx 2\sqrt{\frac{2\lambda}{l}} \tag{13}$$

**Phase Scanning of Arrays** By interpretation of the broadside and end-fire examples, it is clear that a phase delay between elements somewhere between the extremes for the two cases should give a maximum lobe between these extremes. Moreover, if this phase delay is controllable by any means (usually with ferrite or semiconductor devices), the direction of the lobe can be scanned without physical motion of the antenna. This may be most important in large installations that must continually scan a large range of directions in short times, as in airport surveillance radar.

Quantitatively, for the linear array, we see the scanning if we allow the phase delay to be $\Delta\varphi$ between elements. Then, replacing (10) for the end fire,

$$a_n = a_0 e^{-jn\Delta\varphi} \tag{14}$$

Following procedures as for (5) or (12), the space factor here is

$$|S| = \frac{\sin[(N/2)(kd\cos\theta - \Delta\varphi)]}{\sin\frac{1}{2}(kd\cos\theta - \Delta\varphi)}\, a_0 \tag{15}$$

The direction of the principal maximum is then given by

$$kd\cos\theta_m = \Delta\varphi \tag{16}$$

and so can be varied if $\Delta\varphi$ is varied.

This principle can of course be extended to two-dimensional as well as linear arrays, although the number of phases to control then increases.

**Unequally Spaced Arrays** Although the formulation above has been given only for arrays of equal element spacing, unequal spacing of elements provides an additional degree of freedom which may sometimes be used to advantage. Unequally spaced arrays have been used to give greater gain and lower side lobes than an equally spaced array with the same number of elements.[26] The amplitude of excitation of the elements may be retained more nearly constant in the array of unequal spacing. Analysis can be carried out by digital computation once element spacings and excitations are specified.

## 12.20 Radiation from Diffraction Gratings

In Sec. 6.10 we saw the basic idea of the diffraction grating, which has become of increased importance since coherent light has become available from lasers. Here we make use of the array factors developed in Sec. 12.19 to explain the patterns observed for diffraction gratings. The grating could take the form of a parallel array of slits of the type discussed in Sec. 12.14, with each slit forming a radiation source. For practical reasons, these are often engraved lines ("rulings") on a solid reflector rather than open slits, but they act very similarly with regard to radiation pattern.

Consider first the radiation pattern of two parallel slits, each of width $a$, illuminated in phase, and separated by distance d between central axes. Here we find the pattern in the plane normal to the slit axes, so angle $\theta$ is replaced by $\phi$ in Eq. 12.19(5) for the broadside array and we take $N = 2$:

$$|S|^2 = a_0^2 \frac{\sin^2\frac{1}{2}(2kd\cos\phi)}{\sin^2\frac{1}{2}(kd\cos\phi)} = 4a_0^2\cos^2\left(\frac{kd}{2}\cos\phi\right) \tag{1}$$

[26] *D. D. King, R. F. Packard, and R. K. Thomas,* IRE Trans. Antennas and Propagation ***AP-8****, 380 (1960).*

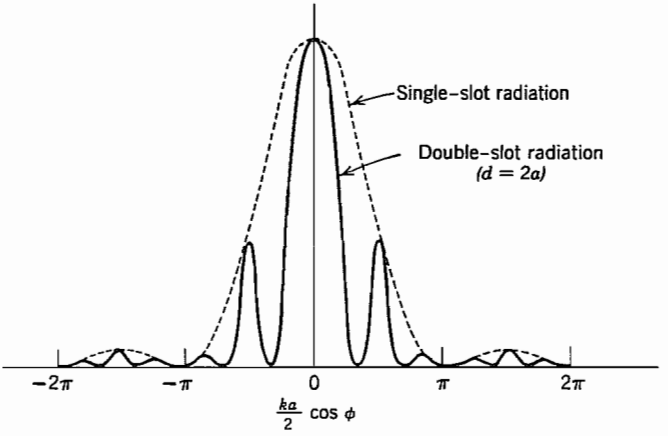


**FIG. 12.20*a*** Fraunhofer intensity pattern for two slits compared with that of one of the slits alone. Slit width is $a$ and spacing $d$.

The radiation intensity is given by Eq. 12.19(3), with $K_0$ representing the radiation intensity for a single slit, Eq. 12.14(7). We let $4a_0^2A = B$ and find

$$K = B\left[\frac{\sin(ka/2\cos\phi)}{ka/2\cos\phi}\right]^2 \cos^2\left(\frac{kd}{2}\cos\phi\right) \tag{2}$$

which is shown in Fig. 12.20*a* for $d = 2a$.

Array factors for larger number of radiators have shapes like that in Fig. 12.19*b*. Shown there is a principal maximum with subsidiary maxima (side lobes). If the spacing $d$ between slits exceeds one wavelength, there will be repeated principal maxima. Photographs of diffraction patterns for different sets of slits are shown in Fig. 12.20*b*. The broad maximum of the single slit is seen with its subsidiary maxima for $N = 1$. With three slits the pattern becomes sharper and the subsidiary maxima may be seen only vaguely. In the case of $N = 20$, the larger number of slits leads to very distinct principal maxima and the intensity of the subsidiary maxima is low enough that they do not register in the photograph. The clear separation of the lines is of utmost importance in the use of diffraction gratings for spectroscopy or other applications where it is desired to separate patterns of different frequency. In practical gratings there are hundreds, or even thousands, of slits (or rulings) so that the principal maxima are very sharp and the subsidiary maxima are very near the principal maxima.

## 12.21 Polynomial Formulation of Arrays and Limitations on Directivity

Schelkunoff[27] has shown that linear arrays with equal element spacings may be formulated as polynomials, with useful results obtained by interpretations of the zeros of the polynomials in the complex plane. If we define

$$\zeta = e^{j\psi} = e^{jkd\cos\theta} \tag{1}$$

[27] *S. A. Schelkunoff,* Bell Syst. Tech. J. **22**, *80 (1943).*

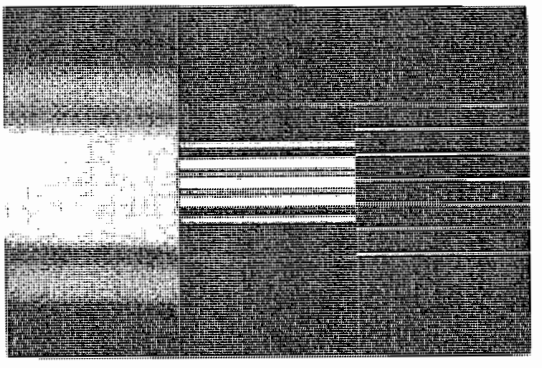


**FIG. 12.20*b*** Diffraction patterns showing the increased sharpness resulting from increasing the number of slits.

then Eq. 12.19(2) may be written as a polynomial in $\zeta$:

$$S = \sum_{n=0}^{N-1} a_n \zeta^n \tag{2}$$

Concentration is now on the properties of $S$ in the complex $\zeta$ plane.

Note first that real $\theta$ corresponds to values of $\zeta$ on the unit circle with phase angles between $-kd$ and $kd$. All, a part, or none of the $N - 1$ zeros of $S$ may occur in this part of the unit circle. When they do so occur, they correspond to true zeros of the pattern, or "cones of silence." The broadside array, Eq. 12.19(5), has its zeros spread out uniformly over the entire unit circle except for the missing one at $\psi = 0$ (Fig. 12.21*a*), where the very large main lobe builds up. One approach to the synthesis of arrays is then that of positioning zeros on this picture so that they are close together where the pattern is to be of small amplitude and farther apart where it is to build up to a relatively large value.

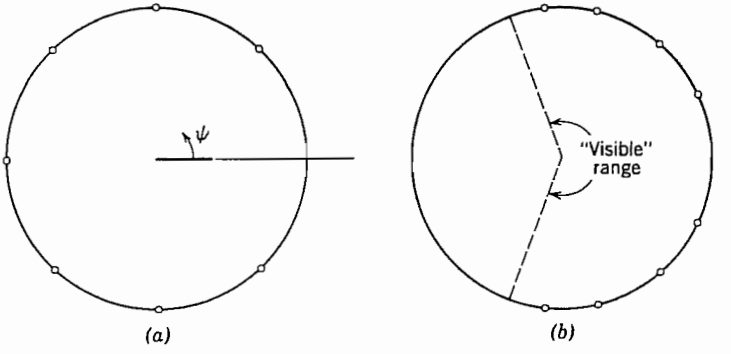


**FIG. 12.21** (a) Location of zeros of polynomial representing a uniform broadside array. (*b*) Positioning of zeros of polynomial to produce a supergain array.

If we limit ourselves to linear arrays with currents in phase, it can be shown that the uniform array (one with all currents of equal amplitude) gives more directivity than arrays with nonuniform excitations. Still greater directivities are possible in principle, however, if one goes to excitations of other phases. Arrays having more directivity than the uniform array are known as *supergain arrays*.

In terms of the picture in the $\zeta$ plane, we see that for an element spacing less than a half-wavelength ($kd = \pi$) the range of real $\theta$ covers only a part of the unit circle. The uniform array, however, has its zeros spread over all the unit circle, so some are "invisible." Schelkunoff has shown that arbitrarily high directivity for a given antenna size is possible in principle by moving the zeros into the range of real $\theta$, properly distributed to give the desired directivity (Fig. 12.21*b*). The trouble here is that a monstrous lobe builds up in the "invisible" range from which the zeros have been eliminated, which might seem to be of no concern but turns out to represent reactive energy and so is of importance. It is surprising to find the rapidity with which this limitation takes over. For high-gain broadside arrays, no significant increase in gain is possible over that of the uniform array before the reactive energy becomes impossibly large.[28] For end-fire arrays, a modest increase is possible and has been utilized in practice.[29] Another way of stating this limitation is that currents of the elements become huge for a given power radiated and fluctuate in phase from one element to the next so that it would be impossible to feed such an array.

A physical picture is provided by looking at the problem from a wave point of view. Imagine that we are attempting to produce a high-gain broadside array with a thin pancake pattern near the equator. We may imagine the distant fields ($H_\phi$ and $E_\theta$) of this pattern expanded in a series of the spherically symmetric TM modes of the type studied in Sec. 10.7. If the pattern is to be sharp, it is clear that waves of very high order are needed to represent this pattern (order of $2\pi/\Delta$ for a narrow beam of angle $\Delta$). A study of the Hankel functions shows that these functions change character at a radius such that $n$ is of the order $kr$, becoming rapidly reactive for radii less than this value. Hence, the antenna boundary must extend approximately to this radius if excessive reactive power is to be avoided. That is,

$$\frac{2r}{\lambda} \approx \frac{n}{\pi} \approx \frac{2}{\Delta} \tag{3}$$

which gives a relation between angle and length equivalent to that for a uniform broadside array, Eq. 12.19(6). The phenomenon is a cutoff of the type found in sectoral horns (Sec. 9.4), where it was found that reactive effects caused an effective cutoff when the cross section became too small to support the required number of half-wave variations in the pattern. The rapidity with which the limitation takes over must again be stressed. For an array 50 wavelengths long, a halving in size from that of the uniform array would require reactive power $10^{59}$ times the radiated power.

[28] *L. J. Chu,* J. Appl. Phys. ***19*** *1163 (1948).*
[29] *W. W. Hansen and J. R. Woodyard,* Proc. IRE ***26****, 333 (1938).*

It should not be inferred from the foregoing discussion that uniform arrays are always best. Often the side-lobe level (13.5 dB) is higher than can be tolerated. Side lobes can be reduced with a sacrifice in directivity. Dolph[30] has given the procedure for finding the array of a given number of elements which gives the lowest side lobes for a prescribed antenna directivity or highest directivity for a prescribed side-lobe level. The polynomial $S(\zeta)$ in (2) has in this case the form of a Chebyshev polynomial.

## 12.22 Yagi–Uda Arrays

One difficulty in using multielement arrays to achieve directivity is the need to provide controlled feeds to the various elements. The so-called Yagi–Uda array avoids this problem by feeding only one element and having other elements with currents induced by the first; correct phasing is achieved by adjusting the size and positions of the other elements.

Consider the situation shown in Fig. 12.22*a* where there is one driven element and one parallel "parasitic" element. The linearity of Maxwell's equations makes it possible to write a set of equations relating the voltages at the center of the antennas to the currents at the feed points:

$$\begin{aligned} V_1 &= Z_{11}I_1 + Z_{12}I_2 \\ V_2 &= Z_{21}I_1 + Z_{22}I_2 \end{aligned} \tag{1}$$

The $Z_{ij}$ are constants that depend upon the lengths $l_1$ and $l_2$ and the separation $d$ of the elements. Using the fact that the voltage at the drive point of element 2 is zero, one

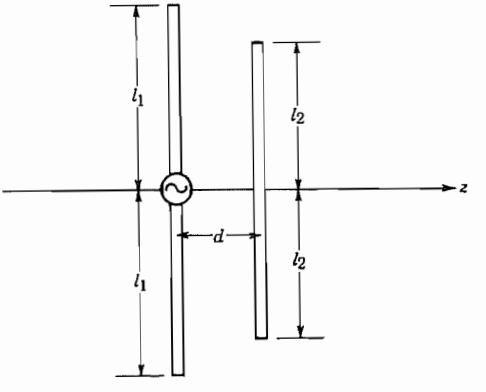


**Fig. 12.22*a*** Driven antenna element with nearby, parallel, parasitic element.

[30] *C. L. Dolph, Proc. IRE* ***34****, 335 (1946). See also R. E. Collin,* Antennas and Radiowave Propagation, *p. 128, McGraw-Hill, New York, 1985.*

finds from (1) that $I_2$ is determined (by induction) by the current $I_1$ and the coefficients in (1):

$$I_2 = -\frac{Z_{21}}{Z_{22}} I_1 \tag{2}$$

The array factor in Eq. 12.19(2) can be written for this array as

$$S(\theta) = a_0 + a_1 e^{jkd\cos\theta} = I_1\left(1 + \frac{I_2}{I_1} e^{jkd\cos\theta}\right) \tag{3}$$

Therefore, we see that the pattern depends upon the spacing $d$ and upon the coefficients $Z_{12}$ and $Z_{22}$.

The methods to be studied in Sec. 12.27 can be used to show that the mutual impedance $Z_{21}$ is rather insensitive to the lengths $2l_1$ and $2l_2$ when they are nearly $\lambda/2$. Therefore, the phase of the current $I_2$ depends, according to (2), mainly upon the self-impedance $Z_{22}$ of element 2. The direction of maximum radiation of course depends upon relative phases of currents $I_1$ and $I_2$.

If the arrangement is such as to maximize radiation in the $-z$ direction, element 2 is called a *reflector*. The maximum directivity is achieved if the spacing $d$ is about $0.16\lambda$. If the driven element has length $2l_1 = \lambda/2$, the length of the reflector should be slightly greater: $0.51 < 2l_2/\lambda < 0.52$.

If the radiation is maximized in the $+z$ direction, element 2 is called a *director*. In this case, the maximum directivity is achieved with a spacing of about $0.11\lambda$. With $2l_1 = \lambda/2$, the director length should be in the range $0.38 < 2l_2/\lambda < 0.48$, that is, somewhat smaller than the driven element.

The simplest array that is called a Yagi–Uda type has both a reflector and a director. The situation is then considerably more complicated because of the interaction of the three elements, but the same conclusions as above are roughly applicable. The reflector is still larger, and the director smaller, than the driven element. The directivity turns out to not depend critically upon the spacings of the director and reflector from the driven element. The input impedance is given by

$$Z_{\text{in}} = Z_{22} + \left(\frac{I_1}{I_2}\right) Z_{21} + \left(\frac{I_3}{I_2}\right) Z_{23} \tag{4}$$

Because of the phasing of the currents, $Z_{\text{in}}$ tends to be low. It can be raised if the driven element is made a folded dipole (Sec. 12.11) for which $Z_{22}$ is four times that of the single dipole.

The addition of other, parallel reflectors has little effect since the field behind the first is small, but additional directors can be added advantageously. Typical antennas for television reception have several directors and have a radiation pattern as shown in Fig. 12.22*b*. Directivities between 10 and 100 are obtainable depending on the number of director dipoles.

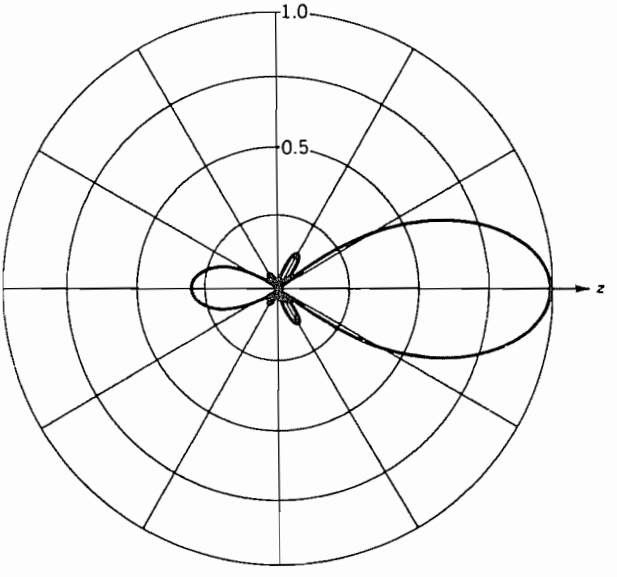


**FIG. 12.22*b*** Intensity pattern of a typical Yagi–Uda-type television receiving antenna, having four directors and one reflector. After W. L. Stutzman and G. A. Thiele, *Antenna Theory and Design*. Wiley, New York, 1981.

## 12.23 FREQUENCY-INDEPENDENT ANTENNAS: LOGARITHMICALLY PERIODIC ARRAYS

The determining factor for the radiation pattern and the impedance of a lossless antenna is the ratio of the dimensions to wavelength. Thus, if an antenna is to be scaled for use at another frequency, all dimensions must be multiplied by the ratio of the wavelengths. If the structural form of an antenna could be defined such that the multiplication of all dimensions by the wavelength ratio for two frequencies would leave the antenna unchanged, that antenna would behave identically at the two frequencies. The earliest work[31] on structures having this property considered an equiangular spiral on either a plane or conical surface with arms having the form $r = r_0 e^{a\phi}$. It is easy to see that a magnification of a structure having this form is identical to the original except for a rotation (which can be an undesirable feature). Frequency independence assumes the unrealizable condition that the spirals start at $r = 0$ (where the feed must be connected) and extend to infinity. Therefore, the properties of such structures are, in practice, only approximately frequency independent. A number of derived forms that eliminate some of the disadvantages of the equiangular spiral have been studied.

In this section we concentrate on a more convenient type of (nearly) frequency-independent antenna.[32] The idealized form is shown in Fig. 12.23*a*, in which the lo-

[31] *V. H. Rumsey,* IRE National Convention Record, *Part I, 114 (1957).*

[32] *R. H. DuHamel and G. C. Chadwick, in* Antenna Engineering Handbook, *(R. C. Johnson and H. Jasik, Eds.), 2nd ed., Chap. 14, McGraw-Hill, New York, 1984.*

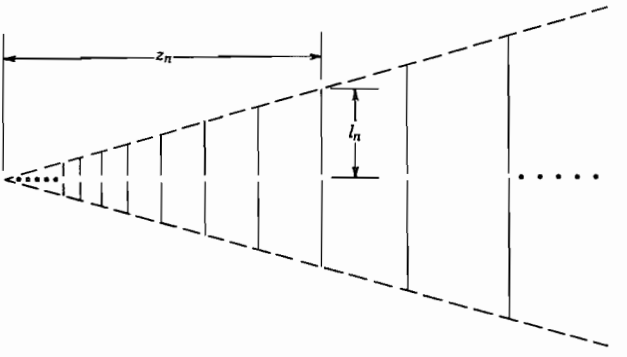


**FIG. 12.23*a*** Logarithmically periodic antenna array.

cations of the parallel-wire elements and their lengths increase from one to the next in the fixed ratio $\tau$:

$$\begin{aligned} z_n &= \tau z_{n-1} \\ l_n &= \tau l_{n-1} \end{aligned} \tag{1}$$

If the wavelength is multiplied by $\tau$, then all arm lengths and positions should be multiplied by $\tau$ so that everywhere the ratio of length to wavelength is the same. The result is a structure that is identical to the original. Therefore, the single structure appears the same at $\lambda_1$, $\tau\lambda_1$, $\tau^2\lambda_1$, and so on. Expressed in terms of logarithms,

$$\log \lambda_n = \log \lambda_1 + (n - 1) \log \tau \tag{2}$$

and correspondingly for frequency,

$$\log f_n = \log f_1 - (n - 1) \log \tau \tag{3}$$

The structure is called *logarithmically periodic.*

An understanding of the radiation properties can be aided by noting the qualitative relationships between three adjacent elements in this antenna and the three-element Yagi–Uda array discussed in the preceding section. It is found from detailed calculations that maximum radiation along the array occurs when the element has a length of about $\lambda/2$. This could be expected from the fact that the element at resonance will have the maximum current for a given drive voltage. Let us consider the resonant element and its two neighbors. We saw in the Yagi–Uda array that the larger acts as a reflector and the smaller as a director, with radiation, therefore, toward the small end of the array.

The input to the transmission line feeding the array is at the small end for a reason to be discussed below. By using alternating connections to the line as shown in Fig. 12.23*b*, and spacing the elements by one-half the element length at that point in the array, the phasing of adjacent elements in the region of maximum radiation is such that the current in the $n + 1$th element leads that in the $n$th by $\pi/2$ rad. Since the $n$th

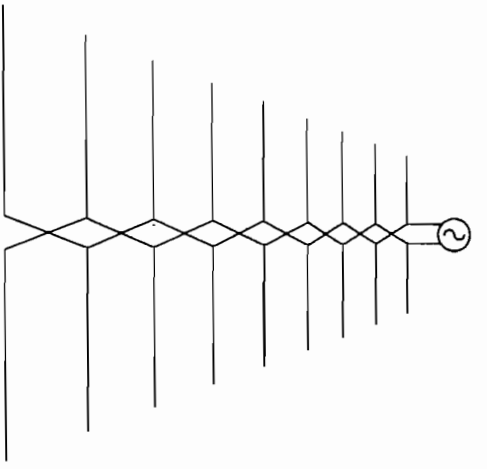

**FIG. 12.23*b*** Manner of connecting antenna elements to the driving transmission line for a logarithmically periodic antenna.

element is resonant ($l_n = \lambda/4$), the spacing to the $n + 1$th element is $\lambda/4$, and its radiation in the direction toward the small end of the array is in phase with that from the $n$th element.

Detailed calculations show that the phase of the transmission-line voltage provided to the dipoles advances uniformly away from the feedpoint up to the region of the strongly radiating dipoles. The amplitude decays slowly because the short elements are radiating inefficiently up to the region of strong radiation. Over a range of a few elements, the voltage level drops by a factor of 10 and then slowly decays over the remainder of the array. The point of maximum radiation moves toward the small end as frequency is increased and vice versa. The pattern and input impedance were earlier said to repeat at wavelengths $\tau''\lambda_1$, and detailed calculations show that there is little variation between those wavelengths. Because any real antenna is of limited length and there is a minimum practical size at the small end, the frequency (or wavelength) range of constant pattern and input impedances is limited. Roughly speaking, the range of operation is bounded by wavelengths equal to twice the lengths of the dipoles at the ends of the array. In fact, since several dipoles are involved in the region of large radiation, the bandwidth is somewhat smaller.

As pointed out above, the need for alternating the dipole connections to the feeding transmission line arises because of feeding from the small end of the array. The reason for not feeding from the large end is that if the $\lambda/2$ resonance for some given frequency were near the small end, the power flowing from the large end would have encountered dipoles of lengths $n\lambda/2$, which would radiate and excite the other resonant dipoles toward the small end with the result of multiple radiation points. Their locations would depend upon frequency so neither the pattern nor the input impedance would remain constant.

## 12.24 INTEGRATED ANTENNAS

Antennas made of metal "patches" which may be placed on dielectrics and fed by microstrip or one of the coplanar transmission lines are small, light, and easy to fabricate. They are especially suitable for use with microwave integrated circuits and so may be called *integrated antennas*. They are also known as *patch antennas*, and those in microstrip form, *microstrip antennas*. There are many variations described in texts and review articles on this subject.[33–36] We will consider here a few simple examples which illustrate some of the special features of this class of antennas.

**Simple Microstrip or Patch Antenna** Figure 12.24*a* shows a rectangular patch placed upon a dielectric with conducting ground plane, excited by an auxiliary microstrip transmission line of much higher characteristic impedance. It is recognized that this is the same configuration analyzed in Sec. 10.6 as a resonator. The resonant modes were found there, approximately, by considering open-circuit boundary conditions at each edge of the patch. Since electric fields are then a maximum at these edges, they provide a source of radiation. For use as a resonator, it is generally important to keep this radiation small, but it is the desired effect when used as an antenna. To calculate the radiation, the electric field at the edges may be represented by magnetic current sheets as explained in Sec. 12.12.

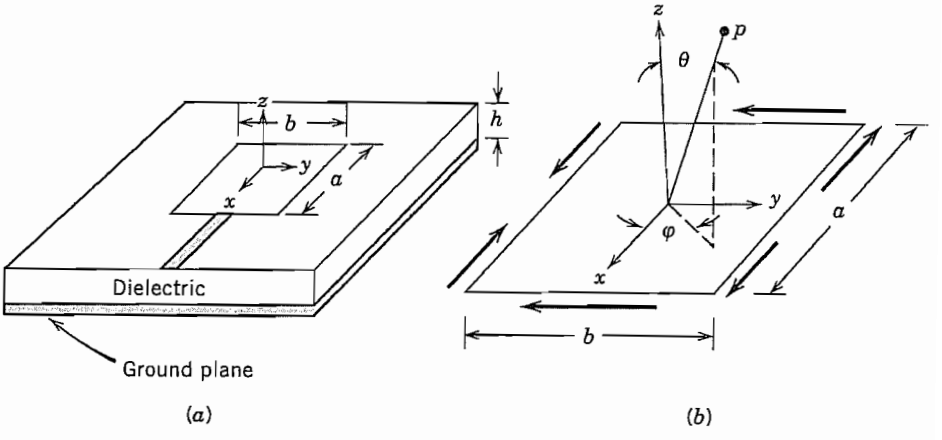


**FIG. 12.24** (a) Rectangular patch antenna in microstrip form. (*b*) Enlarged view of patch. Dark arrows show direction of magnetic currents.

[33] *D. M. Pozar,* Proc. IEEE ***80****, 79 (1992).*
[34] *K. R. Carver and J. W. Mink,* IEEE Trans. Antennas Propagation ***AP-29****, 2 (1981).*
[35] *D. B. Rutledge et al., in* Infrared and Millimeter Waves *(K. J. Button, Ed.), Vol. 10, Academic Press, San Diego, CA, 1983.*
[36] *C. Balanis,* Antenna Theory Analysis and Design, *Sec. 11.7, Wiley, New York, 1982.*

Let us consider the simplest mode with no variations in $z$ or $y$ and one half-sine variation in $x$. This is in effect the resonant standing wave of the microstrip transmission line formed by the patch, with reflections at the open circuit at $x = -a/2$ and also at the junction with the high impedance line at $x = a/2$. With neglect of the fringing effects at the edges, fields within the dielectric of the patch region may be written

$$E_z = E_0 \sin \frac{\pi x}{a} \tag{1}$$

$$H_y = \frac{-jE_0\pi}{\omega\mu a} \cos \frac{\pi x}{a} \tag{2}$$

From Eq. 12.12(2), the electric field along the edges may be replaced by magnetic current sheets of surface density $\mathbf{M}_s = -\mathbf{n} \times \mathbf{E}$, where $\mathbf{n}$ is the outward normal to the surface. Thus, $\mathbf{n} = -\hat{\mathbf{x}}$ at $x = -a/2$, $\hat{\mathbf{x}}$ at $x = a/2$, $-\hat{\mathbf{y}}$ at $y = -b/2$, and $\hat{\mathbf{y}}$ at $y = b/2$. Surface magnetic currents are then

$$\begin{aligned} M_{sy} &= -E_0 && \text{at } x = \pm a/2 \\ M_{sx} &= -E_0 \sin \frac{\pi x}{a} && \text{at } y = -b/2 \\ M_{sx} &= E_0 \sin \frac{\pi x}{a} && \text{at } y = b/2 \end{aligned} \tag{3}$$

Because of the ground plane, there is radiation only in the upper half space, $0 \leq \theta \leq \pi/2$. The ground plane may be taken care of by imaging, which for the parallel magnetic currents doubles their values. The $x$-directed magnetic currents produce little radiation since there are equal and opposite components along the sides as shown in Fig. 12.24*b*. $M_{sy}$ is the same along both sides where it applies, however, so it produces the dominant radiation. From Eq. 12.12(8), the magnetic radiation vector $\mathbf{L}$ for either of the sides, with respect to its center, using $r' = y'$, $\theta' = \pi/2$, and $\phi' = \pi/2$, is

$$\begin{aligned} \mathbf{L}_{y0} &= h \int_{-b/2}^{b/2} (-2E_0 e^{jky' \sin\theta \sin\phi}) dy' \\ &= 4hE_0 \left[ \frac{\sin\left(\frac{kb}{2} \sin\theta \sin\phi\right)}{k \sin\theta \sin\phi} \right] \end{aligned} \tag{4}$$

Now, placing the two sides at $x = \pm a/2$ and adding contributions by the array formulation (Sec. 12.18) with $\theta' = \pi/2$, $\phi' = 0$,

$$\begin{aligned} L_y &= L_{y0}[e^{-jka/2 \sin\theta \cos\phi} + e^{jka/2 \sin\theta \cos\phi}] \\ &= 2L_{y0} \cos\left(\frac{ka}{2} \sin\theta \cos\phi\right) \end{aligned} \tag{5}$$

Fields in the radiation zone may be obtained by using Eqs. 12.12(9) and (10) and

$$\left.\begin{aligned} E_\theta &= -\frac{je^{-jkr}}{2\lambda r} L_\phi = -\frac{je^{-jkr}}{2\lambda r} L_y \cos\phi \\ E_\phi &= \frac{je^{jkr}}{2\lambda r} L_\theta = \frac{je^{-jkr}}{2\lambda r} L_y \sin\phi \cos\theta \end{aligned}\right\} 0 \le \theta \le \pi/2 \tag{6}$$

From a study of the above expressions, it is found that field is a maximum at $\theta = 0$ (normal to the plane) as expected since contributions add in phase in that direction.

These patches are not very efficient radiators, meaning that $Q$ of the resonant mode is relatively high and bandwidth is narrow. Since field strength (6) is proportional to $h$, radiation can be increased by increasing thickness of the dielectric up to the point where guided surface modes in the dielectric can be supported, propagating energy away.

**Integrated Antennas Without Ground Planes** Integrated antennas for use with coplanar strip transmission lines or coplanar waveguides are placed upon a dielectric which generally does not have a ground plane. The major problem then is that the antenna tends to radiate primarily into the dielectric. Radiation may then be taken out the back or in other ways extracted from the dielectric but not always conveniently. The radiation into the dielectric may be explained in a number of ways. One follows from the point of view (Sec. 12.1) that radiation comes about because of phase differences at the observation point from different parts of the radiator. These phase differences obviously increase with increasing dielectric constant. We shall see this effect specifically in the following example.

Consider the dipole and slot antennas on a dielectric filling the half-space (Figs. 12.24*c* and *d*). The fields from the slot antenna are the simplest to calculate since the conducting plane essentially isolates the two half-spaces. Consider an elemental field component $E_x$ of a slot of width $g$ radiating into the dielectric. Equivalent magnetic current surface density is then

$$\mathbf{M} = \hat{\mathbf{y}} \times \hat{\mathbf{x}} E_x = -\hat{\mathbf{z}} E_x \tag{7}$$

The radiation vector $\mathbf{L}$ is then $-jE_x g\,(dz)$ from which we calculate electric field in the radiation zone as

$$dE_\phi = \frac{-je^{-jkr}}{4\pi r} kgE_x dz \sin\theta \tag{8}$$

Since the field is proportional to $k$, it increases with dielectric constant as $\varepsilon^{1/2}$. This is the point made earlier concerning the importance of phase differences over the element. Moreover, the Poynting vector is

$$(P_r)_{av} = \frac{|E|^2}{2\eta} = \frac{|E|^2}{2}\left(\frac{\varepsilon}{\mu}\right)^{1/2} \tag{9}$$

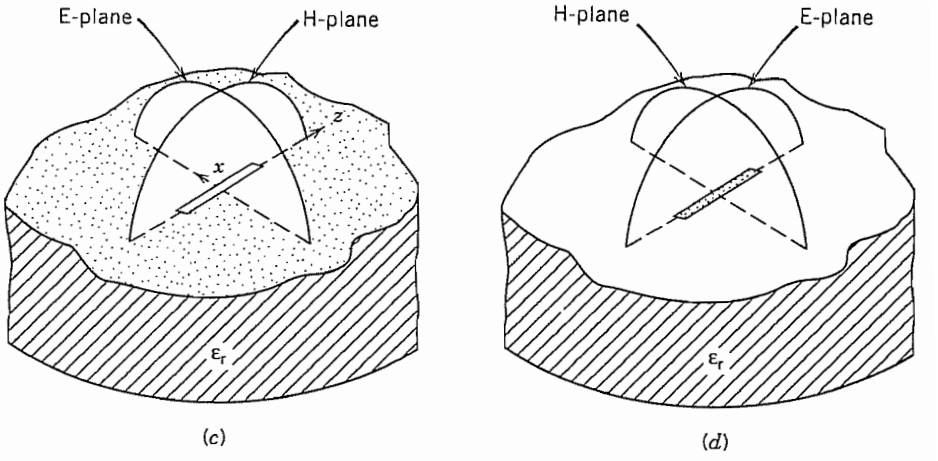


**FIG. 12.24** (*c*) Elementary slot on a dielectric. (*d*) Elementary dipole on a dielectric. Dots indicate metallization.

So the Poynting vector increases as $\varepsilon^{3/2}$. For $\varepsilon_r = 4$, this produces eight times the intensity in the dielectric as compared with that in air.

For the elemental dipole antenna, the patterns in air and the dielectric are quite different in shape. In particular there is a maximum in the H-plane pattern at the critical angle and a null in the E-plane pattern at that angle for the dielectric region.[34] The explanation for the sharp maximum and null is most readily given from reciprocity, viewing it as a receiving antenna (Prob. 12.30e). Patterns are shown for elemental dipoles and slots in Figs. 12.24*e* and *f*.

For both slot and dipole, phase velocity is between that of air and the dielectric, approximately the mean of these values, so this must be used in setting resonant lengths. Also, the fields of dipole and slot are no longer duals of one another as they would be if air or space were on both sides. Booker's formula Eq. 12.16(8), relating impedances holds approximately, however, if mean dielectric constant $\varepsilon_m$ is used.[35] (This applies to more generally shaped strips and complementary slots.)

$$Z_{\text{strip}} Z_{\text{slot}} \approx \frac{1}{4} \frac{\mu}{\varepsilon_m} \tag{10}$$

Of the many variations of these integrated-circuit-type antennas, the flared coplanar strip version pictured in Fig. 12.2*j* is analogous to a horn antenna and has broadband characteristics. Logarithmically periodic antennas (Sec. 12.23) have also been made on dielectrics. Arrays of the elements are important, easily made, and analyzable by standard array theory.

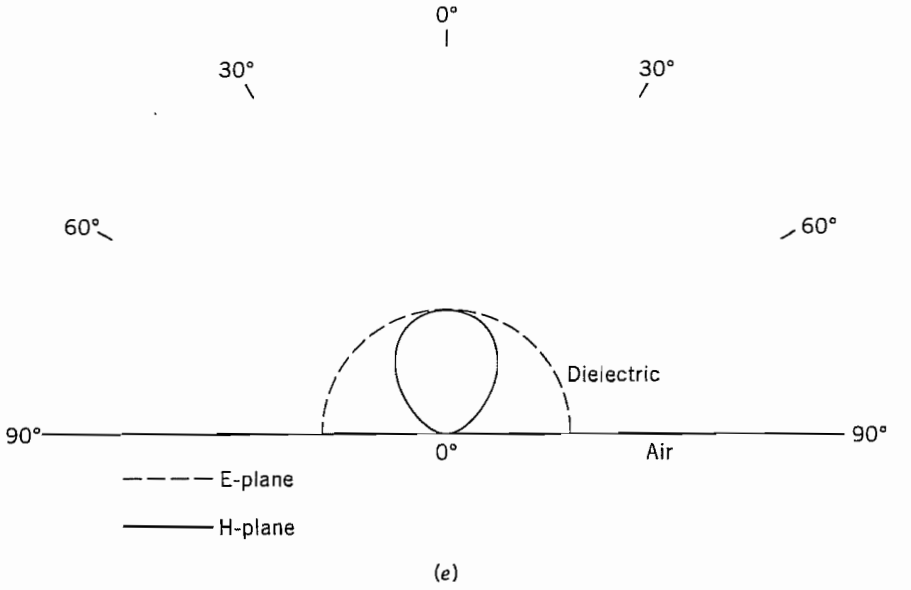


(*e*)

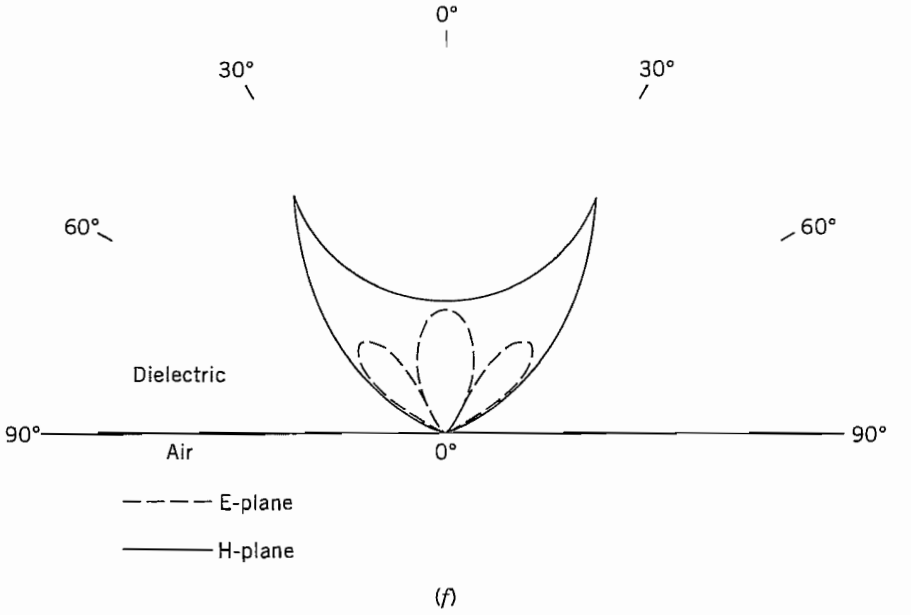


(*f*)

**FIG. 12.24** (*e*) Intensity pattern for elementary slot on dielectric with $\varepsilon_r = 4$. (*f*) Corresponding pattern for elementary dipole on dielectric. From D. B. Rutledge et al. in *Infrared and Millimeter Waves* (K. J. Button, Ed.), Vol. 10, Academic Press, San Diego, CA, 1983.

# Field Analysis of Antennas

## 12.25 The Antenna as a Boundary Value Problem

In our discussion of antennas, we have thus far made assumptions about currents along conductors or fields in the apertures of the system. This approach has proved useful, especially for calculating radiation patterns, directivity, and other aspects of the far-zone solution. One would like, however, to check the assumed current or field distribution and to have better knowledge of the near-zone fields. These last are especially important in calculating antenna impedances, or the couplings between nearby radiating elements. In principle, one has only to solve Maxwell's equations subject to boundary conditions, much as we did for waveguides and cavity resonators. There are only a few shapes for which this has been found possible in analytic form. Powerful numerical methods are rapidly extending the classes of antennas for which field and current distributions can be found.[37] The analytic solutions for the idealized shapes still provide important physical pictures so the boundary value approach to three of these will be presented in this and the following section.

**Spherical and Spheroidal Antennas** One straightforward approach is that of adding wave solutions to fit the boundary conditions, much as we did in static problems and in waveguides. The simplest configuration to illustrate the procedure is the spherical one, illustrated in Fig. 12.25*a*. Although not terribly important in itself, a straightforward extension to spheroidal shapes does lead to more practical results. Field solutions in spherical coordinates have been given in Sec. 10.7. The antenna shown is excited with an azimuthally symmetric $E_\theta$ at the equator, so the symmetric TM set with $E_\theta$, $E_r$, and $H_\phi$ is appropriate. We have seen in Sec. 12.3 that the lowest order of these represents radiation from an infinitesimal dipole, but now we form a series. From Eqs. 10.7(19), using the second Hankel function for the Bessel function in the region extending to infinity,

$$H_\phi(r, \theta) = \sum_{n=1}^{\infty} A_n r^{-1/2} P_n^1(\cos\theta) H_{n+1/2}^{(2)}(kr) \tag{1}$$

$$E_\theta(r, \theta) = \sum_{n=1}^{\infty} \frac{jA_n}{\omega\varepsilon} r^{-3/2} P_n^1(\cos\theta)[krH_{n-1/2}^{(2)}(kr) - nH_{n+1/2}^{(2)}(kr)] \tag{2}$$

If the exact excitation field in the gap were known, the coefficients $A_n$ could be determined from the orthogonality relations for associated Legendre polynomials [Eqs. 10.7(14) and (15)]. Then the boundary values at $r = a$ are

$$E_\theta(a, \theta) = \sum_{n=1}^{\infty} b_n P_n^1(\cos\theta) \tag{3}$$

[37] *W. L. Stutzman and G. A. Thiele,* Antenna Theory and Design, *Chap. 7, Wiley, New York, 1981.*

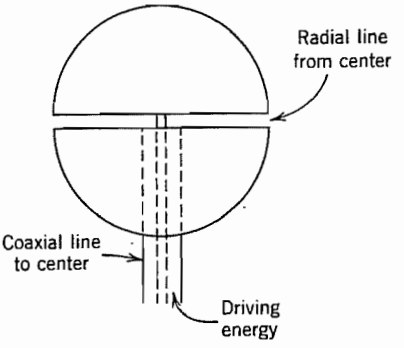


**FIG. 12.25a** Spherical antenna and possible driving system.

where

$$b_n = \frac{2n + 1}{2n(n + 1)} \int_0^{\pi} E_\theta(a, \theta) P_n^1(\cos \theta) \sin \theta \, d\theta \tag{4}$$

If the conductor is good, $E_\theta$ may be made zero everywhere except in the gap, but field is usually not known exactly there. One might assume a form (say a uniform field over a finite gap), but for our purposes we take the gap as infinitesimal, given only that the integral of field is equal to applied voltage. This is equivalent to assuming an impulse or delta function $V_0\delta(\cos \theta)$ in the gap. Then $b_n$ from (4) is readily obtained,

$$b_n = \frac{(2n + 1)P_n^1(0)V_0}{2n(n + 1)a} \tag{5}$$

and by comparison with (2), with $r = a$,

$$A_n = \frac{\omega \varepsilon a^{3/2} b_n}{j[kaH_{n-1/2}^{(2)}(ka) - nH_{n+1/2}^{(2)}(ka)]} \tag{6}$$

Substitution of (6) in (1) and (2) gives the complete solution for the fields around the sphere. To find input admittance, we first calculate current at the gap from the $\theta$-directed surface current $J_{s\theta}$:

$$I = -2\pi a J_{s\theta}(\pi/2) = 2\pi a H_\phi(a, \pi/2) \tag{7}$$

Input admittance is

$$Y = I/V_0 = \sum_{n=1}^{\infty} Y_n \tag{8}$$

and with (1), (5), and (6),

$$Y_n = \frac{j\pi(2n + 1)[P_n^1(0)]^2}{n(n + 1)\eta} \left[ \frac{n}{ka} - \frac{H_{n-1/2}^{(2)}(ka)}{H_{n+1/2}^{(2)}(ka)} \right]^{-1} \tag{9}$$

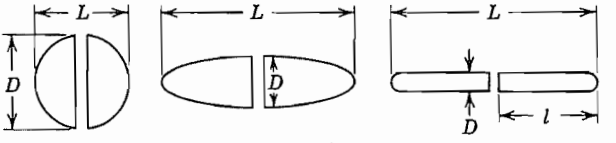


**FIG. 12.25*b*** Transition from sphere to thin spheroidal wire dipole.

It is found that the conductive or real part converges and gives a useful value for this antenna shape. The imaginary or susceptive part does not converge however, since there is infinite capacitance for the infinitesimal gap. One can make an estimate of the finite number of terms to retain for a finite gap size, but in a practical case the connection to the feed line has much to do with the actual input capacitance. In any event the principles and difficulties of finding exact field solutions are well illustrated by this example.

Stratton and Chu[38] used a similar approach but with prolate spheroidal wave functions for the more practical, spheroidal antennas illustrated in Fig. 12.25*b*. Several features associated with past antenna knowledge are shown by their analysis. Resonance (zero reactance) is near the half-wave condition, but not exactly there. Resistance at the resonant condition is near the 72-Ω value known for filamentary half-wave dipoles (see Sec. 12.5). Fatter antennas give broader bandwidth (i.e., less variation of input impedance about the resonant point). For thin antennas ($L/D \gg 1$) the analysis shows current distribution well approximated by a sinusoid, as assumed in our earlier calculations for wire antennas.

**The Biconical Antenna and Its Extensions** Another shape for which the boundary value problem may be formulated in terms of a series of spherical wave solutions is that of the biconical antenna used as an example for qualitative discussion in Sec. 12.1. This has been especially important in giving the picture of the antenna as a transducer between waves on the input transmission system and waves in space. Referring to Fig. 12.1, the solutions for the exterior region, $r > l$, are of the same form as (1) and (2). For the interior region, $r < l$, the Bessel function selected is $J_{n+1/2}(kr)$, and a second solution[39] for the associated Legendre function is required to satisfy the two boundary conditions of $E_r = 0$ at $\theta = \psi$ and $\pi - \psi$. The continuity condition at $r = l$ requires that $E_\theta$ and $H_\phi$ be continuous for $\psi \leq \theta \leq \pi - \psi$ and $E_\theta$ be zero over the conducting caps $0 < \theta < \psi$ and $\pi - \psi < \theta < \pi$. Tai[40] and Smith[41] carried out the matching exactly for certain angles, but probably most useful are some approximate

[38] *J. A. Stratton and L. J. Chu,* J. Appl. Phys. ***12****, 236, 241 (1941).*

[39] *The second solution is often designated* $Q_n^1(\cos\theta)$ *but for general angles* $\psi$, n *is not an integer so that* $P_\nu^1(-\cos\theta)$ *may then be shown to be a linearly independent second solution. See, for example, S. A. Schelkunoff,* Proc. IRE ***29*** *493 (1941); S. A. Schelkunoff and C. B. Feldman,* Proc. IRE ***30****, 512 (1942).*

[40] *C. T. Tai,* J. Appl. Phys. ***20****, 1076 (1949).*

[41] *P. D. Smith,* J. Appl. Phys. ***19****, 11 (1948).*

matchings carried out by Schelkunoff for relatively small-angle cones. One of his methods expands the far-zone fields calculated from a sinusoidal distribution of currents along the cones in spherical TM modes for the exterior region, then shows that they are nearly equal term by term to the modes of the interior region. All these higher-order modes, inside and outside, are shown to act exactly as a terminating impedance for the TEM mode on the biconical transmission-line system, and this termination may be transformed to the source at the origin by transmission-line theory.

The characteristic impedance and load admittance of the transmission-line representation are, respectively,

$$Z_0 = \left(\frac{\eta}{\pi}\right) \ln \cot\left(\frac{\psi}{2}\right) \tag{10}$$

$$Y_L = \frac{1}{Z_0^2} \sum_{m=0}^{\infty} b_m J_{2m+3/2}(kl) H^{(2)}_{2m+3/2}(kl) \tag{11}$$

where

$$b_m = \frac{30\pi kl(4m + 3)}{(m + 1)(2m + 1)} \tag{12}$$

The input impedance plotted from these expressions as functions of $l/\lambda$ show the same general features as those given above for the spheroidal antenna (with some differences for shape) for lengths $2l \approx \lambda/2$, but were also extended to larger values of $l/\lambda$. In the vicinity of the antiresonance, $2l \approx \lambda$, input resistance is high (order of thousands of ohms) and very sensitive to antenna diameter.

Schelkunoff extended his point of view to dipole antennas of other shapes by considering them to have essentially the same load impedance as the biconical antenna, with this impedance transformed to the input by a nonuniform transmission-line theory depending upon the configuration of the antenna. In the cylindrical dipole of Fig. 12.25*c*, for example, an element at radius $r$ from the origin may be considered a section of biconical transmission line with $\psi \approx a/r$. As $r$ varies, $Z_0$ varies, but nonuniform transmission-line theory may be used to transform $Y_L$ of (11) to the input. Curves of input resistance and reactance calculated by Schelkunoff in this way are shown in Figs. 12.25*d* and *e*. The values of $Z_0$ shown are the average values over the length of the dipole. Note that bandwidth is greater for the fatter antennas (lower $Z_0$).

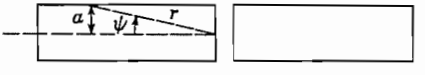


**FIG. 12.25c** Cylindrical dipole interpreted as a nonuniform transmission line.

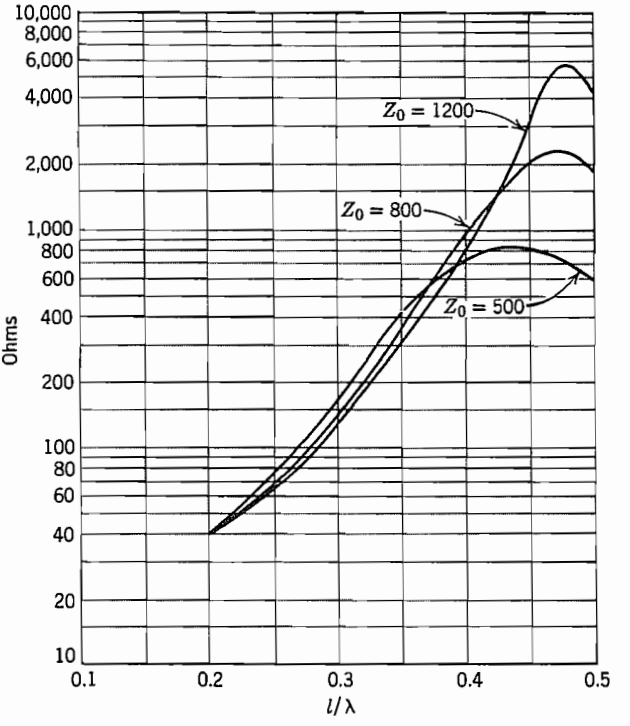


**FIG. 12.25*d*** Input resistance for cylindrical dipole antenna. From S. A. Schelkunoff, *Proc. IRE* **29**, 493 (1941).

The biconical model is also useful in telling something about the current distribution along dipole antennas. The current in the dominant TEM wave of the loss-free biconical line is exactly sinusoidal, so departures from a sinusoidal distribution are due either to losses, the higher-order modes near the end of the antenna, or the perturbations arising from nonuniform line effects if the shape is other than biconical. For low-loss, long, thin antennas, these effects are small so that the sinusoidal assumptions made earlier are reasonable.

## 12.26 Direct Calculation of Input Impedance for Wire Antennas

The spheroidal and biconical antennas considered in the preceding section were shown to approximate wire antennas in the limit, but it may seem more natural to work with a cylindrical structure from the start. Much work has been done on the cylindrical

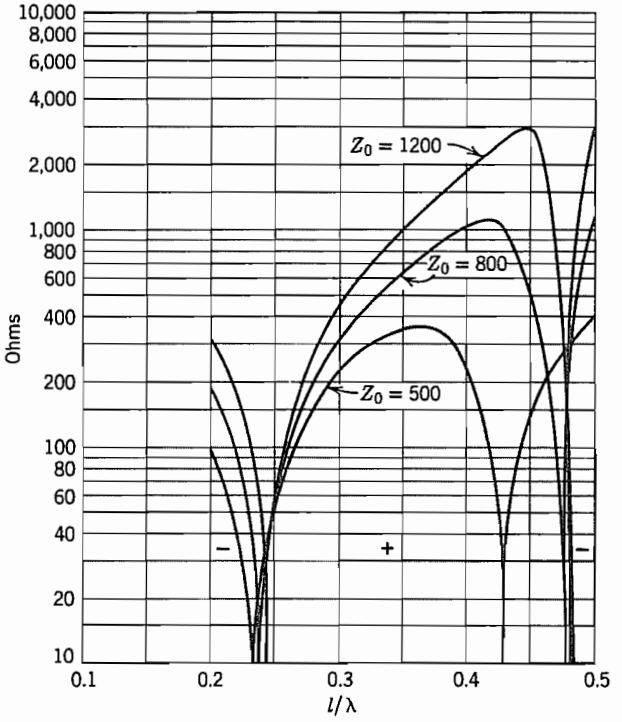


**FIG. 12.25e** Input reactance for cylindrical dipole antenna. From S. A. Schelkunoff, *Proc. IRE* **29**, 493 (1941).

configuration,[42] generally based upon an integral equation approach. We will see how this equation is set up and used with approximations to obtain antenna impedance.

Consider a circular cylindrical radiator of length $2l$ and radius $a$ with an infinitesimal gap in the center (Fig. 12.26). The cylinder is a perfectly conducting tube with negligibly thin walls so end currents can be neglected. The electric field $E_{az}(z)$ is zero on the surface at $r = a$ except in the gap at the center where we assume it can be represented by a delta function so that

$$-\int_{-l}^{l} E_{az}(z)\,dz = V \quad \text{and} \quad E_{az}(z) = 0 \quad \text{for} \quad z \neq 0 \tag{1}$$

where $V$ is the applied voltage. Let us construct a surface $S$ just outside the radiator and have the current $J_{az}(z)$ that flows on the surface of the radiator flow, instead, on

[42] *For examples: R. S. Elliott,* Antenna Theory and Design, *Chap. 7, Prentice Hall, Englewood Cliffs, NJ, 1981; R. E. Collin,* Antennas and Radiowave Propagation, *Sec. 2.9, McGraw-Hill, New York, 1985; J. D. Kraus,* Antennas, *2nd ed., Chap. 10, McGraw-Hill, New York, 1988; C. Balanis,* Antenna Theory Analysis and Design, *Chap. 7, Wiley, New York, 1982.*

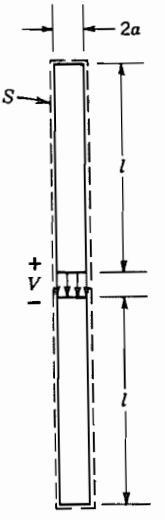


**FIG. 12.26** Circular cylindrical dipole radiator used in calculation of terminal impedance by emf method. The spacing between $S$ and the cylinder is infinitesimal.

the surface $S$. Then the conducting cylinder can be removed and the fields outside $S$ are the same as in the original situation. Additionally, we place an arbitrary (but later to be specified) current $I_b(z)$ along the axis. Since both currents are inside $S$, we can apply the reciprocity theorem quoted in Eq. 11.3(3),

$$\oint_S (\mathbf{E}_a \times \mathbf{H}_b - \mathbf{E}_b \times \mathbf{H}_a) \cdot \mathbf{dS} = 0 \tag{2}$$

where $\mathbf{E}_a$ and $\mathbf{H}_a$ are fields of current $J_a$ and fields $\mathbf{E}_b$ and $\mathbf{H}_b$ are those of current $I_b$.

Assuming very small radius $a$, the fields on the end surfaces of $S$ can be neglected. Also making use of symmetry in $\phi$, (2) becomes

$$\int_{-l}^{l} 2\pi a[E_{az}(a, z)H_{b\phi}(a, z) - E_{bz}(a, z)H_{a\phi}(a, z)]\,dz = 0 \tag{3}$$

The field $H_{a\phi}(a, z)$ can be put in terms of current since

$$2\pi a H_{a\phi}(a, z) = 2\pi a J_{sa}(z) = I_a(z) \tag{4}$$

Then from (3) with (1) and (4), we get

$$2\pi a H_{b\phi}(a, 0)V = -\int_{-l}^{l} E_{bz}(a, z)I_a(z)\,dz \tag{5}$$

Assuming radius $a$ small, we can make the approximation

$$2\pi a H_{b\phi}(a, 0) \approx I_b(0) \tag{6}$$

Since $I_b(z)$ is arbitrary, we can take it to be identical with $I_a(z)$. Using these arguments and dropping the now-superfluous subscripts $a$, we have

$$I(0)V = -\int_{-l}^{l} E_z(a, z)I(z)dz \tag{7}$$

and the induced emf formula for input impedance becomes

$$Z = \frac{V}{I(0)} = -\frac{1}{I^2(0)}\int_{-l}^{l} E_z(a, z)I(z)dz \tag{8}$$

To make use of (8), we first assume a current distribution $I(z)$ and calculate the field $E_z(z)$ that $I(z)$ would produce along the surface of $S$ at $r = a$ and then perform the integration. Using the sinusoidal current distribution in Eqs. 12.5(1) that has been shown to be reasonably accurate for thin antennas and the retarded potential (Sec. 3.21), the electric field $E_z$ along the surface $S$ can be found to be

$$E_z = -\frac{j\eta}{4\pi} I_m \left(\frac{e^{-jkr_1}}{r_1} + \frac{e^{-jkr_2}}{r_2} - 2\cos kl\,\frac{e^{-jkr}}{r}\right) \tag{9}$$

where $I_m$ is the peak value of the standing current wave and the other quantities are

$$\begin{aligned} r_1 &= [(l - z)^2 + a^2]^{1/2} \\ r_2 &= [(l + z)^2 + a^2]^{1/2} \\ r &= (a^2 + z^2)^{1/2} \end{aligned} \tag{10}$$

Substituting (9) in (8) gives the impedance

$$Z = j30\left(\frac{I_m}{I(0)}\right)^2 \int_{-l}^{l} \sin k(l - |z|)\left(\frac{e^{-jkr_1}}{r_1} + \frac{e^{-jkr_2}}{r_2} - 2\cos kl\,\frac{e^{-jkr}}{r}\right)dz \tag{11}$$

Equation (11) can be evaluated numerically and/or can be put in terms of tabulated functions, *sine integrals*, $\mathrm{Si}(x)$ and *modified cosine integrals*, $\mathrm{Cin}(x)$.[43] The results indicate that in this approximation the resistive part of $Z$ is independent of radius $a$ but the reactance is not.

The impedance formula (8) can be recast into a form that is *stationary* with respect to the choice of $I(z)$; that is, no first-order error is made in calculation of $Z$ when the guess for $I(z)$ contains first-order errors.[44]

Study of (8) shows that this analysis is related to the circuit approach of Sec. 4.12, and the self-impedance determination is a generalization of the method of calculating inductance by considering induced fields from an equivalent current on the axis of the wire (Sec. 4.7).

[43] *E. C. Jordan and K. G. Balmain,* Electromagnetic Waves and Radiating Systems, *2nd ed., pp. 540–547, Prentice Hall, Englewood Cliffs, NJ, 1968.*

[44] *R. S. Elliott,* Antenna Theory and Design, *p. 305, Prentice Hall, Englewood Cliffs, NJ, 1981.*

## 12.27 Mutual Impedance Between Thin Dipoles

When arrays of dipoles are used, interactions between them affect the impedances seen by the feed system at their drive points. Also, a dipole with a reflector is equivalent to a pair of dipoles so the terminal impedance is similarly affected. Circuit equations relating terminal voltages and currents can be written for an array of $n$ dipoles:

$$\begin{aligned} V_1 &= Z_{11}I_1 + Z_{12}I_2 + \cdots + Z_{1n}I_n \\ V_2 &= Z_{21}I_1 + Z_{22}I_2 + \cdots + Z_{2n}I_n \\ &\vdots \\ V_n &= Z_{n1}I_1 + Z_{n2}I_2 + \cdots + Z_{nn}I_n \end{aligned} \tag{1}$$

The input impedance for dipole 1 is

$$Z = \frac{V_1}{I_1} = Z_{11} + Z_{12}\frac{I_2}{I_1} + \cdots + Z_{1n}\frac{I_n}{I_1} \tag{2}$$

In the absence of terminal currents on the other dipoles $Z = Z_{11}$, which is usually assumed to be the terminal impedance of the isolated dipole calculated in the preceding section. (The currents induced on the open-circuited neighboring dipoles produce an important reaction on the one excited only if they are extremely close or the length is near $n\lambda/2$.) The off-diagonal terms represent the mutual effects and are called *mutual impedances*. It is further assumed that mutual impedances can be calculated between any two of the dipoles with the others open-circuited and not producing significant effect on the pair being considered.

Let us consider two dipoles as shown in Fig. 12.27*a* where we have made them

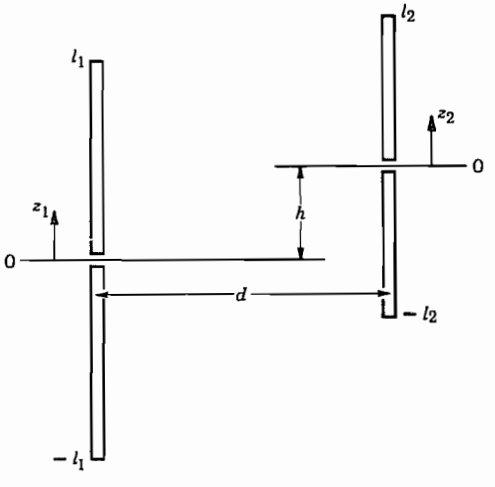


**Fig. 12.27*a*** Model for mutual impedance calculation for a pair of thin dipoles.

parallel but not necessarily of the same length or having their centers in the same plane. The mutual impedance is defined as the ratio of the open-circuit voltage in dipole 1 produced by a current in dipole 2 to the terminal current of dipole 2:

$$Z_{12} = \frac{(V_1)_{oc}}{I_2(0)} \tag{3}$$

This is recognized as an extension of mutual inductance ideas with retardation included. It can be argued from the general reciprocity theorem (see Prob. 12.27) that

$$Z_{12} = -\frac{1}{I_1(0)I_2(0)} \int_{-l_2}^{l_2} E_z^1(z_2) I_2(z_2) dz_2 \tag{4}$$

Here $I_2(z_2)$is the assumed current distribution in dipole 2 with terminal value $I_2(0)$, and $E_z^1(z_2)$ is the electric field along the surface of dipole 2 that would exist in its absence if a current were impressed on dipole 1 with terminal value $I_1(0)$. The electric field $E_z^1(z_2)$ can be expressed by Eq. 12.26(9) with $l$ being $l_1$ in the present problem, if we make the usual assumption of sinusoidal current distribution for $I_1$. In this case,

$$\begin{aligned} r &= [d^2 + (h + z_2)^2]^{1/2} \\ r_1 &= [d^2 + (h + z_2 - l_1)^2]^{1/2} \\ r_2 &= [d^2 + (h + z_2 + l_1)^2]^{1/2} \end{aligned} \tag{5}$$

where the displacements $d$ and $h$ are shown in Fig. 12.27*a*. Then making $I_2(z_2)$ also sinusoidal [$I_2(z_2) = I_{m2} \sin k(l_2 - |z_2|)$] one finds

$$Z_{12} = \frac{j30}{(\sin kl_1)(\sin kl_2)} \int_{-l_2}^{l_2} \left( \frac{e^{-jkr_1}}{r_1} + \frac{e^{-jkr_2}}{r_2} - 2 \cos kl_1 \frac{e^{-jkr}}{r} \right) \sin k(l_2 - |z_2|) dz_2 \tag{6}$$

A typical result is shown in Fig. 12.27*b* for two half-wave dipoles with no vertical displacement ($h = 0$) as a function of spacing $d$.

It should be noted that the result (6) is not dependent on the radii of the dipoles as long as they are small compared with wavelength and, by the same reasoning, the dipoles need not be of circular cross section for this result to apply.

## 12.28 Numerical Methods: The Method of Moments

Numerical methods have become most important for the analysis and design of radiating systems, as with other aspects of electromagnetics. Field solutions have been obtained by a variety of methods[37] but often only a global quantity, such as antenna impedance, is needed. In that case, as explained in Sec. 7.3, the method of moments is the desirable approach. We will set down the basis for this method as applied to a long straight

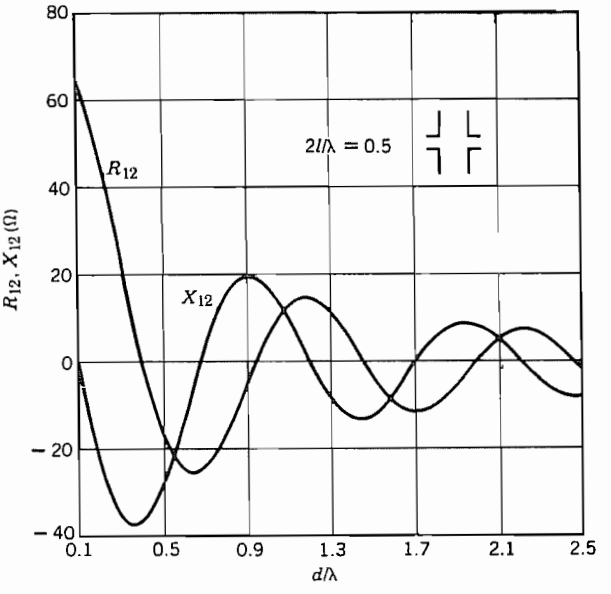


**FIG. 12.27*b*** Real and imaginary parts of mutual impedance between half-wave dipoles with zero vertical separation [($h = 0$ in Fig. 12.27*a*)] as a function of spacing. From R. S. Elliott, *Antenna Theory and Design*, © 1981, p. 333. Reprinted by permission of Prentice Hall, Englewood Cliffs, NJ.

antenna of small radius. Much of this is closely related to the integral equation development of Sec. 12.26.

We start with the assumption that impressed field $\mathbf{E}_i$ is known. The scattered field $\mathbf{E}_s$ resulting from the currents on the antenna must then just cancel $\mathbf{E}_i$ over the surface of the conductor, assumed perfectly conducting:

$$\mathbf{E}_i + \mathbf{E}_s = 0 \qquad \text{on } S \tag{1}$$

For the straight antenna, currents and fields are along the wire, so may be treated as scalars. If the antenna is thin, current may be taken as on the axis, as in Sec. 12.26. The scattered field at $z$ may then be found by integrating contributions from current along the antenna:

$$E_s(z) = \int_0^L I(z')G(z,z')dz' \tag{2}$$

$G(z,z')$ is a weighting function, called a Green's function (Appendix 5), giving the contribution to $E_s$ at $z$ from current element at $z'$. Using (1),

$$E_i(z) = -\int_0^L I(z')G(z,z')dz' \tag{3}$$

$E_i$ is known but current is unknown, so this is an integral equation for determination of $I(z)$. There are several approaches to solving this, but here we expand $I$ in a set of basis functions,

$$I(z) = \sum_{n=1}^{N} I_n F_n(z) \tag{4}$$

We next substitute this in (3), multiply by $F_m(z)$, and integrate.

$$\int_0^L E_i(z)F_m(z)dz = -\sum_{n=1}^{N} I_n \int_0^L\int_0^L F_n(z')G\ (z,z')F_m(z)dz\,dz' \tag{5}$$

or

$$V_m = \sum_{n=1}^{N} Z_{nm}I_m \tag{6}$$

where

$$V_m = \int_0^L E_i(z)F_m(z)dz \tag{7}$$

$$Z_{nm} = -\int_0^L\int_0^L F_n(z')G(z,z')F_m(z)dz\,dz' \tag{8}$$

Equation (6) may be written as a matrix equation with $V_m$ known, $Z_{mn}$ determinable, and the set of $I_m$ to be solved for by inverting the matrix. Current is then known and may be used for antenna impedance or loss from finite conductivity. The hard part is the determination of $Z_{mn}$. If sinusoidal basis functions are used, $Z_{mn}$ becomes the mutual impedance between two sinusoidal elements, as in Sec. 12.27. Richmond[45] made use of overlapping sinusoids, dividing the length $L$ into $N + 1$ segments of length $d$ and defining

$$F_n(z) = \frac{\sin\ k\ (d-|z-z_{m+1}|)}{\sin\ kd} \tag{9}$$

These are illustrated in Fig. 12.28 for $N = 3$, although many more segments would be chosen for an accurate solution unless the antenna is very short. Expressions for the mutual impedances (8) between the $m$th and $n$th sinusoidal element are available in the literature, but are complicated enough that computer solution is needed. For relatively short antennas, approximations to $Z_{mn}$ make the problem tractable by scientific calculator.[46] Other basis functions have been used, including rectangular and triangular pulses.[47]

[45] *J. H. Richmond,* IEEE Trans. Antennas Propagation **AP-18**, *694 (1970).*
[46] *E. H. Newman,* IEEE Trans. Educ. **31**, *193 (1988).*
[47] *R. E. Collin,* Antennas and Radiowave Propagation, *Sec. 2.10, McGraw-Hill, New York, 1985.*

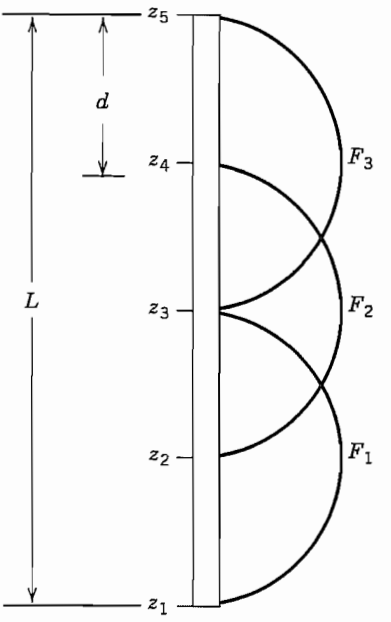


**FIG. 12.28** Straight antenna with overlapping sinusoids as basis functions for numerical analysis.

# Receiving Antennas and Reciprocity

## 12.29 A TRANSMITTING–RECEIVING SYSTEM

The discussion in previous sections has generally implied that the radiating system was to be used as a transmitting antenna, exciting waves in space from some source of high-frequency energy. The same devices useful for transmission are also useful for reception, and it will be seen that the quantities already calculated (such as the pattern, directivity, and input impedance for transmission) are the useful parameters in the design of a receiving system also. This might at first seem surprising, since the two problems have some noticeable differences. In the transmitting antenna, a generator is generally applied at localized terminals, and waves that are set up go out in space approximately as spherical wavefronts. In the receiving antenna, a wave coming in from a distant transmitter approximates a portion of a uniform plane wave, and so sets up an applied electric field on the antenna system quite different from that associated with the localized sources in the transmitting case. As a consequence, the induced fields must

be different so that total field meets the boundary conditions of the antenna, and the current distribution in general is different for the same antenna on transmission or reception. The currents set up on the receiving antenna system by the plane wave will convey useful power to the load (probably through a transmission line or guide), but will also produce reradiation or scattering of some of the energy back into space. The mechanism of this scattering is exactly the same as that discussed for radiation from a transmitting antenna, but the form may be different for a given antenna because of the different current distribution.

Thus, we seem to have somewhat different pictures of the mechanism of transmitting and receiving electromagnetic radiation. Reciprocity theorems related to those already discussed (Sec. 11.3) provide ties between the two phenomena such as the following:

1. The antenna pattern for reception is identical to that for transmission.
2. The input impedance of the antenna on transmission is the internal impedance of the equivalent generator representing a receiving system.
3. An effective area for the receiving antenna can be defined and, by reciprocity, is related to the directivity (Sec. 12.6).

These points will be discussed in this and following sections. An excellent treatment in more detail has been given by Silver.[48]

We wish to begin the discussion by considering the transmitting and receiving antennas with intermediate space (Fig. 12.29*a*) as a system in which energy is to be transferred from the first to the second. We select terminals in the feeding guide where voltage and current may be defined in the manner explained in Sec. 11.2, and similarly select a reference in the guide from the receiving antenna. The region between, including both antennas, the space, and any intermediate conductors and dielectric (assumed linear), may be represented as a two port or transducer as indicated in Fig. 12.29*b*. That is,

$$V_1 = Z_{11}I_1 + Z_{12}I_2 \tag{1}$$

$$V_2 = Z_{21}I_1 + Z_{22}I_2 \tag{2}$$

The systems discussed in Chapter 11, for which proofs of (1) and (2) were given, were assumed to be closed by conducting boundaries, whereas the present system extends to infinity. The theorems given there, however, can be extended to regions extending to infinity[49] because of the manner in which fields die off there.

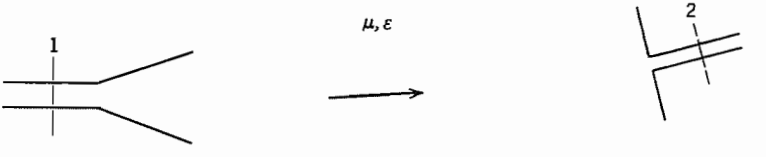


**FIG. 12.29*a*** A system of transmitting and receiving antennas.

[48] *S. Silver,* Microwave Antenna Theory and Design, *Chap. 2, IEEE Press, Piscataway, NJ, 1984.*

[49] *W. K. Saunders,* Proc. Natl. Acad. Sci. USA ***38****, 342 (1952).*

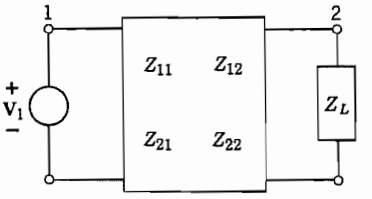


**FIG. 12.29b** Equivalent representation for Fig. 12.29*a*.

The present system is specialized in another respect in that the coupling impedance $Z_{12}$ in (1) is very small for a large separation between transmitter and receiver. It may then be neglected in (1), and the impedance coefficient $Z_{11}$ is just the input impedance of the transmitting antenna calculated by itself:

$$V_1 \approx Z_{11}I_1 \approx Z_A I_1 \tag{3}$$

The coupling term in (2) cannot be neglected, since this coupling is the effect being studied. Equation (2), however, can be represented by the usual equivalent circuit of Thévenin's theorem (Prob. 11.2f) in which an equivalent voltage generator $I_1Z_{21}$ is connected to the load impedance $Z_L$ through an antenna impedance $Z_{22}$ (which is essentially the input impedance of antenna 2 if driven as a transmitter). Thus, because of the small coupling, the reaction of the receiving antenna on the transmitting antenna can be neglected and the equivalent circuit separated as in Fig. 12.29*c*.

The equivalent circuit will be discussed again later. For the moment, we shall discuss transmission over the system from another point of view. For this purpose, an *effective area* of the receiving antenna is defined so that the useful power removed by the receiving antenna is given by this area multiplied by the average Poynting vector (power density) in the oncoming wave:

$$W_r = A_{er}P_{av} \tag{4}$$

Like directive gain defined previously, $A_{er}$ is in general a function of direction about the antenna and of the condition of match in the guide. When not otherwise specified, it will be assumed to be the value for a matched load. The power density at the receiver is the power density of an isotropic radiator ($W_t/4\pi r^2$) multiplied by directive gain of the transmitting antenna in the given direction. Therefore, from (4),

$$W_r = W_t \frac{A_{er}}{4\pi r^2} g_{dt} \tag{5}$$

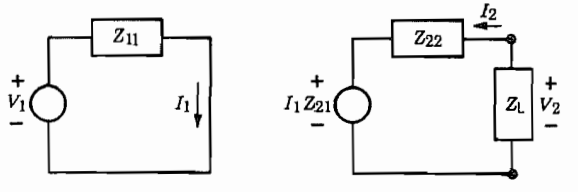


**FIG. 12.29c** Approximate equivalent circuit neglecting reaction of receiver back on transmitting system.

where $W_t$ is the power transmitted, $r$ is the distance between transmitter and receiver, $g_{dt}$ is the directive gain of the transmitting antenna, and $A_{er}$ is the effective area of the receiving antenna. We will see in Sec. 12.30 that effective area always is related to directive gain by the same constant; the constant may be found for any specific antenna and any direction and then applied to all other cases. It was seen in Sec. 12.14, for an aperture with an area $A$ large enough to ignore source currents on the surfaces surrounding it, that

$$(g_d)_{max} = \frac{4\pi}{\lambda^2} A \tag{6}$$

The last term in (6) follows from recognition that the power $W_r$ received through a large aperture oriented perpendicular to $\mathbf{P}$ is $P_{av}A$. Making use of the above-mentioned general applicability of the constant $4\pi/\lambda^2$, (5) may be written in either of the following forms given by Friis.[50] Subscripts $r$ and $t$ refer to receiving and transmitting antennas, respectively:

$$\frac{W_r}{W_t} = \frac{\lambda^2 g_{dr} g_{dt}}{(4\pi r)^2} = \frac{A_{er} A_{et}}{\lambda^2 r^2} \tag{7}$$

## 12.30 Reciprocity Relations

From the equivalent circuit of Fig. 12.29*c*, we can obtain a different form for the power delivered to the receiving antenna. For this purpose, let us assume that there is a conjugate match

$$Z_L = Z_{22}^* = R_{r2} - jX_{r2} \tag{1}$$

which is known to be the condition for maximum power transfer from the equivalent generator to the load. The power delivered to the load under this condition is

$$W_r = \frac{|I_1 Z_{21}|^2}{8R_{r2}} \tag{2}$$

If the transmitting antenna has radiation resistance $R_{r1}$, transmitted power is

$$W_t = \tfrac{1}{2}|I_1|^2 R_{r1} \tag{3}$$

so

$$\frac{W_r}{W_t} = \frac{|Z_{21}|^2}{4R_{r1}R_{r2}} \tag{4}$$

By comparing (4) with Eq. 12.29(5), we see that

$$|Z_{21}|^2 = \frac{R_{r1}R_{r2}g_{d1}A_{e2}}{\pi r^2} \tag{5}$$

[50] *H. T. Friis,* Proc. IRE **34**, *254 (1946).*

If we now reverse the roles of transmitting and receiving antennas, we find for the transfer impedance in the reverse direction

$$|Z_{12}|^2 = \frac{R_{r2}R_{r1}g_{d2}\,A_{e1}}{\pi r^2} \tag{6}$$

By the reciprocity argument of Sec. 11.3 (modified so that it applies to a region extending to infinity), $Z_{12}$ and $Z_{21}$ are equal, so we conclude

$$\frac{A_{e1}}{g_{d1}} = \frac{A_{e2}}{g_{d2}} \tag{7}$$

The antennas in the foregoing argument were arbitrary, so it follows from (7) that the ratio of effective area to directive gain for all antennas is the same. As discussed in Sec. 12.29, the constant of proportionality is known from large-aperture theory to be $\lambda^2/4\pi$. It could also be shown for other specific antennas, such as the Hertzian dipole,[51] or for the small loop antenna.

Although, for large apertures effective area equals actual area, this is not true for small antennas. In fact, for the Hertzian dipole, we found the directivity to be 1.5, so the maximum effective area is

$$(A_e)_{max} = \frac{\lambda^2}{4\pi}(g_d)_{max} = \frac{3}{8\pi}\lambda^2 \qquad \text{(for dipole)} \tag{8}$$

which is finite and sizable even though antenna size is infinitesimal.

Another relation following from reciprocity is that the pattern of a given antenna is the same for transmission and reception. This is useful because the pattern may then be calculated or measured in the easiest way and then be used for both transmission and reception designs. To show this, imagine, as in Fig. 12.30*a*, that antenna 2 is moved about the arc of a circle to measure the pattern of antenna 1. Let $\theta = 0$ be the angle of maximum response (position *a*) and angle $\theta$ (position *b*) be a general position. Then, if 1 is transmitting and 2 receiving, the power received in position *b*, as compared with position *a*, by (4) is

$$\frac{W_{2b}}{W_{2a}} = \frac{|Z_{21}|_b^2}{|Z_{21}|_a^2} \tag{9}$$

If 2 is transmitting and 1 receiving, the powers received for the two positions are related by

$$\frac{W_{1b}}{W_{1a}} = \frac{|Z_{12}|_b^2}{|Z_{12}|_a^2} \tag{10}$$

Because of reciprocity $|Z_{12}|_a = |Z_{21}|_a$, and similarly for *b*, so the ratios (9) and (10) are the same. Thus, the same relative power pattern will be measured with antenna 1 transmitting or receiving. The same result can be argued from the arrangement in Fig. 12.30*b*.

[51] *D. O. North, RCA Rev.* **6**, *332 (1942).*

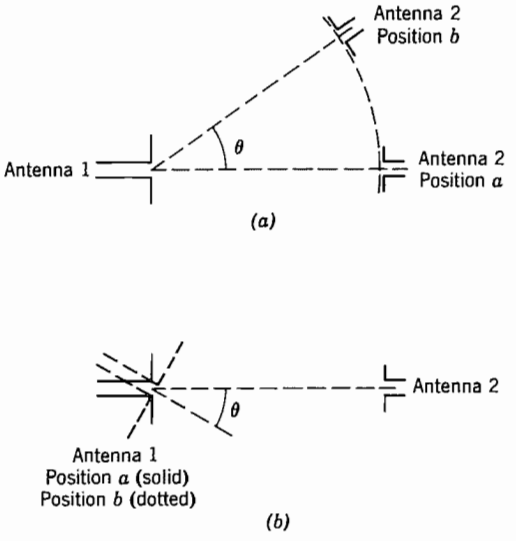


**FIG. 12.30** Possible system for pattern measurement.

It is, of course, important to remember that the reciprocity relation may be violated if the transmission path contains a medium such as the ionosphere, which may not have strictly bilateral properties. It is obvious that frequency must be kept constant when receiver and transmitter are interchanged. Also, if there are obstacles or other secondary radiators in the field, they must keep their same position relative to the system when the interchange is made. (See Prob. 12.30*b*.)

## 12.31 EQUIVALENT CIRCUIT OF THE RECEIVING ANTENNA

For a study of the circuit problem in matching the antenna to a receiver, the second part of the equivalent circuit of Fig. 12.29*c* is useful and is repeated in Fig. 12.31*a*. In this the internal impedance of the generator $Z_{22}$ is essentially the input impedance of the same antenna if driven at the same terminals:

$$Z_{22} \approx Z_{i2} \tag{1}$$

This follows by the same argument given for antenna 1 in Sec. 12.29, meaning that reaction back through $Z_{21}$ is negligible *when the antenna is driven.*

The voltage generator in Fig. 12.31*a* is given from Eq. 12.29(2) as $I_1 Z_{21}$, but transmitter current and transfer impedance are not convenient parameters for most calculations, so other forms in terms of the power density of the oncoming wave are preferable. By substitution from Eq. 12.29(4) and Eq. 12.30(2), we can find this voltage in terms of the average Poynting vector or power density of the oncoming wave $P_{av}$, the radiation resistance of the receiving antenna $R_{r2}$, and the effective area $A_{e2}$. (The effective area

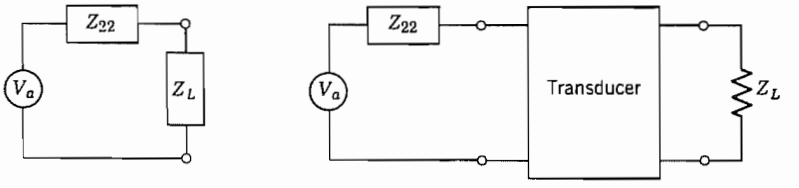


**FIG. 12.31** (a) Equivalent circuit of receiving antenna for power transfer calculations. (*b*) Circuit for receiving antenna coupled to the load through a transducer.

is calculated on the assumption of a matched load, but may be a function of the orientation of the antenna with respect to the oncoming wave.)

$$|V_a| = |I_1 Z_{21}| = (8R_{r2}A_{e2}P_{av})^{1/2} \tag{2}$$

The equivalent circuit is useful, for example, in computing the transfer of power from the antenna to the useful load through a transmission line which may have discontinuities, matching sections, or filter elements. All these may be lumped together as a transducer, as explained in the preceding chapter (Fig. 12.31*b*), and the problem from here on is a standard circuit calculation. It must be emphasized, as in any Thévenin equivalent circuit, that the equivalent circuit was derived to tell what happens in the load under different load conditions, and significance cannot be automatically attached to a calculation of power loss in the internal impedance of the equivalent circuit. In the present case, it is tempting to interpret this as the power reradiated or scattered by currents on the receiving antenna, and one would conclude that as much power is scattered under a condition of perfect match as is absorbed in the load. This conclusion is not true, except in special cases where the current distribution may be the same for reception as for transmission.

## PROBLEMS

**12.3a** An inspection of Eqs. 12.3(3) shows that there are in-phase parts other than those considered in forming the power flow. Taking into account all terms, show that the result (6) is correct for average power radiated.

**12.3b** Study the $n = 2$ TM wave and show that it corresponds to a quadrupole field, that is, a field from two small current elements at right angles.

**12.3c** Show that the fields of Eqs. 12.3(8) are those of a first-order spherical TE wave of Sec. 10.7.

**12.3d** Plot $|H_\phi|$ of the Hertzian dipole (appropriately normalized) versus $kr$ for $\theta = \pi/2$ and note (approximately) near-zone, far-zone, and transition regions. Do similarly for $|E_\theta|$.

**12.3e** Compare the near-zone fields of the magnetic dipole with the static fields of Sec. 2.10, explaining why the factor $\mu$ had to be added in applying duality. Check dimensions of the three equations in Eq. 12.3(8).

**12.3f** Compare currents required to radiate 100 W from a Hertzian dipole of length 0.1 wavelength and a current loop of circumference 0.1 wavelength.

**12.3g** Show that a circularly polarized wave may be formed in the far zone if a Hertzian dipole is placed at the center of a small current-carrying loop, the dipole being directed along the axis of the loop. Give the relation of currents in the dipole and the loop.

**12.4a** Verify the relations of Eq. 12.4(6) as the only field components of **H** remaining if components with higher power of $r^{-1}$ are neglected.

**12.4b** As in Prob. 12.4a, verify Eqs. 12.4(7).

**12.4c** Verify Eqs. 12.4(14) and (15).

**12.4d*** For the small loop antenna of radius $a \ll \lambda$, assume current distribution uniform around the loop, $I = \hat{\phi} I_0$. Take the $z$ axis perpendicular to the plane of the loop and find $A_\phi$ in the far zone. From this, obtain fields and compare with those of the magnetic dipole of Sec. 12.3. Also calculate radiation intensity and total power radiated.

**12.4e** A square loop of wire lying in the $x$–$y$ plane carries uniform current $Ie^{j\omega t}$. Sides of length $a$ are small enough compared with wavelength that each side may be considered a current element as in Sec. 12.3. Find fields in the far zones and compare with those from a circular loop of the same area, Eq. 12.3(8).

**12.5a*** Although Eq. 12.5(6) may be readily integrated numerically, it can also be evaluated in terms of tabulated functions. Let $u = \cos\theta$, separate denominator by partial fractions, and show that for $\eta = 120\pi$,

$$W = 30I_m^2 \{C + \ln 2kl - \mathrm{Ci}(2kl) + \tfrac{1}{2}(\sin 2kl)[\mathrm{Si}(4kl) - 2\,\mathrm{Si}(2kl)] + \tfrac{1}{2}(\cos 2kl)[C + \ln(kl) + \mathrm{Ci}(4kl) - 2\mathrm{Ci}(2kl)]\}$$

where

$$\mathrm{Si}(x) = \int_0^x \frac{\sin x'}{x'}\,dx', \qquad \mathrm{Ci}(x) = -\int_x^\infty \frac{\cos x'}{x'}\,dx', \qquad C = 0.5772\ldots.$$

**12.5b** Following the procedure in Sec. 12.5, find the far-zone fields and radiated power if the antenna is loaded in such a way that current $I$ is substantially constant along the antenna, even though $kl$ is not negligibly small.

**12.5c** For antennas that are short in comparison with wavelength, and not end-loaded, current distribution is nearly linear from a maximum at the center to zero at the ends. For such a short, symmetric dipole, give the mathematical form for current and obtain far-zone fields.

**12.5d** Obtain far-zone fields for a straight antenna with current assumed to have a quadratic distribution with $z$, $I(z) = I_m[1 - (z/l)^2]$.

**12.5e*** Obtain Eq. 12.5(4) by integrating far-zone contributions to $E_\theta$ from small current elements (Hertzian dipoles) along the antenna, assuming current distribution as in (1). Make appropriate far-zone approximations.

**12.6a** Plot polar patterns of field and intensity for a full-wave antenna with $2l = \lambda$.

**12.6b** How many lobes are there in the pattern for a straight antenna with $kl = n\pi$, where $n$ is an integer? For $kl = m\pi/2$ where $m$ is an odd integer?

**12.6c** Find the direction of maximum directive gain and directivity of a dipole of length $3\lambda/2$, for which the pattern is pictured in Fig. 12.6*b*. Use $W$ from Prob. 12.5a.

**12.6d** Find the directivity for the antenna with assumed current distribution as in Prob. 12.5b.

**12.7a** Compare the currents that would be required in a half-wave dipole and a small dipole of height $0.05\lambda$ to produce 100 W of radiated power from each. For both antennas to have the same radiation efficiency, assuming materials with the same surface resistivity, what should be the ratio of radii?

**12.7b** Simpson's rule is useful for evaluation of radiation integrals. If the area to be evaluated is divided into $2m$ even-numbered portions by $2m + 1$ lines spaced an equal distance $\Delta$ apart, and values of the function at these lines are $f_0, f_1, \ldots, f_{2m+1}$, the area under the curve is approximately

$$I = \frac{\Delta}{3}[(f_0 + f_{2m}) + 4(f_1 + f_3 + \cdots + f_{2m-1}) + 2(f_2 + f_4 + \cdots + f_{2m-2})]$$

Use this to find the radiation resistance of a half-wave dipole, taking $m = 3$. Compare with the value 73.09 $\Omega$ found by more precise methods.

**12.7c** Find the expression for radiation resistance of the antenna with assumed current as in Prob. 12.5b. Plot versus $l/\lambda$ for $0 < l/\lambda < 0.2$.

**12.7d** The current in the definition for radiation resistance, Eq. 12.7(1), is sometimes taken as maximum current along the antenna rather than input current. This is especially useful in estimating current level on the antenna needed for a given power when the assumed current distribution has a zero at the input. Calculate and plot $R_r$ on both bases for $0 \leq kl \leq \pi$. (This requires numerical integration of Eq. 12.5(6) or tables for evaluation of the result of Prob. 12.5a.)

**12.8** Prove by a study of the resulting vector potential the *same vertical direction, opposite horizontal direction* rule for image currents given in Sec. 12.8.

**12.9a** Plot the form of radiation intensity as a function of $\theta$ of a wire with traveling wave for $kl = \pi, 2\pi, 4\pi$.

**12.9b** For large $kl$, obtain the value $\theta_m$ for maximum radiation from the wire with traveling wave and plot versus $kl$.

**12.9c** Suppose the traveling wave on the wire has a different phase constant $\beta$ than the free space $k$. Find radiation intensity for this case. For a slow wave on the wire ($\beta > k$) describe qualitatively the main effects on the pattern.

**12.9d** As in Prob. 12.9c, but assume attenuation so that current along the wire is $I_0 \exp[-(\alpha + j\beta)z']$.

**12.10a** Show that Eq. 12.10(9) applies to any antenna with horizontal currents distance $h$ above perfectly conducting earth.

**12.10b** Analysis has been given for a V antenna with traveling wave from the vertex of the V to the wide end. Show that the same pattern results (for a given $kl$) if the V is reversed in direction, with the traveling waves propagating from the wide end to the vertex.

**12.10c** V antennas may also be made with standing waves in the two arms in place of the traveling waves considered in Sec. 12.10. For example, the radiation pattern of the dipole of length $3\lambda/2$ sketched in Fig. 12.6*b* has maximum radiation at an angle 42.5 degrees from the wire axis. If two such wires form a V with angle 85 degrees between them, one would then expect maxima in the forward and reverse directions. Sketch the expected pattern.

**12.10d** For the V antenna with standing waves, it is found that interaction between arms modifies the simple superposition assumed in Prob. 12.10c. For $0.5 < l/\lambda < 3$, an empirical formula gives optimum angle $2\alpha = 60(\lambda/l) + 38$ degrees with resulting directivity $(g_d)_{max} = 1.2 + 2.3(l/\lambda)$ [W. L. Weeks, *Antenna Engineering*, McGraw-Hill, New York, 1968, p. 141]. Plot $2\alpha$ and $(g_d)_{max}$ versus $l/\lambda$ over the range of validity.

**12.11** For the folded dipole pictured in Fig. 12.11*b*, one obvious mode that might seem to be excited is the parallel-wire transmission line mode with equal and opposite currents in the parallel conductors. With the length from input terminals to shorted ends approximately a quarter-wavelength, estimate the input impedance for such a mode and explain why it is not much excited by an input line of a few hundred ohms characteristic impedance.

**12.12** Demonstrate that Eqs. 12.12(5) and (6) do satisfy 12.12(3), with **A** and **F** satisfying inhomogeneous Helmholtz equations.

**12.13a*** From Eq. 12.13(2) we see that the elemental plane-wave source is equivalent to crossed electric and magnetic infinitesimal dipoles. Superpose directly the far-zone fields of these from Sec. 12.3 to obtain Eqs. 12.13(4) and (5). (Note the required transformation of coordinates axes for this demonstration.)

**12.13b** Suppose **E** and **H** in an aperture are not related as in a plane wave, but by a general wave impedance $Z_w$, so that $E_x/H_y = -E_y/H_x = Z_w$. Give the modified form of Eq. 12.13(6). How is the paraxial approximation for apertures, Eq. 12.13(10), modified in this case?

**12.14a** Analyze the rectangular aperture with uniform illumination without making the paraxial approximation (i.e., for $\theta$ not necessarily small) and compare with Eq. 12.14(2).

**12.14b** Analyze, using the paraxial approximation, the far-zone field from a rectangular aperture with no variation in $y$ but a quadratic variation in $x$:

$$E = E_0\left[1 - \left(\frac{2x}{a}\right)^2\right], \qquad -\frac{a}{2} \le x \le \frac{a}{2}$$

**12.14c** In calculating radiated power for the rectangular aperture, we have utilized power conservation and found the flow through the aperture. Check this, using approximations appropriate to small $\theta$, from the far-zone field, Eq. 12.14(2).

**12.14d** For the circular aperture with uniform illumination, suppose that all radiation was confined to a cone of angle $\theta_0$ given by Eq. 12.14(12) and was of constant amplitude over this cone. Give the directivity and compare with Eq. 12.14(13), explaining the difference.

**12.14e** For $ka = 5$ and $ka = 10$, plot $K$ versus $\theta$ for the circular aperture with uniform illumination. Find beam width and directivity. Comment on the effect of larger $ka$.

**12.14f*** As in Prob. 12.14c, use the far-zone field and paraxial approximations to check radiated power from the circular aperture.

**12.14g** Find far-zone fields from an "elliptic" gaussian distribution,

$$E(x', y') = E_0 e^{-(x'/w_1)^2} e^{-(y'/w_2)^2}.$$

As in the text, aperture size is large compared with either $w_1$ or $w_2$.

**12.14h** An annular aperture with uniform plane-wave illumination extends from $r' = b$ to $r' = a$. Find angle of the first zero if $b/a = \frac{1}{2}$.

**12.15** Modify Eq. 12.15(3) to account for a possible reflection coefficient $\rho$ in the aperture. *Hint:* Refer to Prob. 12.13b.

**12.16a** Prove that the image of a magnetic current in a perfectly conducting plane requires horizontal currents in the same direction for source and image. In what sense is the field for the resonant slot the dual of the field for the half-wave dipole?

**12.16b*** For the open end of a coaxial line of radii $a$ and $b$, set up the problem of determining power radiated, assuming the electric field of the TEM mode as the only important field in the aperture. Make approximations appropriate to a line small in radius compared with wavelength, and show that the equivalent radiation resistance referred to the open end is

$$R = \frac{3\eta}{2\pi^3}\left[\frac{\lambda^2 \ln(b/a)}{\pi(b^2 - a^2)}\right]^2$$

Calculate the value for $a = 0.3$ cm, $b = 1$ cm, $\lambda = 30$ cm. What standing wave ratio would this produce in the line?

**12.16c*** In Prob. 12.16b assume the magnetic field of the TEM mode at the open end of sufficient magnitude to account for the power calculated there. Show that a recalculation of power radiated including effects from this magnetic field leads to only a small correction to the first calculation. Take radii small compared with wavelength.

**12.16d*** Read one of the references on the Babinet principle and supply the derivation of the relation between slot conductance and dipole resistance found in Eq. 12.16(7).

**12.17a** Utilizing the relation for effective permittivity of disks given in Sec. 12.17, estimate the radius of disks and the spacing (assumed uniform) if $\varepsilon_r = 1.5$ is desired for use at a frequency of 10 GHz.

**12.17b** Utilize Eq. 12.17(2) to solve for $d(r)$ in terms of $d(0)$, $D$, $r$, and $v_p/c$. Plot $d(r)$ versus $r$ if $d(0) = 0.1$ m, $D = 1$ m, and the waves between plates act as $TE_1$ modes with $\lambda = 0.1$ m and plate spacing 0.075 m. Show modified shape if full wavelengths are subtracted once $d(r) > \lambda$.

**12.18a** Find $K$ and sketch the radiation pattern versus $\phi$ at $\theta = \pi/2$ if phase is as in the Fig. 12.18*b* but $I_2 = I_1/2$.

**12.18b** As in Prob. 12.18a but $I_2 = I_1$ in magnitude and phase. Then repeat for $I_2 = -I_1$.

**12.18c** An infinitely long parallel-wire transmission line propagates the TEM mode and would not be considered radiating, although one of finite length may. Consider such a finite-length line as an array of two wires carrying traveling waves as in Sec. 12.9 with currents of opposite sign. Take length as $l$ and spacing $d$ and find the expression for radiation intensity. Examine the behavior as $kl \to \infty$.

**12.18d** Consider a radiator with only vertical currents and a radiation intensity $K$. It is placed a distance $h$ above a plane, perfectly conducting earth. Find an expression for total radiation intensity $K_T$ corresponding to Eq. 12.10(9).

**12.19a** Explain the statement of the text that directivity of an array of elements is not the product of array directivity and element directivity. Illustrate with a high-directivity array made up of low-directivity elements.

**12.19b** Considering only the array factor, plot the direction of maximum radiation $\theta_m$ for a linear array versus the normalized phase delay $\Delta\varphi/kd$ between elements. What can you say about the relative sensitivities of $\theta_m$ to changes in $\Delta\varphi$ for nearly end-fire versus nearly broadside arrays?

**12.20a** Sketch patterns similar to Fig. 12.20*a* for $d = 4a$, $d = 6a$.

**12.20b** Obtain the expression for $K$ of a diffraction grating with $N = 4$. Sketch $K$ versus $(ka/2)\cos\phi$ with $d = 2a$ and compare with Fig. 12.20*a*.

**12.21a** The factored form of the polynomial of Eq. 12.21(2) is

$$S = C(\zeta - \zeta_1)\cdots(\zeta - \zeta_{N-1})$$

Find the locations of the zeros of a broadside array with $N = 4$.

**12.21b** Consider making a five-element linear array to be "supergain" by choosing $kd = \pi/2$ and placing the zeros at $\zeta = e^{\pm j\pi/6}, e^{\pm j\pi/3}$. Find the coefficients of the resulting polynomial and interpret in terms of required current excitation.

**12.21c** A potential analog of the linear array problem can be set up and has been utilized in array synthesis [T. T. Taylor and J. R. Whinnery, *J. Appl. Phys.* **22**, 19 (1951)] although numerical methods are now preferable. Show that if the logarithm of the factored form of Prob. 12.21a is taken, the result may be interpreted in terms of potential and flux about line charges.

**12.22a** For a three-element Yagi–Uda array with element 1 a passive reflector, element 2 driven by voltage $V_2$, and element 3 a passive director, write the equivalent of Eq. 12.22(1) and solve for $I_1, I_2, I_3$ in terms of $V_2$.

**12.22b** Estimate the directivity for the array with pattern sketched in Fig. 12.22*b*, assuming for simplicity that the given pattern also applies in planes normal to that shown.

**12.23a** Sketch a log-periodic array with seven elements, starting with $l_0 = 0.1$ m, $z_0 = 0.05$ m, and $\tau = 1.1$. Using the physical arguments of Sec. 12.23, estimate the frequency range over which this might be expected to radiate effectively.

**12.23b** Design a five-element log-periodic array to operate between frequencies 500 and 800 MHz.

**12.24** A microstrip patch antenna is in the form of a circular disk on dielectric with a ground plane. When fed by a coaxial line at the center as shown in Fig. P12.24, an

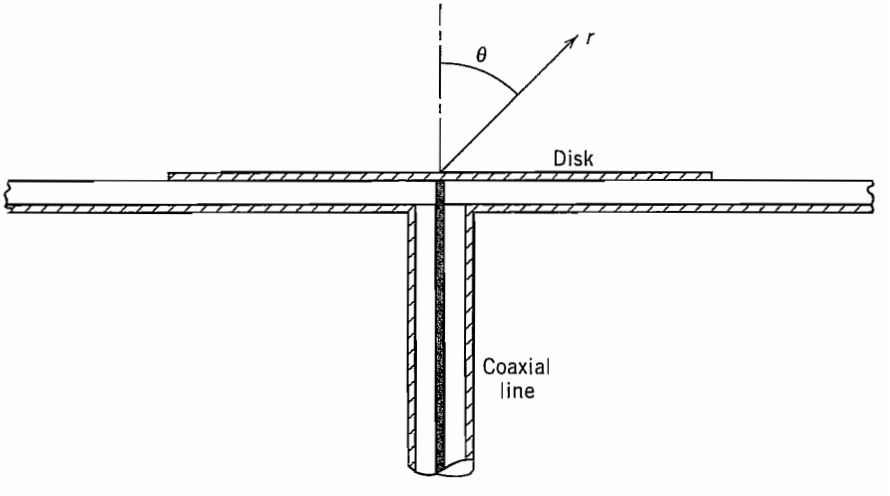


**FIG. P12.24**

axially symmetric mode, as analyzed in Sec. 9.3, is excited. (Antisymmetric modes radiate more strongly but the symmetric mode is simpler to analyze.) For a dielectric with $\varepsilon_r = 9$ and $f = 30$ GHz, find the radius of the disk for the first symmetric resonant mode, neglecting fringing effects. Find the radiation vector $\mathbf{L}$ for the air region above the disk in terms of the edge field $E_0$, taking the spherical coordinate axis as a continuation of the coaxial line axis. Evaluate the integral approximately by expanding the exponential in the integral in a power series.

**12.25a** The $Z_0$ for cylindrical antennas in Figs. 12.25*d* and *e* is the average of $Z_0$ from Eq. 12.25(10), with $\psi = a/r$. Show for a cylindrical antenna of length $l$ and radius $a$ that this yields

$$Z_0 = 120[\ln (2l/a) - 1]$$

What values of $l/a$ correspond with $Z_0 = 1200$? $Z_0 = 800$? $Z_0 = 500$?

**12.25b** Defining bandwidth as the frequency range for which $|Z| < \sqrt{2}Z_{\min}$, estimate from Figs. 12.25*d* and *e* the ratio of bandwidths for $l/\lambda$ near 0.25, for antennas of $Z_0 = 1200\ \Omega$ and $Z_0 = 500\ \Omega$.

**12.26a*** Verify Eq. 12.26(9).

**12.26b*** Find the input impedance formula corresponding to Eq. 12.26(11) for a short antenna so loaded that the current is uniform along its length.

**12.26c** An approximate solution of Eq. 12.26(11), valid where $1.3 \leq kl \leq 1.7$ and $0.0016 \leq a/\lambda \leq 0.0095$, is given by (see Elliott[3])

$$Z = [122.65 - 204.1kl + 110(kl)^2] - j\left[120\left(\ln\frac{2l}{a} - 1\right)\cos kl - 162.5 + 140kl - 40(kl)^2\right]$$

Calculate the input impedance for a dipole with $kl = \pi/2$ and $a/\lambda = 0.005$. Compare with the result for the $\lambda/2$ filamentary dipole.

**12.26d*** It can be shown that Eq. 12.26(11) can be integrated with the assumption that $a \ll \lambda$ and $a \ll l$ to give

$$Z = \frac{j60}{\sin^2 kl}\{[4\cos^2 kl][S(kl)] - [\cos 2kl][S(2kl)] - [\sin 2kl][2C(kl) - C(2kl)]\}$$

where

$$C(kl) = \ln\frac{2l}{a} - \frac{1}{2}\,\mathrm{Cin}(2kl) - \frac{j}{2}\,\mathrm{Si}(2kl)$$

and

$$S(kl) = \frac{1}{2}\,\mathrm{Si}(2kl) - \frac{j}{2}\,\mathrm{Cin}(2kl) - ka$$

Use tables of $\mathrm{Si}(x)$ and $\mathrm{Cin}(x)$ integrals to calculate the input impedance for a dipole with $kl = \pi/2$ and $a/\lambda = 0.005$ and confirm the result found by the simpler formula in Prob. 12.26c.

**12.27** Give the proof of Eq. 12.27(4). Use reciprocity as in Sec. 12.26.

**12.29a** Calculate power received corresponding to a transmitted power of 100 W and a distance between transmitter and receiver of $10^3$ m under the following conditions:

(i) Directivity of transmitting antennas = 1.5; effective area of receiver = 0.40 $m^2$.

(ii) Directivity of both antennas = 2; wavelength = 0.10 m.

(iii) Effective area of both antennas = 1 $m^2$; wavelength = 0.03 m.

**12.29b** Synchronous satellites orbit at about $4 \times 10^4$ km from the earth. About what diameter would you need for a uniformly illuminated circular aperture antenna on such a satellite to give full earth coverage if frequency is 7.5 GHz? (Earth radius ≈ 6370 km.) What power would have to be transmitted from the satellite if the earth stations have antennas 4 m in diameter and the receivers are capable of responding with acceptable error to signals of $10^{-10}$ W? Repeat for a satellite with earth coverage reduced to a region of diameter 100 km.

**12.30a** Calculate the effective area for a half-wave dipole antenna. Compare with that for the infinitesimal dipole.

**12.30b** If the antennas are in free space, the pattern of 1 may be measured, as was described in Fig. 12.30*a*, by moving antenna 2 about the arc of a circle or as in Fig. 12.30*b* by rotating 1 about an axis to give the same relative position. Explain why the same results might not be obtained by the two methods if there are fixed obstacles in the transmission path.

**12.30c** For the data of Prob. 12.29*a*(ii) and the radiation resistance of both antennas equal to 50 Ω, calculate $|Z_{12}|$. Now, allowing separation $r$ to vary, find the separation for which magnitude of $Z_{12}$ becomes comparable to real part of $Z_{11}$.

**12.30d** An integrated antenna placed on a dielectric as in Fig. 12.24*d* is used as a receiving antenna. Explain why more signal will be induced in the antenna when irradiated from the dielectric region than from air. By reciprocity, this explains why, as a transmitting antenna, it radiates more strongly into the dielectric region.

**12.30e** As in Prob. 12.30d, use the integrated antenna of Fig. 12.24*d* as a receiving antenna, and reciprocity, to explain the special features of Fig. 12.24*f* at the critical angle.

**12.31a** To demonstrate that a power calculation in the internal impedance of a Thévenin equivalent circuit does not necessarily represent the power lost internally, consider the source of constant voltage 100 V coupled to a resistance load of 2 Ω through the series-parallel resistances shown in Fig. P12.31*a*. Calculate the actual power lost in the generator, and compare with that calculated by taking load current flowing through the internal impedance of a Thévenin equivalent circuit.

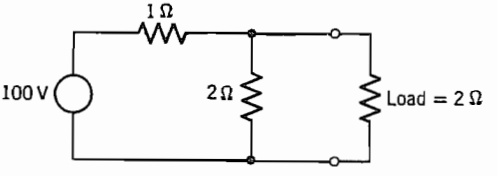


**FIG. P12.31*a***

**12.31b** An antenna having an input impedance on transmission of $70 + j30$ Ω is used on reception by connecting directly to a 50-Ω transmission line which is perfectly matched to a pure resistance load. The effective area is 0.40 $m^2$. Find the power transfer to the load if the antenna is in a plane wave field of 100 μV/m. Compare this with the power that could be obtained with a conjugate match to the antenna impedance.